University of Nevada, Reno

Impacts of Reservoir Operations with Extreme Hydrologic and Climatic Conditions on Fish Sustainability below Shasta Lake

A thesis submitted in partial fulfillment of the
requirements for the degree of Master of Science in Hydrogeology

by

Joseph Reginald Sapin

Dr. Laurel Saito/Thesis Advisor

August, 2014

We recommend that the dissertation

prepared under our supervision by

JOSEPH R SAPIN

entitled

Impacts of Reservoir Operations with Extreme Hydrologic and Climatic Conditions on Fish Sustainability below Shasta Lake

be accepted in partial fulfillment of the

requirements for the degree of

MASTER OF SCIENCE

Laurel Saito, Ph.D., Advisor

Balaji Rajagopalan, Ph.D., Committee Member

Derek Kauneckis, Ph.D., Graduate School Representative

David W. Zeh, Ph. D., Dean, Graduate School

August, 2014

Abstract

Reservoir managers on the Sacramento River are required by law to provide artificial cold water habitat downstream for endangered winter-run Chinook salmon. At Shasta Lake, a temperature control device was installed on Shasta Dam that allows selective withdrawal of reservoir water at different elevations. There is debate, however, about whether selective withdrawal will be effective under uncertain future conditions such as climate change and extreme hydrologic conditions not observed in the historical record. This study examines the ability of providing artificial cold water habitat by coupling a stochastic model for model input generation with a two-dimensional hydrodynamic model capable of simulating selective withdrawal at Shasta Lake. Input from water managers was used to examine variations to stochastically generated scenarios under various operations schedules. A generalized operations schedule was found to perform better in maintaining cold water habitat than either an all-out-the-bottom or all-out-the-uppermost schedule in most cases, even though the all-out-the-uppermost schedule maximized the in-reservoir cold water pool in all simulations.

Table of Contents

List of Figures

List of Tables

Chapter 1: General Introduction

Project Background

Changing the flow patterns and habitat of natural lotic river systems by the construction of artificial lentic reservoirs creates a major problem for migrating salmon species that can no longer reach their native cold water spawning habitat (Collier et al. 1996; Graf 2006; Yates et al. 2008). To lessen the riverine impact on salmon and improve water quality, altered release schedules from dam operations can be implemented to improve the downstream habitat and long-term sustainability of salmon populations (Collier et al. 1996; Petts 1989; Poff et al. 1997; Stanford et al. 1996). Selective withdrawal structures to create altered release schedules are often utilized to manage the downstream hydrograph and create suitable habitat for threatened and endangered salmon species such as the Chinook salmon in northern California (Bartholow et al. 2001; Olden and Naiman 2010).

Shasta Lake, part of the Central Valley Project, is the largest storage reservoir in California (USBR 2003) and is operated for downstream fish conservation among other uses including hydroelectric power generation (USBR 2004). In 1997, a temperature control device (TCD) began operating at Shasta Dam that allows selective withdrawal to regulate downstream water temperatures while maximizing hydropower generation (Hanna et al. 1999). Revised reservoir operations are implemented using the TCD to create downstream habitat to promote the propagation and survival of the endangered winter-run Chinook salmon (Bartholow et al. 2001). Hydrodynamic modeling of the reservoir-river system is useful to inform downstream temperature control operations

(Caldwell et al. 2009), however, uncertainty in the system cannot be fully captured by modeling inputs limited to the historical record (Apipattanavis et al. 2007).

Methods Development

This project represents the integration of previously developed methods to address the effects of hydrologic and climatic uncertainty for artificial stream temperature management on the Sacramento River. In the 1990's researchers at Colorado State University developed and calibrated a CE-QUAL-W2 (W2; Cole and Wells 2011) model capable of simulating selective withdrawal through the TCD at Shasta Lake (Bartholow et al. 2001; Hanna et al. 1999; Saito et al. 2001). The researchers found that selective withdrawal using blended operations could reduce the impact of downstream temperature exceedances (Hanna et al. 1999), and that TCD operations were likely to have little impact on the in-reservoir fish populations (Saito et al. 2001). They also found that management of reservoir volume would benefit reservoir limnology better than adjustments to TCD operations alone could achieve.

For the current study, the calibrated W2 model and simulation methods of Hanna et al. (1999) were implemented for two-dimensional hydrodynamic modeling of Shasta Lake and assessment of simulated outflow temperatures. A macro utility was developed to run W2 and prepare output data for analysis of simulated outflow temperatures and calculated in-reservoir cold water pool. A tradeoff analysis was also conducted to evaluate the cost of meeting downstream temperature with selective withdrawal schedules in terms of in-reservoir cold water pool depletion.

To capture a greater uncertainty for the system than is present in the historical record, a stochastic model developed by Nowak et al. (2010) was used to generate W2 inputs of extreme hydroclimate conditions. This method uses a K-nearest neighbor bootstrap resampling technique modified from the work of Sharma et al. (1997) and Prairie et al. (2007) to create synthetic datasets from the historical record with values beyond the historical record while maintaining statistics of the historical record. Synthetic Shasta Lake inflow datasets of extreme wet and extreme dry conditions were generated using this method. The method was also used to create complementary synthetic weather and stream temperature datasets required for input into the W2 model. The uncertainty associated with temperature increases due to climate change were also incorporated into the synthetic W2 inputs by forcing the forecasted temperature increases of peer-reviewed climate studies (California Climate Change Center 2012; USBR 2011).

Incorporating the input of reservoir managers into the modeling process was an integral goal of this project. Two workshops were conducted to gain insight into what issues they were most interested in seeing modeled for impacts on downstream temperature regulation. The first workshop in February 27, 2013 was held in Redding, CA with representatives from academic institutions, government agencies, non-profit organizations and American Indian tribal representatives. Feedback from the first workshop was used to develop modeling scenarios for input into W2 that included a wet year with a dry fall, a wet year with a warm fall and a two year drought. A second workshop was held at the US Bureau of Reclamation office in Sacramento, CA on May 28, 2014 to present modeling results based on guidance from the first workshop and to obtain additional guidance for the refinement of W2 modeling methods.

Thesis Overview

This thesis is divided into five chapters. Chapter one (this chapter) provides background and an introduction to project motivations and methods. The second chapter is a manuscript focusing on the development of synthetic W2 inputs of extreme wet and extreme dry conditions using modifications to the methods of Nowak et al. (2010). The third chapter is a manuscript discussing results of downstream temperature assessment and in-reservoir cold water pool reserve using the inputs developed in chapter two and climate change predictions and feedback from the first workshop. The fourth chapter consists of recommendations provided by reservoir managers at the second workshop for refinement of modeling methods. The fifth chapter provides a summary of results and a conclusion to this thesis. The appendices contain information and data not included in previous chapters.

References

Apipattanavis S, Podesta G, Rajagopalan B, Katz R. 2007. A semiparametric multivariate and multisite weather generator. *Water Resources Research* 43: W03432.

Bartholow J, Hanna RB, Saito L, Lieberman D, Horn M. 2001. Simulated limnological effects of the Shasta Lake temperature control device. Environmental Management 27(4):609-626.

Caldwell, RJ, Danner E, Pike A, Rajagopalan B, Melton FS, Lindley S, and Nemani RR. 2009. An Integrated Framework for Improved Stream Temperature Predictions to Mitigate Fish Mortality. AGU Fall Meeting, Dec. 14-18, San Francisco, CA.

California Climate Change Center. 2012. Our Changing Climate: Vulnerability and Adaptation to the increasing Risks from Climate Change in California. A Summary

Report on the Third Assessment from the California Climate Change Center. CEC-500-2012-007.

Cole TM, Wells SA. 2011. CE-QUAL-W2: a two-dimensional, laterally-averaged, hydrodynamic and water quality model, version 3.7. User manual. Instruction Report EL-11-1. Washington (DC): US Army Corps of Engineers.

Collier M, Webb RH, Schmidt JC. 1996. Dams and rivers: a primer on the downstream effects of dams. Denver (CO): US Geological Survey. US Geological Survey circular no. 1126.

Graf WL. 2006. Downstream hydrologic and geomorphic effects of large dams on American rivers. Geomorphology 79:336-360.

Hanna RB, Saito L, Bartholow JM, Sandelin J. 1999. Results of simulated temperature control device operations on in-reservoir and discharge water temperatures using CE-QUAL-W2. Journal of Lake and Reservoir Management 15(2):87-102.

Olden JD, Naiman RJ. 2010. Incorporating thermal regimes into environmental flows assessments: modifying dam operations to restore freshwater ecosystem integrity. Freshwater Biology 55:86-107.

Nowak K, Rajagopalan B, Prairie J. 2010. A non-parametric stochastic approach for multisite disaggregation of annual to daily streamflow. *Water Resources Research* 46:W08529.

Petts GE. 1989. Perspectives for ecological management of regulated rivers. In: Gore JA, Petts GE, editors. Alternatives in regulated river management. Boca Raton: CRC Press. p 3-24.

Poff NL, Allan JD, Bain MB, Karr JR, Prestegaard KL, Richter BD, Sparks RE, Stromberg JC. 1997. The natural flow regime: a paradigm for river conservation and restoration. BioScience 47:769-784.

Prairie J, Rajagopalan B, Lall U, Fulp T. 2007. A stochastic nonparametric technique for space-time disaggregation of streamflows. Water Resources Research 43: W03432.

Saito L, Johnson BM, Bartholow J, Hanna RB. 2001. Assessing ecosystem effects of reservoir operations using food web-energy transfer and water quality models. Ecosystems 4:105-125.

Sharma A, Tarboton DG, Lall U. 1997. Streamflow simulation: a nonparametric approach. *Water Resources Research* 33(2): 291-308.

Stanford JA, Ward JV, Liss WJ, Frissell CA, Williams RN, Lichatowich JA, Coutant CC. 1996. A general protocol for restoration of regulated rivers. Regulated Rivers 12:391-413.

[USBR] US Bureau of Reclamation. 2003. Shasta Reservoir Area Inventory: Shasta Dam and Reservoir, California. Prepared by MWH. February 2003. 21 p.

[USBR] US Bureau of Reclamation. 2004. Long-Term Central Valley Project Operations Criteria and Plan: CVP-OCAP. Sacramento, CA: US Bureau of Reclamation, Mid-Pacific Division. 238 p.

[USBR] US Bureau of Reclamation. 2011. Reclamation, SECURE Water Act Section 9503(c) – Reclamation Climate Change and Water, Report to Congress.

Yates D, Gallbraith H, Purkey D, Huber-Lee A, Sieber J, West J, Herrod-Julius S, Joyce B. 2008. Climate warming, water storage, and Chinook salmon in California's Sacramento Valley. Climatic Change 91:335-350.

Chapter 2: A nonparametric stochastic alternative to generate inputs for modeling impacts of extreme hydrologic and climatic conditions

[1]Joseph Sapin, [2]Balaji Rajagopalan, [3]Laurel Saito, [4]R Jason Caldwell

[1]Graduate Research Assistant
Graduate Program of Hydrologic Sciences
University of Nevada – Reno, Mail Stop 186
Reno, NV, USA 89577

[2]Professor
Department of Civil, Environmental and Architectural Engineering
University of Colorado – Boulder, Campus Box 428
Boulder, CO, USA 80309

[3]Associate Professor
Department of Natural Resources and Environmental Science
University of Nevada – Reno, Mail Stop 186
Reno, NV, USA 89577

[4]Senior Project Engineer
Leonard Rice Engineers, Inc.
1221 Auraria Pkwy, Denver, CO USA 80204

Abstract

Hydrologic and climatic uncertainty is increasing in the western United States, and with it the need for models capable of capturing this uncertainty beyond what is seen in the historical record. Realistic modeling inputs of uncertain and extreme hydrologic and climatic conditions were created using a non-intensive, stochastic alternative to watershed-based generation methods. The synthetic inputs reproduced the historical statistics of climate and inflow, but produced extreme wet and dry conditions beyond those seen in the historical record. The extreme conditions created for input into the model offer water managers and modelers the ability to assess the impacts of unprecedented hydrologic conditions without the investment in a large-scale watershed based model. The approach developed can be applied for other situations where combined flow, temperature, and climate inputs are needed for analysis of uncertain events. Modifications to the generation of temporal disaggregation could also lead to further refinement of the stochastic process with increased variability in the intra-annual synthetic hydrology.

Keywords

Lake Shasta, Disaggregation, Streamflow, Stream Temperature, Weather Generator

Introduction

The climate and hydrology of the western United States is in a state of increasing uncertainty. Winter and spring temperatures are increasing (Cayan et al. 2001), and spring snowpack in Northern California has decreased by 50% or more on average since 1950 (Mote et al. 2005). Mote et al. (2005) found that spring snowpack in the mountains of Northern California and the Cascades have the greatest sensitivity to reduction due to temperature changes and regional warming in the western United States. Warming temperatures are also expected to result in earlier spring snowmelt runoff for the western United States that could lead to increased winter and early springtime floods and extended periods of summer drought (Stewart et al. 2004).

Because of this uncertainty, reservoir managers are under increased pressure to ensure that changes in hydrology and climate will not affect their ability to meet obligations of downstream stakeholders, including downstream fisheries. The construction of dams across the western United States during the 20th century disrupted downstream river ecosystems and impeded the upstream migration of salmon species (Botsford and Brittnacher 1998). In some cases, species that were adapted to much colder upstream waters were subjected to stream temperatures that were warmer than their biology could tolerate. Many important fish species in the western United States experienced population declines to such low levels that they were listed for protection under the Endangered Species Act (USFWS 2014).

Evaluating the effects of reservoir management under increasingly uncertain conditions to provide adequate habitat for downstream fisheries can be addressed with computer modeling. Many numerical models, such as CE-QUAL-W2 (Cole and Wells 2011), have the ability to simulate reservoir operations and the effects of operations decision making on downstream water temperature, which provides useful information about the sustainability of downstream fisheries (Hanna et al. 1999). Modeling to assess impacts of uncertain future conditions could benefit from uncertain inputs beyond what is available in the historical record to enable analysis of possible unforeseen events and inform future decision making strategies for reservoir management.

Many models generally used for generation of uncertain inputs, such as large-scale watershed models (e.g., Variable Infiltration Capacity (VIC), Hydrological Simulation Program—Fortran (HSPF), Precipitation-Runoff Modeling System (PRMS), etc.), are time and budget intensive. Parametric statistical methods offer an alternative to intensive watershed-based models for generating flow input and require relatively low computational power. However, because parametric methods require data to fit a certain distribution, they can underrepresent anomalous behaviors within a system. Nonparametric methods also suffer from the drawback of requiring transformations into normal distributions for systems with several variables and seasons. Even when data are successfully transformed, model performance in the transformed space does not guarantee performance in the untransformed space. Even basic non-normal features such as bimodality, common in rainfall patterns, are typically not captured by the limitations of parametric methods (Apipattanavis et al. 2007).

With increased computing power over the last several decades, nonparametric stochastic methods have increased in popularity and are now being used frequently in stochastic simulation (Nowak et al. 2010). Synthetic hydrodynamic modeling inputs generated using non-parametric methods benefit from the generation of ensembles that transmits the uncertainty from one step to the next in the input, modeling and output phases (Appipattanavis et al. 2007). The generation of synthetic ensembles in an integrated framework has been shown to capture uncertainty in the stochastic generation and disaggregation of synthetically generated datasets (Nowak et al. 2010, Tarboton et al. 1998, Prairie et al. 2007).

Nowak et al. (2010) developed a nonparametric daily disaggregation method for disaggregating monthly and annual streamflow to daily streamflow values. This work was built off of previous nonparametric methods presented by Tarboton et al. (1998) that was subsequently improved by Prairie et al. (2007) to be more robust, computationally more manageable, and to always produce positive values. This method is easy to implement, is data driven, is non-assumptive, and can capture non-normality and non-linear data characteristics. It is also a very robust method in that it can perform disaggregation at multiple time and space scales. The disaggregated flows generated are rich in variety and can produce flows outside of the range of observed historical values (Nowak et al. 2010). Nowak et al. (2010) applied these methods to the disaggregation of daily streamflow simulations at three gauges on the San Juan River in southwestern Colorado where other methods failed due to the mismatch between the parametric distributions appropriate for daily flows versus annual flows.

Our objective in this study was to create realistic modeling inputs of uncertain and extreme hydrologic and climatic conditions using a non-intensive, stochastic alternative to watershed-based generation methods. By implementing modifications to the methods of Nowak et al. (2010), we created necessary hydrologic and meteorologic inputs for a CE-QUAL-W2 model of Shasta Lake on the Sacramento River in California, where questions about reservoir operations for temperature management for downstream fisheries under extreme conditions were being investigated. The approach developed can be applied for other situations where combined flow, temperature, and climate inputs are needed for analysis of uncertain events.

Methods

Site Description

Shasta Lake is a large, deep and dendritic waterbody located roughly 32 kilometers (20 miles) downstream of the headwaters of the Sacramento River watershed in Northern California and 16 kilometers (10 miles) north of the city of Redding. It is the largest storage reservoir in California, and supports an excellent fishery of both cold water and warm water species (USBR 2011). The reservoir has four main tributaries: the Sacramento River, the McCloud River, the Pitt River, and Squaw Creek. According to the Parameter-elevation Relationships on Independent Slopes Model (PRISM; PRISM 2014) data for climate normals between 1981 – 2010, Shasta Lake receives average annual precipitation of about 160 cm, with annual maximum temperatures of 23 °C and an annual minimum temperature of 10 °C.

CE-QUAL-W2

CE-QUAL-W2 (W2) is a two-dimensional hydrodynamic and water quality model (Cole and Wells 2011). For the modeling effort on Shasta Lake, inputs of daily inflows, outflows and stream temperature as well as subdaily meteorology were needed. W2 also has the capability of simulating selective withdrawal in which outflows can be distributed at different outlet elevations. The W2 model for Shasta Lake was calibrated to in-reservoir measurements from 1995 (Hanna et al. 1999, Saito et al. 2001). Calibration metrics for the current version of the model are provided in chapter 3.

Because W2 was to be used to evaluate outflow stream temperatures, W2 input requirements chosen for stochastic generation included daily inflows, daily inflow temperatures and hourly meteorology. Hourly meteorology was needed to replicate diurnal temperature variations in the reservoir. To generate these inputs, three types of data were obtained: incoming streamflow, incoming stream temperature and site meteorology (Table 1).

Table 1. Locations and descriptions of data downloaded for the project.

Station Name	Latitude	Longitude	Period of Record	Data Type	Source
USGS 11368000 McCloud River Above Shasta Lake CA	40.958°	122.218°	10/1/1945 – 9/30/2011	Streamflow	USGS[a]
USGS 11365000 Pit River Near Montgomery Creek CA	40.844°	122.001°	10/1/1944 – 9/30/2011	Streamflow	USGS[a]
USGS 11342000 Sacramento River A Delta CA	40.940°	122.416°	10/1/1944 – 9/14/2012	Streamflow	USGS[a]
USGS 11365500 Squaw Creek Above Lake Shasta CA	40.857°	122.119°	10/1/1944 – 9/30/1966	Streamflow	USGS[a]
CDEC DLT Sacramento River at Delta	40.939°	122.417°	11/1/89 – 9/13/2012	Stream Temperature	CDEC[b]
CDEC PMN Pit River near Montgomery Creek	40.843°	122.016°	5/1/1990 – 9/13/2012	Stream Temperature	CDEC[b]
CDEC MSS McCloud River above Shasta Lake	40.958°	122.219°	11/1/1989 – 9/13/2012	Stream Temperature	CDEC[b]
NOAA AWS 725920 REDDING MUNICIPAL	40.518°	122.299°	1/1/1994 – 13/31/2010	Air Temperature, Relative Humidity, Wind Speed, Wind Direction, Cloud Cover	NOAA[c]
USBR hydrologic data Shasta Lake, CA	40.719°	122.419°	1/1/1944 – 12/31/2010	Computed Daily Inflow (adjusted for precip and evap), Reservoir Storage, Reservoir Elevation, Outlet Release	USBR[d]

a. US Geological Survey (USGS) - http://waterdata.usgs.gov/ca/nwis/
b. California Data Exchange Center (CDEC) - http://cdec.water.ca.gov/
c. National Oceanic and Atmospheric Administration - http://www.ncdc.noaa.gov/
d. US Bureau of Reclamation (USBR)

Overview of stochastic approach

Stochastic generation of modeling inputs was implemented with a disaggregation process and generated flows with corresponding water temperatures and weather as shown in Figure 1. The incoming streamflow values were generated first in a three step process and the incoming stream temperature and site meteorology were subsequently generated to complement the results of the synthetic streamflow values. The streamflows were generated by an initial resampling of aggregate annual inflow from the historical record which was subsequently disaggregated to daily values and then further disaggregated spatially among the incoming tributaries. The inputs of stream temperature and meteorology were also resampled from the historical record to correspond with the conditions and timesteps produced by the streamflow generator.

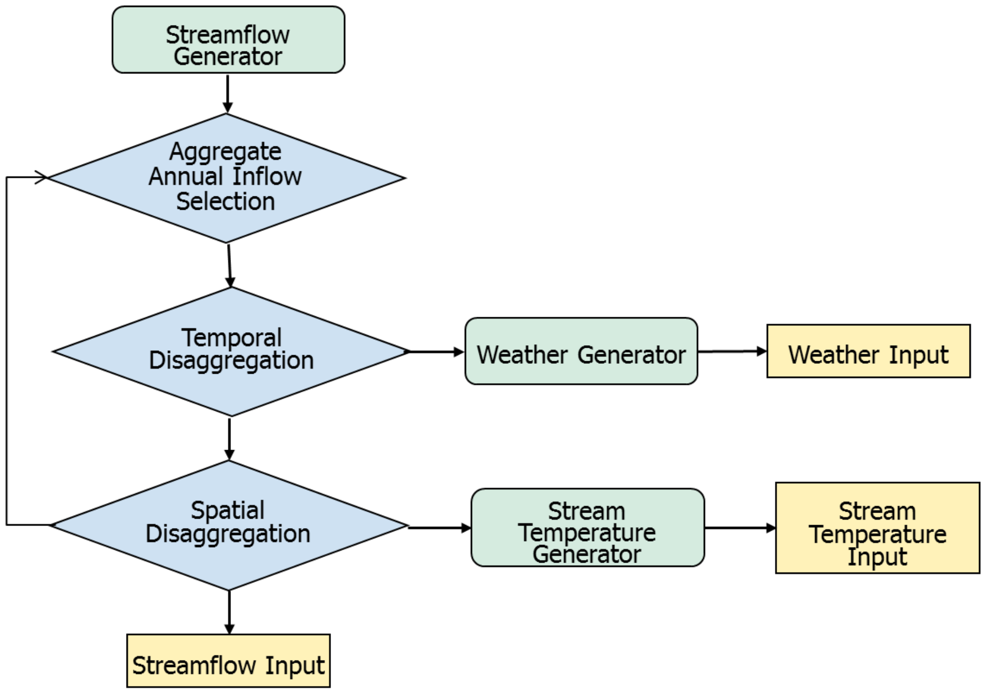

Figure 1. Overview of the stochastic generation process

Development of stochastic daily Shasta Lake inflows

Using modified stochastic methods from Nowak et al. (2010), an annual streamflow value was first selected from the time series of the calendar year sum of the US Bureau of Reclamation (USBR) computed inflows for 1946 - 2010. The USBR computed inflows are the aggregate daily inflows into Lake Shasta for all tributaries that have been adjusted for gains from precipitation and losses from evaporation. The inflow selection program was written such that the annual streamflow value could be selected randomly or with a weighting factor to preferentially select a high or low streamflow year as implemented by Apipattanavis et al. (2007).

A k-nearest neighbor (k-NN) algorithm was then applied to select a year of similar annual inflow magnitude to the one initially selected by the program where the number of neighbors chosen to sample from was equal to the square root of the length of record being sampled. The daily inflow values of the k-NN year selected were divided by the annual inflow value of the k-NN year to create a "daily proportion vector" such that each day was a fraction of the k-NN annual inflow value. The aggregate annual streamflow of the initially selected year was then disaggregated temporally into daily aggregate streamflow values by multiplying it by the daily proportion vector created using the k-NN year.

Next, the daily aggregate streamflow values were disaggregated spatially by multiplying them with a proportion vector based on the fraction of daily inflow attributed to each tributary according to gauged USGS streamflow observations for each day of the daily proportion vector. Since the USGS streamflow record of Squaw Creek ends in 1966, the Squaw Creek component of the daily proportion vector post-1966 was set to its daily average contribution in the historical record (2.1%). Each simulation of the stochastic streamflow generator created a synthetic matrix dataset consisting of 365-day streamflow vectors for 61 years, the length of the original USBR computed inflow dataset used[1]. Fifty simulations were run to create an ensembled array of 365 day stochastic streamflow matrices with a total of 3050 synthetic years created.

Streamflow inputs of uncertain events were constructed using a percentile flow selection process of stochastically generated streamflow ensembles. First, a weighting factor preferentially selected either wet or dry annual streamflow values. The weighting

---

[1] 1964, 1965, 2007 and 2008 were not used because of long data gaps in the USGS datasets

factor sorted the historical record of annual inflows to list from either wettest to driest or vice-versa. The weight was assigned from the top down defined by a discrete decreasing kernel (Lall and Sharma 1996), with the top value assigned the highest weight. The probability of selection was determined by the assigned weights of the annual inflows.

Wet year ensembles were generated using a weighting factor that preferentially selected wet years in the k-NN selection process. The 99^{th} percentile flow year of the entire generated ensemble was then saved as a 365 day streamflow vector for later input as an extreme wet year into the W2 model. Dry year ensembles were generated with a weighting factor that preferentially selected dry years in the k-NN selection process. The 1^{st} percentile flow year of the entire generated ensemble was selected at the conclusion of the simulations for input into the W2 model as an extreme dry year.

Development of stochastic daily stream temperatures

Daily stream temperature values for each tributary were stochastically generated using a k-NN algorithm that selected days in the California Data Exchange Center (CDEC) stream temperature dataset that were similar in streamflow magnitude to the synthetic values generated from the spatial disaggregation. The length of the sampling record was limited to a seven day window that encompassed three days ahead and three days after the Julian day being generated. The corresponding stream temperature values for the days selected by the k-NN process were assembled into an appropriate vector for input into the W2 model.

Development of stochastic sub-daily meteorology

Sub-daily weather data used for input into the stochastic weather generator included cloud cover, wind speed, wind direction, air temperature and dew point temperature obtained from CDEC. Data gaps in the CDEC dataset from 1994 - 2010 collected for the Redding Municipal Airport were filled using linear interpolation. This dataset was then adjusted for application at Shasta Lake using algorithms in Saito (1999).

Site meteorology inputs were stochastically generated using the results of the temporally disaggregated streamflow generation results (*Figure 2*). For each day in the 365 day aggregate streamflow vector, a two-dimensional Euclidian distance k-NN algorithm was used to select a day in the USBR dataset that had an aggregate daily inflow value similar in magnitude to the magnitude of the streamflow and an air temperature similar to the day selected for streamflow in the streamflow generator. The length of the sampling record was limited to a seven day window that encompassed three days ahead and three days after the Julian day being generated to improve computational efficiency. To ensure that adjacent day weather was realistically compatible, the algorithm included a check that the 12 am air temperature was within the variance of the historical record (5.79°C) for the transition from the 11 pm air temperature of the previous day. The sub-daily weather for the k-NN day selected was then used to create a year-long matrix of sub-daily weather data that corresponded to the daily streamflow values of the extreme wet year or extreme dry year.

Statistical analysis of streamflow generation

A statistical analysis was conducted of temporally and spatially disaggregated streamflows generated from 50 simulations of 61 year ensembles using random annual inflow selection. The interquartile range of monthly aggregate streamflow, monthly variance and monthly skew for the 3050 synthetic years generated were compared to the monthly mean streamflow, monthly variance and monthly skew of the historical record, respectively.

Results

50 simulations of 61 year ensembles were run with random selection of annual inflow. Both temporal and spatially disaggregated streamflow generations were comparable to the mean, skewness and variance of the historical record (*Figure 2*; Appendix A). March is the wettest month of the year on average for the study area while the late summer months of July, September and October are on average the driest months of the year. The variability of streamflow is highest in the winter months with some very wet Januarys, whereas the summer months have the lowest variability. The simulations produced a bias of overrepresenting the variance of the streamflow during the month of January. The simulations also produced a bias of underrepresenting the skew of the streamflow in the months of June and July. Preferential selection of the aggregate annual inflow values using a weighting factor was effective in biasing the selection of the wet and dry years from the historical record for the creation of extreme wet and dry scenarios (*Figure 3*).

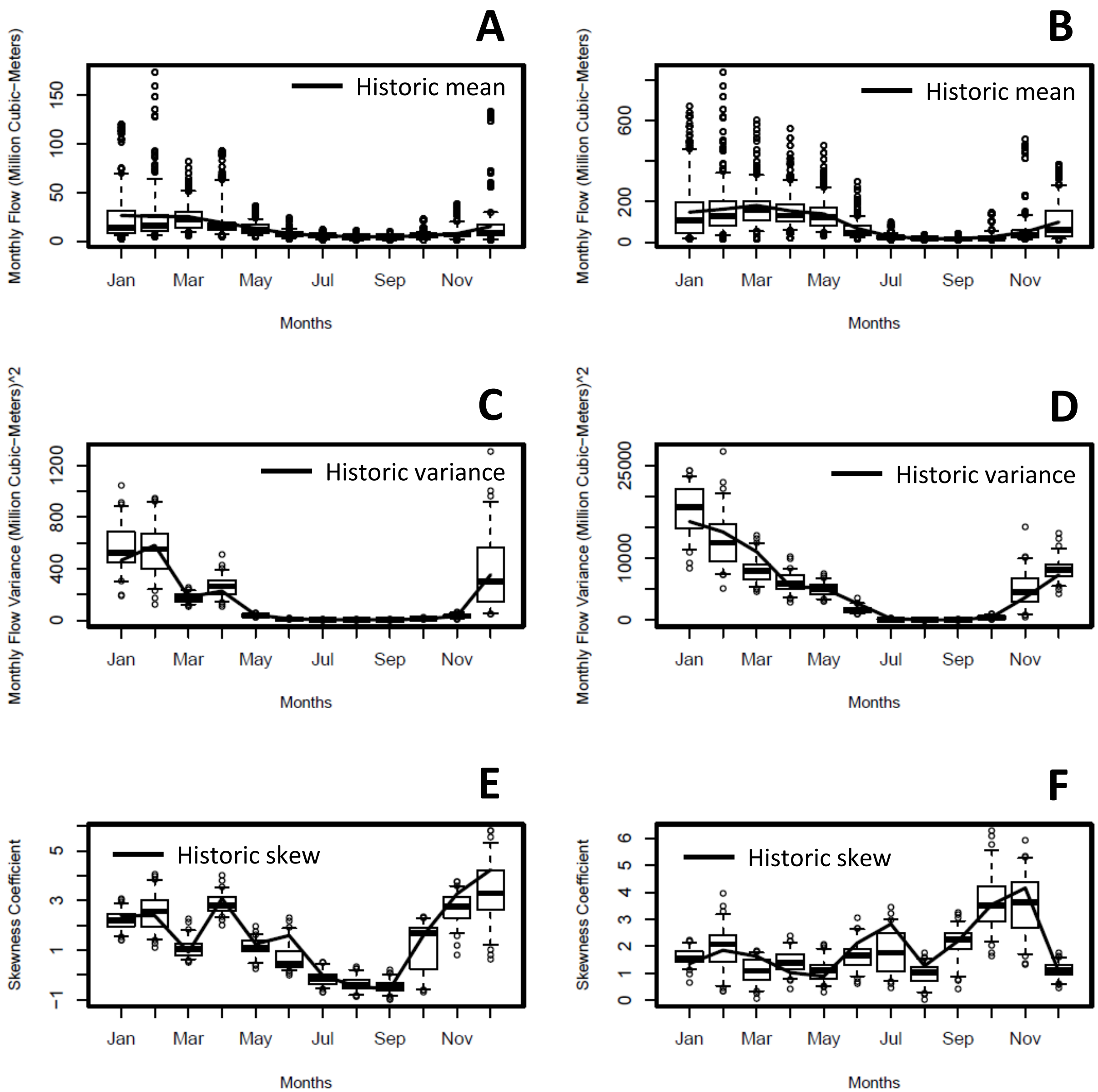

Figure 2. Statistical analysis of streamflow disaggregation from 50 simulations of 61 year ensembles using random annual inflow selection. Solid lines represent observed statistics. Boxplots represent interquartile range of stochastically simulated streamflow ensembles: (A) mean aggregate streamflow from temporal disaggregation; (B) mean Sacramento River streamflow from spatial disaggregation; (C) aggregate streamflow variance from temporal disaggregation; (D) Sacramento River streamflow variance from spatial disaggregation; (E) aggregate streamflow skewness from temporal disaggregation; (F) Sacramento River streamflow skewness from spatial disaggregation (Sacramento River).

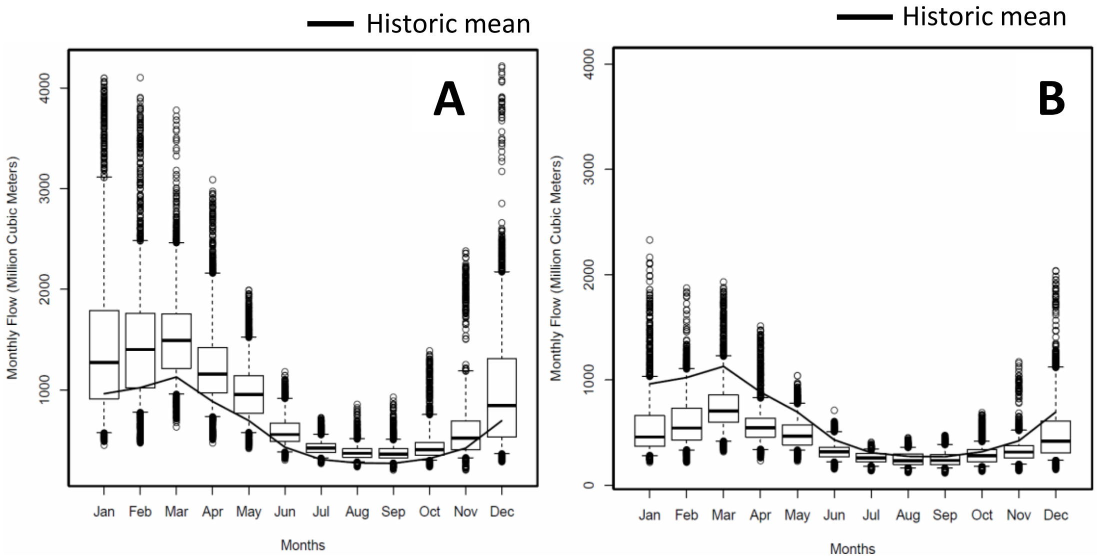

Figure 3. Statistical analysis of aggregate monthly streamflow generation using weighted annual inflow selection from 50 simulations of 61 year ensembles of the streamflow generator. Solid lines represent historic statistics. Boxplots represent interquartile range of synthetic streamflow: (A) mean monthly streamflow from wet year weighting; (B) mean monthly streamflow from dry year weighting.

The extreme wet year (i.e., the 99th percentile selection from 50 simulations of 61 year ensembles with preferential selection of wet annual streamflow values) included extreme flooding with springtime inflow values beyond what was seen in the historical record (*Figure 4*). The synthetic streamflow in the month of March was almost 620 million cubic meters (500,000 acre feet) larger than the highest outlier in the historical record. Streamflows during the months of August and September were also higher than their respective largest outliers in the historical record.

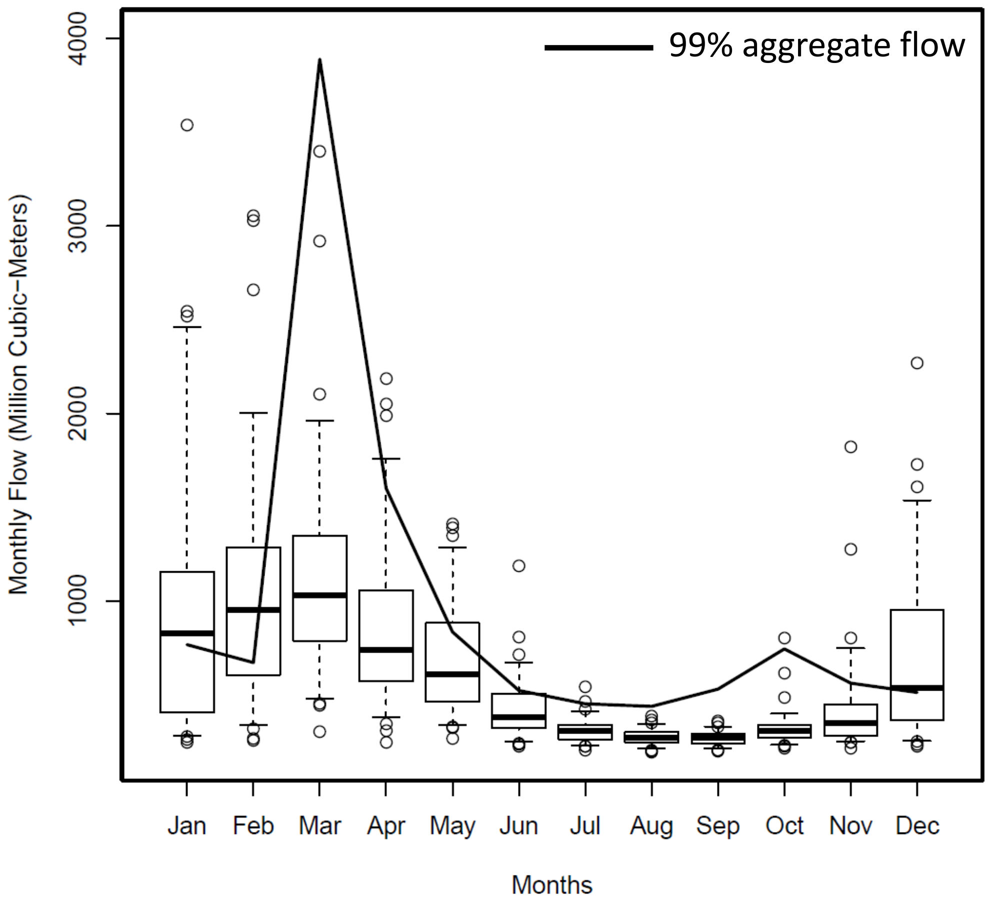

Figure 4. Extreme wet year (99th percentile flow) from 50 simulations of 61 year ensembles using weighting factor to preferentially select wet years from the historical record. Solid line represents percentile flow selection. Boxplots represent interquartile range of historical streamflow measurements.

The 1st percentile selection from 50 simulations of 61 year ensembles with preferential selection of dry annual streamflow values produced a year of extreme dryness well below the average inflow into Lake Shasta in a given year (Figure 5). The furthest deviation from the historical mean occurred again for the month of March where the streamflow was simulated at 5% of the historical mean streamflow.

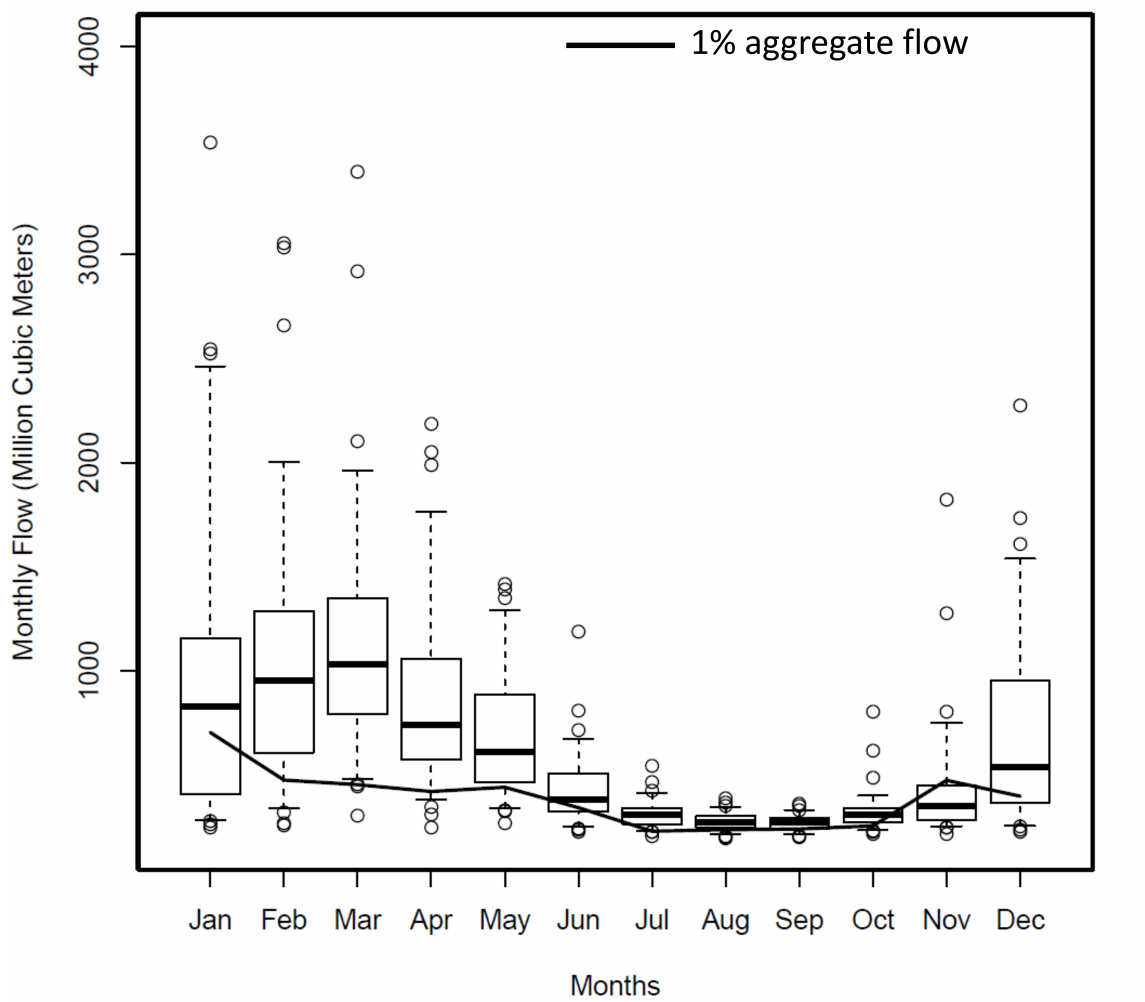

Figure 5. Extreme dry year (1st percentile flow) from 50 simulations of 61 year ensembles using weighting factor to preferentially select dry years from the historical record. Solid line represents percentile flow selection. Boxplots represent interquartile range of historical streamflow measurements.

The approach for generating weather and stream temperatures produced reasonable synthetic values as demonstrated by examining statistical analysis of results generated using the median synthetic streamflow year from 50 simulations of 61 year ensembles of the streamflow generator using random annual inflow selection (Figure 6 & Figure 7). It also generated reasonable inputs of cloud cover, wind speed, wind direction and dew point temperature (Appendix B). The meteorological inputs generated using a separate k-NN resampling of both the extreme wet and extreme dry years produced complementary weather years reflective of their respective inputs. Air temperatures produced for both the extreme wet year and the extreme dry year were well within the range of the historical record (*Figure 8*). In addition, daily average air temperatures of the extreme wet year were on average 0.27°C lower than the air temperatures of the extreme dry year with temperatures and 3.06°C lower during the simulated springtime flooding period of March.

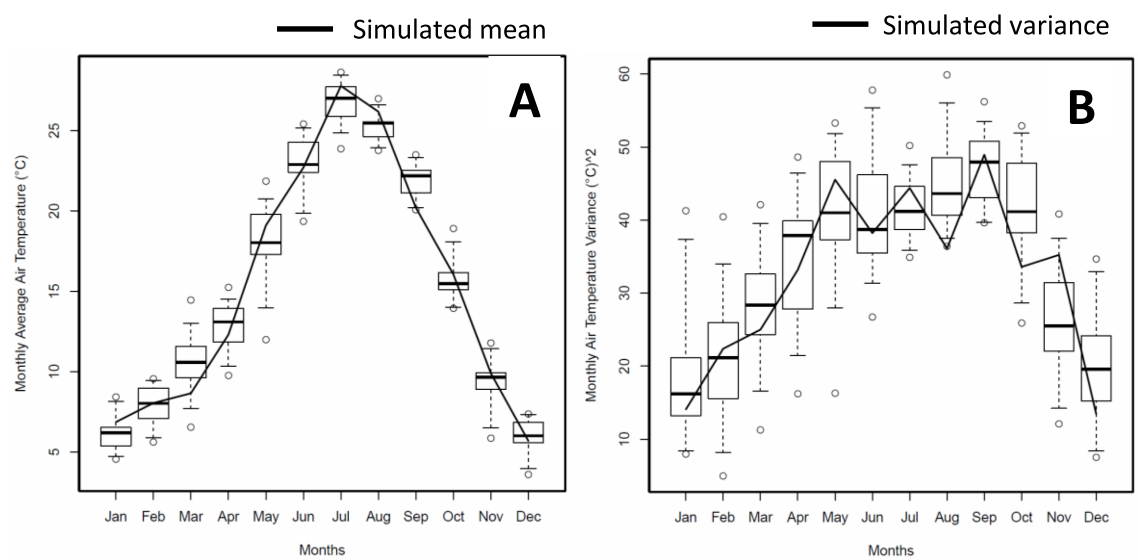

Figure 6. Statistical analysis of air temperature generation using median synthetic streamflow year as input from 50 simulations of 61 year ensembles of the streamflow generator using random annual inflow selection. Solid lines represent simulated statistics. Boxplots represent interquartile range of historical air temperature: (A) mean monthly air temperature; (B) mean monthly air temperature variance.

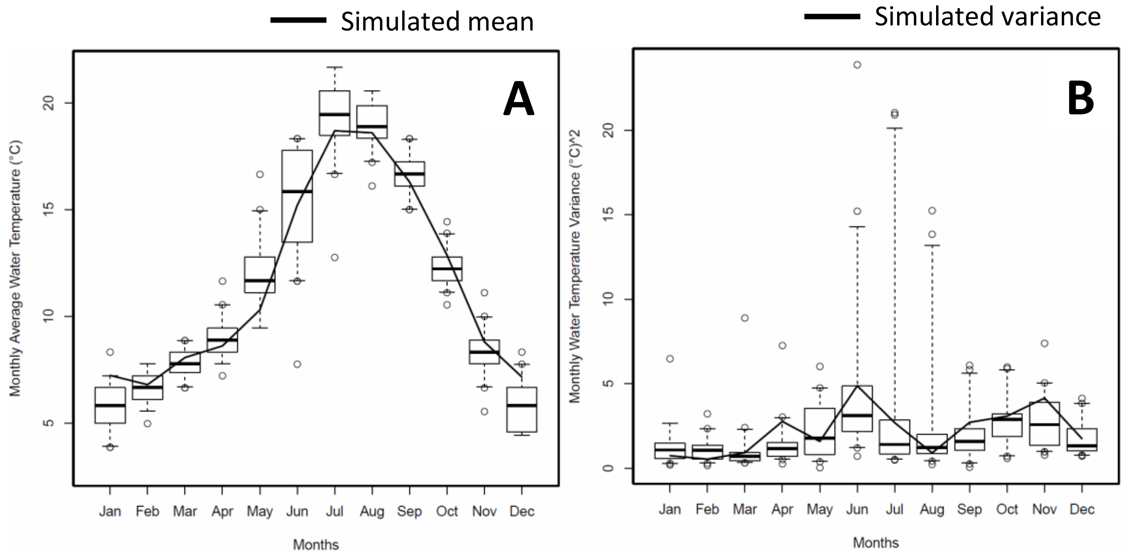

Figure 7. Statistical analysis of stream temperature generation using median synthetic streamflow year as input from 50 simulations of 61 year ensembles of the streamflow generator using random annual inflow selection. Solid lines represent simulated statistics. Boxplots represent interquartile range of historical stream temperature: (A) mean monthly stream temperature; (B) mean monthly stream temperature variance.

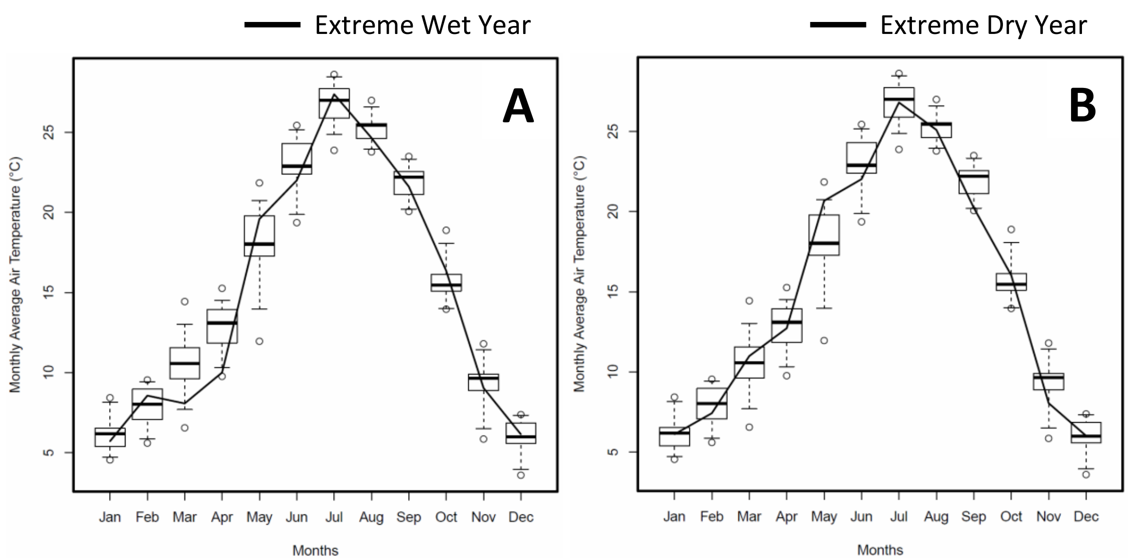

Figure 8. Mean daily air temperature of Shasta Lake generated using k-NN resampling of temporal disaggregation for (A) extreme wet year and (B) extreme dry year. Solid line represents simulated air temperature. Boxplots represent interquartile range of historical air temperature.

Another k-NN resampling of both the extreme wet and extreme dry years produced stream temperature values corresponding to their inputs. Stream temperatures produced for the extreme wet year and the extreme dry year matched the nature of the historical record (*Figure 9*). Stream temperatures produced for the extreme dry year are on average 0.32°C higher than the stream temperature for the extreme wet year. This difference was especially pronounced during the month of July where the average temperature difference was 1.78°C.

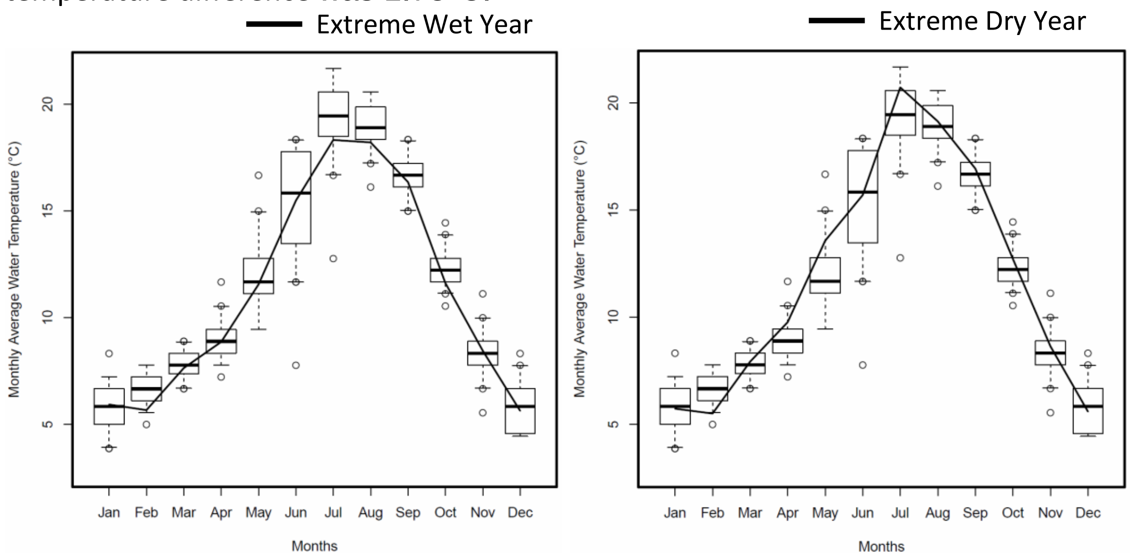

Figure 9. Mean daily stream temperature of the Sacramento River generated using k-NN resampling of spatial disaggregation for (A) extreme wet year and (B) extreme dry year. Solid line represents simulated stream temperature. Boxplots represent interquartile range of historical stream temperature.

Discussion

The extreme conditions created for input into the model offer reservoir managers and modelers the ability to assess reservoir operations under unprecedented hydrologic conditions without the investment in a large-scale watershed-based model. The nonparametric methods used in this study are non-intensive, computationally efficient methods that can be implemented with a limited dataset in a short timeframe.

One commonly cited drawback of nonparametric methods is that they restrict simulations of extremes because the vast majority of simulations in a nonparametric sampling will not generate extreme events (Srikanthan and McMahon 2001). We found that the percentile selections gravitated towards the mean as more simulations were conducted, so that when more than 100 simulations were conducted the 99th and 1st percentile flow selections were no longer selecting simulations with values beyond the historical record. However, extreme events can be generated by percentile selection of 50 to 100 simulations. Therefore, the generation of extreme events with percentile selection works best with a lower, yet still representative, number of simulations in the stochastic process.

The inputs created fulfilled the hydrologic and meteorologic inputs for a CE-QUAL-W2 model, a model capable of assessing operational changes in reservoir management to mitigate downstream water temperature risks. Many watersheds such as the Sacramento River in California are under stringent state and federal regulation to maintain downstream temperatures within a certain threshold for the protection of endangered and threatened species. With increased uncertainty in how climate change is likely to affect the ability of reservoir managers to maintain downstream temperatures within required thresholds, models such as these are useful in forecasting operational strategies. Our methods fulfilled all required inputs for such a model, and did it in a way that reflected the nature of the system while generating uncertain inputs beyond what has been seen in the historical record.

A major difficulty faced in generating realistic meteorologic inputs was creating a synthetic data set that had reasonable air temperature transitions from one day to the next. By selecting the k-NN using a Euclidian distance based on two dimensions (streamflow and air temperature), a synthetic dataset was produced that was within the variance of the historical record in a computationally efficient manner (*Figure 8*). Implementation of these methods can be useful for other situations of stochastic generation where the synthetic data set is unable to settle on a realistic solution when conditioned to only one parameter of the historical record.

The methods also proved versatile in creating realistic inputs with a limited set of data. The CDEC stream temperature data set was limited to 23 years, so only a handful of days in that record in a seven day window were useable in selecting stream temperature values similar to the stream magnitudes generated by the streamflow generator. Limiting the number of neighbors to choose from in the stochastic process was an effective strategy in creating realistic outputs (*Figure 9*).

A useful modification to the methods presented would be to create proportion vectors for the temporal disaggregation with sub-yearly malleability. For example, proportion vectors that can be adjusted for seasonal variability would allow for the stochastic generation of anomalous years such as one with a wet spring and a dry fall. The sub-yearly adjustable proportion vector could be applied to other input variables as well such as weather. Applying a weighted seasonal disaggregation to the weather inputs could be used to create unseasonable conditions such as a year with an abnormally hot fall period.

It would also be interesting to incorporate some aspects of climate change into the simulation of stochastic streamflows to model potential future impacts on the system. The incorporation of projected future flows, such as those developed by Vano et al. (2014) for the Colorado River, as an input dataset into stochastic streamflow generation would add to the robustness of the method and capture a further degree of uncertainty not included in the historical record. A future study that creates stochastically generated streamflows based on projected future streamflows to examine the effectiveness of downstream temperature control by reservoir operation in a watershed under those conditions would be a worthwhile investigation.

Conclusions

By implementing modifications to the methods of Nowak et al. (2010), realistic inputs of extreme hydrologic and climatic conditions were created. The inputs produced maintained the statistical nature of the system both spatially and temporally, and preserved relationships between inflows (*Figure 2*), weather (*Figure 8*) and stream temperatures (*Figure 9*). The generation of arrayed ensembles though multiple simulations was utilized to capture a greater amount of uncertainty in the system. The methods produced extreme inputs for the model beyond what has been measured in the historical record using preferential selection of wet and dry annual inflow values with subsequent selection of the 99th and 1st percentile flow of a simulated array (*Figure 4* & *Figure 5*).

CE-QUAL-W2 is a model capable of assessing operational changes in reservoir management to mitigate downstream water temperature risks. The extreme conditions created for input into the model offer reservoir managers and modelers the ability to assess the reservoir under unprecedented hydrologic conditions without the investment in a large-scale watershed-based model. This approach can be applied for other situations where computer simulated modeling of combined flow, temperature, and climate inputs are needed for analysis of uncertain events. The method could be improved upon by increasing the intra-annual variability in the synthetic hydrology.

Acknowledgements

Funding for this project was provided by the National Oceanic and Atmospheric Administration (NOAA SARP Award Number NA12OAR4310093). Workshops for interaction with reservoir managers were organized and administered by Derek Kauneckis of the University of Nevada Reno. Assistance with model output assessment was provided by Joel Hupp, Alexes Garrett and Helaine Berris, all of the University of Nevada Reno.

References

Apipattanavis S, Podesta G, Rajagopalan B, Katz R. 2007. A semiparametric multivariate and multisite weather generator. *Water Resources Research* 43: W03432.

Botsford LW and Brittnacher JG. 1998. Viability of Sacramento River Winter-Run Chinook Salmon. Conservation Biology, 12(1):65-79.

Cayan, DR., Kammerdiener SA, Dettinger MD, Caprio JM, and Peterson DH. 2001. Changes in the onset of spring in the western United States. Bull. Amer. Meteor. Soc., 82:399–415.

Cole TM, Wells SA. 2011. CE-QUAL-W2: a two-dimensional, laterally-averaged, hydrodynamic and water quality model, version 3.7. User manual. Instruction Report EL-11-1. Washington (DC): US Army Corps of Engineers.

Hanna RB, Saito L, Bartholow JM, Sandelin J. 1999. Results of simulated temperature control device operations on in-reservoir and discharge water temperatures using CEQUAL-W2. Lake Reserv Manage 15(2):87-102.

Lall, U, and Sharma A (1996), A Nearest Neighbor Bootstrap For Resampling Hydrologic Time Series, Water Resour. Res., 32(3), 679–693

Mote PW, Hamlet AF, Clark MP, Lettenmaier DP. 2005. Declining mountain snowpack in western north America. American Meteorlogical Society, 86(1):39-49.

Nowak K, Rajagopalan B, Prairie J. 2010. A non-parametric stochastic approach for multisite disaggregation of annual to daily streamflow. *Water Resources Research* 46:W08529.

Prairie J, Rajagopalan B, Lall U, Fulp T. 2007. A stochastic nonparametric technique for space-time disaggregation of streamflows. Water Resources Research 43: W03432.

PRISM Climate Group, Oregon State University, http://prismmap.nacse.org/nn/, accessed 6/17/14.

Saito L. 1999. Interdisciplinary modeling at Shasta Lake. Fort Collins: Colorado State University. 341 p. [Ph.D. dissertation]

Saito L, Johnson BM, Bartholow J, Hanna RB. 2001. Assessing ecosystem effects of reservoir operations using food web-energy transfer and water quality models. Ecosystems 4:105-125.

Stewart IT, Cayan DR, Dettinger MD. 2004. Changes in snowmelt runoff timing in western north American under a ‘business as usual’ climate change scenario. Climate Change, 62:217-232.

Srikanthan R. and McMahon TA. 2001. Stochastic generation of annual, monthly and daily climate data: A review. Hydrology and Earth Systems Sciences, 5(4):653-670.

Tarboton DG, Sharma A, and Lall U. 1998. Disaggregation procedures for stochastic hydrology based on nonparametric density estimation, Water Resources Research, 34(1):107-119.

[USBR] US Department of the Interior, Bureau of Reclamation. 2011. Fisheries and Aquatic Ecosystems Technical Report. Shasta Lake Water Resources Investigation. Sacramento: US Department of the Interior, Bureau of Reclamation, Mid-Pacific Region.

[USFWS] US Fish and Wildlife Service. Environmental Conservation Online system. Accessed 2/10/2014. http://www.fws.gov/endangered/

Vano, Julie A., and Coauthors, 2014: Understanding Uncertainties in Future Colorado River Streamflow. Bull. Amer. Meteor. Soc., 95, 59–78.

Chapter 3: Reservoir Operations and Extreme Hydrologic and Climatic Conditions: Impacts on Fish Sustainability below Shasta Lake

[1]Joseph Sapin, [2]Laurel Saito, [3]Balaji Rajagopalan, [4]Derek Kauneckis, [5]Blair Hanna, [6]Arthur Dai

[1]Graduate Research Assistant
Graduate Program of Hydrologic Sciences
University of Nevada – Reno, Mail Stop 186
Reno, NV, USA 89577

[2]Associate Professor
Department of Natural Resources and Environmental Science
University of Nevada – Reno, Mail Stop 186
Reno, NV, USA 89577

[3] Professor
Department of Civil, Environmental and Architectural Engineering
University of Colorado – Boulder, Campus Box 428
Boulder, CO, USA 80309

[4]Associate Professor
Department of Political Science
University of Nevada – Reno, Mail Stop 302
Reno, NV, USA 89577

[5]Consultant
Water and Earth Technologies, Inc.,
1225 Red Cedar Circle, Fort Collins CO, 80524

[6]Undergraduate Research Assistant
University of Arizona, Tucson
Tucson, AZ, USA 85721

Abstract

Since the construction of Shasta Dam on the Sacramento River in 1945, Chinook salmon have been prevented from reaching their natural cold-water habitat for spawning. In 1997 the US Bureau of Reclamation began operating a temperature control device on Shasta Dam that enabled selective withdrawal of reservoir outflows for downstream temperature control without sacrificing power generation. However, there are concerns about the ability of the temperature control device to be as effective in uncertain and future hydroclimate conditions. We investigated this issue by combining stochastic inflow generation with two-dimensional hydrodynamic modeling of reservoir operations and interactions with reservoir managers to examine the ability of the temperature control device to meet downstream temperature objectives under extreme and uncertain hydroclimatic conditions. The stochastically generated inputs produced unprecedented circumstances that have not been observed in the historical record. We examined the synthetic outflows from calendar year CE-QUAL-W2 simulations for their ability to meet downstream temperature targets, and the tradeoffs of late season in-reservoir cold water pool reserve. The results suggest that selective withdrawal schedules with the TCD device reduce exceedances of outflow temperatures overall compared to more traditional dam operations such as all-out-the-bottom and all-out-the-uppermost elevations. A generalized operations schedule was also shown to minimize the drawdown tradeoff of the cold water pool in meeting these temperature objectives.

Introduction

The Chinook salmon, also known as King salmon, were once the most abundant salmon species in the Central Valley Region of California (Yoshiyama et al. 1998). They are an important commercial fishing species, especially for the Sacramento River where the first commercial salmon hatchery in the United States was established (McGinnis 1984). Winter-run Chinook once spawned during summer in cold water of Sacramento River tributaries supplied by snowmelt of Mount Shasta. However, after construction of numerous dams in the Sacramento River watershed, including Shasta Dam, salmon populations declined significantly, and in 1989 the winter-run Chinook salmon were listed as a protected species under federal and California State Endangered Species Acts. The list status was changed to endangered in 1994 (Saito et al. 2001).

Shasta Reservoir is now operated to artificially create cold water habitat downstream of the dam to promote salmon spawning where it did not naturally occur before dam construction (Yates et al. 2008). Reservoir operations are also affected because the Biological Opinion for the Sacramento River recommends the release of cold water in summer and fall to reduce salmon mortality (Hanna et al. 1999). The critical period for spawning and egg survival for winter-run Chinook salmon is September and October where being over the temperature target by only 2°C could prove detrimental for spawning and egg survival (Kilgour et al. 1985). Because of this, biological criteria for the health of the salmon have been developed and downstream temperature targets are enforced by the State of California.

To enable more effective downstream temperature control for fish propagation while maximizing hydropower generation, a temperature control device (TCD) was installed on Shasta Dam and began operating in 1997 (Hanna et al. 1999). Before TCD installation, selective withdrawal to meet downstream temperature targets occurred through fixed outlets. The highest elevation outlet was at 281 meters (922 feet) and the lowest elevation outlet was at 220 meters (720 feet; Bartholow et al. 2001). Operation of the reservoir for temperature targets led to releases that bypassed the penstocks to the power plant, resulting in an estimated $63 million in lost power generation (Hanna et al. 1999). Installation of the TCD allowed water taken from different elevations in the reservoir to be run through the penstocks to generate hydropower. It was also possible to withdraw water from lower elevations than before TCD installation (Hanna et al. 1999). Simulations by Hanna et al. (1999) and Bartholow et al. (2001) indicated TCD operations reduced exceedances of downstream temperature targets in the fall and throughout the year.

Climate change may affect the ability of using reservoir operations to manage downstream temperatures, particularly increases in winter and springtime temperatures (Cayan et al. 2001). Temperatures are estimated to increase by 2.8 to 8.6 °C in the San Joaquin / Sacramento Basin over the next century depending on emissions levels (USBR 2011b; California Climate Change Center 2012). Spring snowpack in northern California is highly sensitive to temperature change, and has reduced by more than 50% on average since 1950 (Mote et al. 2005). Warming temperatures increase the likelihood for early spring snowmelt runoff and thereby increase the hazard for winter and springtime flooding. It can also prolong the timespan of a summer drought (Stewart et al. 2004).

Reservoir managers are also required to follow the Operations Criteria and Plan (OCAP) for the Central Valley Project and the State Water Project (USBR 1997; USBR 2008). The OCAP includes operational guidelines for reservoir and river management that are consistent with applicable laws and sensitive to impacts on listed species and designated critical habitat. These operational guidelines include water temperature requirements specific to the life history and sustainability of Chinook salmon on the Sacramento River. Managers are required to uphold the State Water Resources Control Board Water Rights Order 90-5 (SWRCG WRO 90-5) that requires downstream temperature control for winter-run salmon “to the extent controllable” (USBR 2008). SWRCG WRO 90-5 sets a downstream chronic temperature threshold standard of 13.3°C (56°F) that results in fines if exceeded for 72 hours or more and an acute temperature threshold standard of 13.6°C (56.5°F) that results in fines anytime it is exceeded.

One way to examine the ability to meet downstream temperature needs of the Chinook salmon on the Sacramento River is through modeling. A model capable of simulating TCD operations on Shasta Lake is CE-QUAL-W2 (W2). W2 is a two-dimensional hydrodynamic and water quality model distributed by the U.S. Army Corp of Engineers (USACE; Cole and Wells 2011). The W2 model for Lake Shasta was calibrated to measured water temperature data collected by the USGS throughout the reservoir in 1995 (Hanna et al. 1999). The model was also used to evaluate ecosystem impacts of selective withdrawal (Saito et al. 2001).

The primary research objective of this study was to examine the downstream temperature effects of outflow operations at Shasta Lake under extreme hydrologic and climatic conditions, and the effects of these operations on sustainability of the winter-run Chinook salmon population on the Sacramento River. To achieve this, our methodology consisted of a three part process. Because the use of the historic record as modeling input may not be adequate to address the climatic and hydrologic uncertainties associated with climate change, we first developed extreme hydrologic and climatic conditions for input into the Shasta W2 model using modified stochastic methods of Nowak et al. (2010). Nowak et al. (2010) developed a nonparametric, stochastic method that is capable of creating synthetic datasets from the historical record that are outside the range of the historical record yet still maintain the nature of the system. Completion of the first step using stochastic approaches to generate model inputs based on the historical record is described in detail in chapter two. The next steps involved simulation of Shasta Dam TCD operations in W2 and analysis of modeled outflow results in regards to meeting downstream and in-reservoir water temperature objectives and are the focus of the current chapter.

Methods

Site Description

Located 16 km (10 miles) north of Redding on the Sacramento River (Figure 10), Shasta Lake is the largest storage reservoir in California with a surface area of 119 square kilometers (29,500 acres), a maximum depth of 157 meters (515 feet), and a storage capacity of over 5,550 million cubic meters (4.5 million acre feet; Higgs and Vermeyen 1999). Shasta Lake stores and releases water for uses that include irrigation, navigation control, fish conservation, municipal and industrial use, and protection of the Sacramento-San Joaquin Delta from saltwater intrusion. Inflows to the reservoir are primarily from four tributaries: the Sacramento River, the McCloud River, the Pitt River, and Squaw Creek. The reservoir also supports an excellent fishery of both cold water and warm water species. On the far shore of the Sacramento River below Shasta Dam is the Livingston Stone Fish Hatchery, which is involved in fish culture related to winter-run Chinook salmon recovery (USBR 2011a).

Shasta Dam has a maximum outflow capacity of 5,267 m^3/s (186,000 ft^3/s). There are 18 outlets on the face of the dam, each 2.4 m (7.9 ft) in diameter. The power plant below the dam has 5 penstocks carrying water from the dam with an installed capacity over ½ million kilowatts (USBR 2012). Water is usually run through the 5 penstocks of the hydroelectric plant which has a maximum capacity of 498 m^3/s (17,500 ft^3/s; Higgs and Vermeyen 1999).

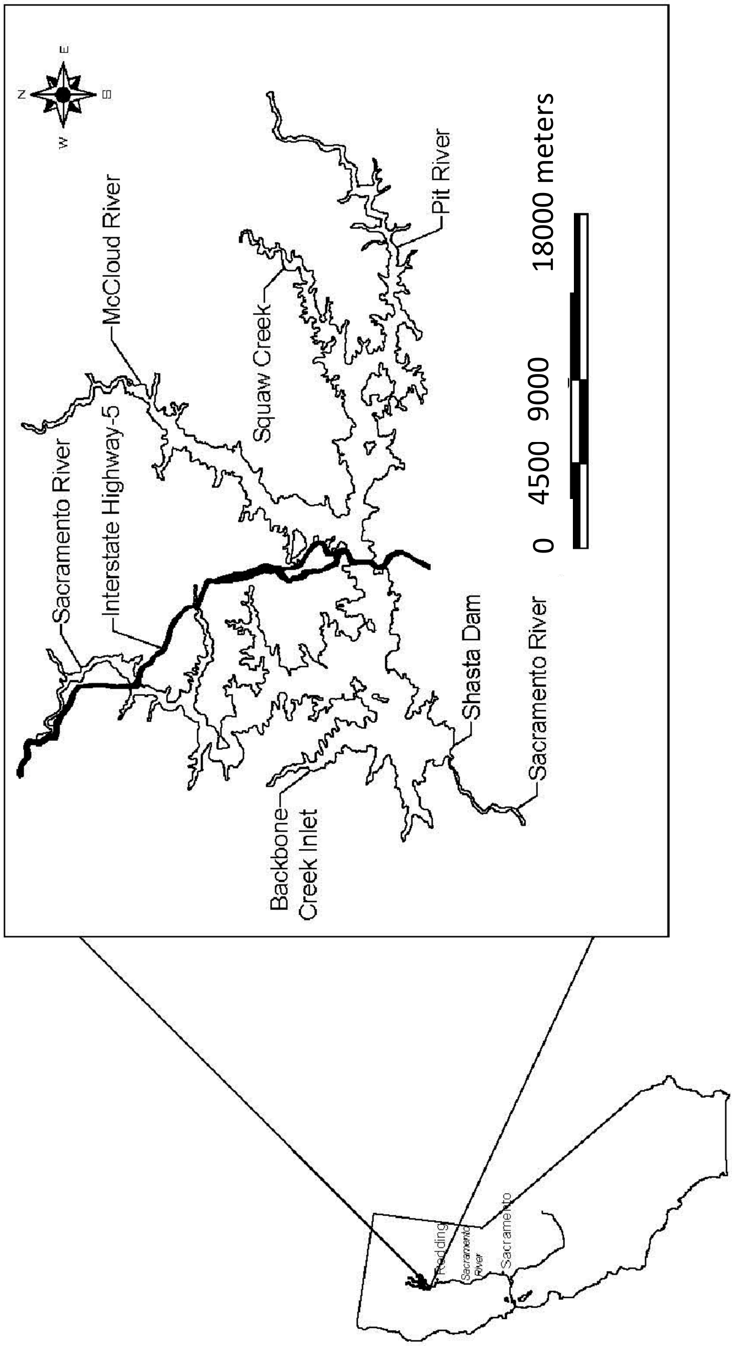

Figure 10. Shasta Dam, reservoir and tributaries.

Data for Modeling Inputs

To assess the ability of using TCD operations to meet temperature guidelines we developed calendar-year simulations that required daily inputs of inflows, inflow temperatures and outflows to W2. To capture diurnal variations in meteorology we used subdaily inputs of meteorology. W2 also required a starting day water surface elevation. Data for stochastic generation of synthetic data for W2 inputs were obtained from the US Geological Survey, the California Data Exchange Center, the National Oceanic and Atmospheric Administration and the US Bureau of Reclamation (Table 2):

Table 2. Sources of data for stochastic input generation

Data Type	Period of Record	Source
Streamflow[a] USGS stations at McCloud River (11368000), Pit River (11365000), Sacramento River (11342000), and Squaw Creek (11365500)	10/1/1944 – 9/30/2011	USGS[b]
Stream Temperature[c] CDEC stations at McCloud River (MSS), Pit River (PMN), and Sacramento River (DLT)	11/1/89 – 9/13/2012	CDEC[d]
Air Temperature, Relative Humidity, Wind Speed, Wind Direction, Cloud Cover NOAA AWS 725920 Redding Municipal Airport	1/1/1994 – 12/31/2010	NOAA[e]
Computed Daily Inflow, Reservoir Storage, Reservoir Elevation, Outlet Release USBR operations data at Shasta Lake, CA	1/1/1944 – 12/31/2010	USBR[f]

a. Squaw Creek (USGS station 1365500; representing ~2% of total lake inflow) record of streamflow ends in 1966. Later flows assumed to be 2.1% of total inflows based on historical proportions.
b. US Geological Survey (USGS) - http://waterdata.usgs.gov/ca/nwis/
c. McCloud River stream temperatures were used for Squaw Creek because Squaw Creek stream temperatures were not available.
d. California Data Exchange Center (CDEC) - http://cdec.water.ca.gov/
e. National Oceanic and Atmospheric Administration (NOAA) - http://www.ncdc.noaa.gov/
f. US Bureau of Reclamation (USBR); computed daily inflows represent total inflows to the reservoir after adjustment for precipitation and evaporation.

Stochastic Input Generation

Stochastic inputs of streamflow quantities, temperatures and site meteorology for the W2 model were generated using a k-nearest neighbor (k-NN) bootstrap resampling approach modified from the methods of Nowak et al. (2010). Percentile selection of stochastically generated streamflow was used to generate years of extreme hydrologic conditions, such as an extreme wet year and an extreme dry year. Corresponding stream temperatures and weather were then stochastically generated based on the magnitude of incoming streamflow. The stochastic methods produced streamflows outside the range of the historical record while still maintaining the statistical nature of the system. A full description of the stochastic methods and data used to generate the W2 inputs is provided in chapter two.

Conditions of increasing air temperatures under climate change were also modeled for each of the scenarios. Two ranges of projected average temperature increase by 2100 to the San Joaquin / Sacramento Basin based on emissions were presented in California Climate Change Center (2012). We used their estimates of future air temperature for high emissions (4.6 – 8.6 °C) and low emissions (2.8 – 6.0 °C) to set up climate change scenarios by increasing air temperatures for extreme wet or dry scenarios (*Table 3*). These temperature increase predictions correspond to what the USBR submitted in a 2011 report to Congress (USBR 2011b). Temperature increases were applied to the air temperatures for the 15th of each month and linearly interpolated for days in between.

Table 3. Monthly air temperature increases (°C) for the high and low emissions scenarios.

Scenario	Jan	Feb	Mar	April	May	June	July	Aug	Sept	Oct	Nov	Dec
Low emissions	2.8	3	3.5	4.5	5.5	6	6	6	5.5	4.5	3.5	3
High emissions	4.6	5	5.5	6.5	7.5	8	8.6	8	7.5	6.5	5.5	5

We also collaborated with reservoir managers to develop modeling scenarios of most concern to them. The managers suggested modeling scenarios of multi-year drought and unanticipated fall conditions (i.e., wet year with dry fall or wet year with warm fall). A two-year drought scenario was developed by repeating inputs of the extreme dry year for an additional year. A wet year with a dry "fall" was created by combining the first 145 Julian days of the stochastically generated streamflows of the extreme wet year with the remaining days of the extreme dry year. Julian day 145 was chosen because there is a streamflow cross-over point for the inflow hydrographs of the stochastically generated scenarios (*Figure 11*), and minimal alteration of the stochastically generated hydrographs is desirable since they replicate the statistical nature of the system (chapter two). A wet year with a warm fall was developed by forcing the high emissions temperature increases for the extreme wet year onto the meteorology of the extreme wet year for the critical salmon rearing months of September and October. The scenarios chosen for modeling are listed in Table 4.

Table 4. Stochastically generated scenarios for modeling in CE-QUAL-W2

Scenario #	Description
1	Extreme wet year
2	Extreme dry year
3	Extreme wet year with a dry fall
4	Extreme wet year with a warm fall
5	Extreme wet year with low emissions climate change
6	Extreme wet year with high emissions climate change
7	Extreme dry year with low emissions climate change
8	Extreme dry year with high emissions climate change
9	Two year drought

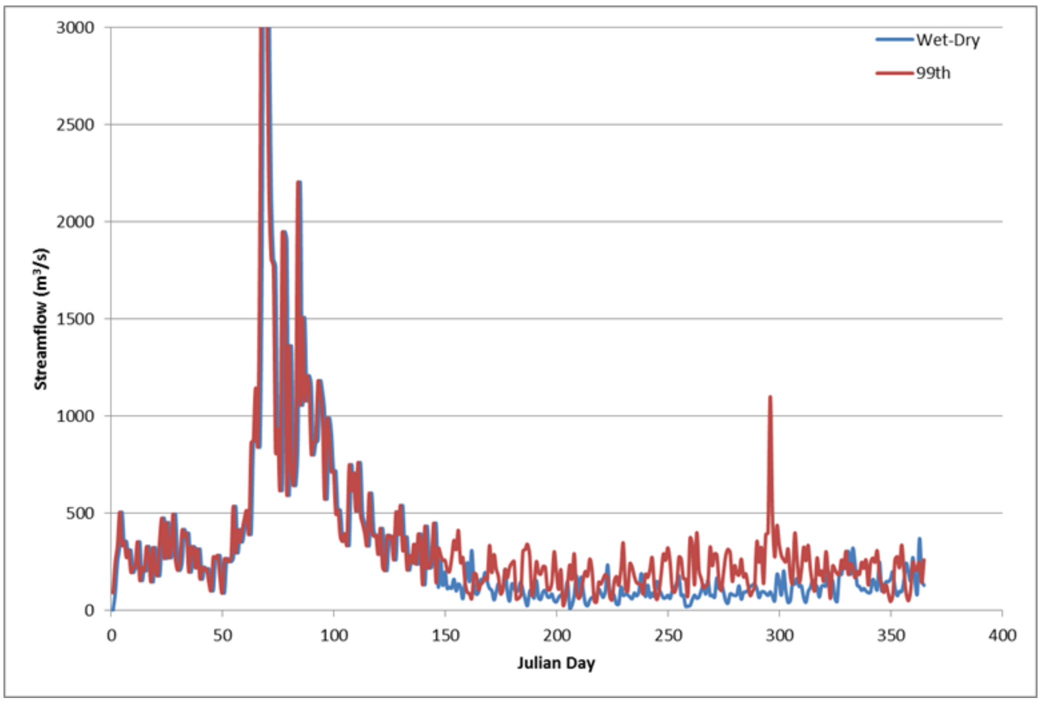

Figure 11. Comparative streamflow hydrographs showing the separation of the wet year with a dry fall from the extreme wet year.

CE-QUAL-W2 Setup

The W2 model of Shasta Lake described in Bartholow et al. (2001) and Hanna et al. (1999) was upgraded to version 3.7 and recalibrated to 1995 data. Calibrated parameters (Table 5) resulted in an average R^2 of 0.966 and average root mean squared error (RMSE) of 0.947°C for 931 observations. Unless stated otherwise, all boundary conditions of the W2 model were the same as in Hanna et al. (1999). W2 requires a starting day surface elevation that we based on a calendar year stochastically selected from the historical record that was used for daily streamflow disaggregation (chapter two).

Table 5. Calibrated values for the W2 model: *wind sheltering coefficient (WSC), coefficient of bottom heat exchange (CBHE), temperature of the sediments (TSED) and light extinction coefficients (EXH20 and BETA).*

WSC	CBHE ($m^{0.5}sec^{-1}$)	TSED (°C)	EXH20 (m^{-1})	BETA
1.0	7.0 E-8	15.9	0.40	0.45

Outflow Generation

Outflows were based on the storage of the year selected for daily streamflow values from the historical record, where the outflows were the difference of incoming streamflow from the storage curve. Adjustments were made to the raw output of synthetic outflows to match OCAP guidelines (*Table 6*; USBR 2008).

Table 6. Adjustments to initial estimates of synthetic outflows to meet OCAP guidelines.

Minimum Outflow	90 m^3/s (3,180 cfs)
Maximum Outflow	2237 m^3/s (79,000 cfs)
Minimum Submergence of Active TCD Gate	10.7 m (35 ft) above bottom of gate for elevations 219.5, 249.3 and 281.3 m. 6.1 m (20 ft) above bottom of gate for elevation 311.5 m

The daily rate of outflow change was also set to a maximum of 15% higher or lower than the previous simulated day. This value was chosen as an appropriate daily interpretation for the average of the integrated seasonal OCAP requirements for hourly ramping restrictions of outflow at Shasta Lake (USBR 2008).

Modeled TCD Operations

Three separate calendar year schedules of TCD operation were modeled for each scenario. The first was to run all release water out of the lowest elevation TCD gate (219.5 m). The second was to run all release water out of the highest TCD gate possible without violating minimum submergence criteria of an active TCD gate (*Table 6*). The third was a generalized TCD operations schedule used in Hanna et al. (1999; *Table 7*), with adjustments made to satisfy gate submergence criteria. For the two year drought, the generalized operations schedule was run for the first simulated year and then varied to the bottom, uppermost and generalized operations as appropriate for the TCD operations schedule of interest for the second year.

Table 7. Generalized TCD operations schedule by Julian Day based on Hanna et al. (1999)

Start day	**End day**	**Gate Elevation (m)**
0	120	311.5
121	181	281.3
182	243	249.3
244	334	219.5
335	365	311.5

Downstream Temperature Control Assessment

An assessment of outflow temperatures was conducted to examine if TCD operations at Shasta Lake can assist with meeting federally mandated monthly downstream temperature targets for Chinook salmon on the Sacramento River in California under the scenario conditions. The temperature targets used were those from Hanna et al. (1999; Table 8) that are based on OCAP guidelines for the tail waters of Shasta Lake (USBR 1997).

Degree-days were calculated as a metric for how well simulated operations of Shasta Dam TCD can meet these downstream temperature requirements. Degree-days measure both the degrees above the target temperature and the number of days over the target temperature. For example, both one degree above a target temperature for two days and two degrees above the target temperature for one day would result in a calculation of two degree days above the target temperature. The sums of degree-days over the temperature target between May 1 and December 1 (Julian days 121 – 335) for each scenario using each TCD schedule were determined. The sum of degree-days over the acute temperature (13.6 °C) standard and the chronic temperature standard (13.3 °C) throughout the calendar year were estimated as well.

Table 8. Release temperature targets to be used in the simulation of Shasta's temperature control device (Hanna et al. 1999).

Month	**Target Temperature (°C)**	**Additional Criteria**
January	13.9	Or as warm as possible
February	13.9	Or as warm as possible
March	12.8	Or as warm as possible
April	12.8	
May	8.3	
June	8.3	
July	8.3	
August	8.3	
September	10.0	
October	11.1	
November	10.0	
December	10.0	Or as warm as possible

Cold Water Pool Reserve Assessment

To analyze the ability of TCD operations to maintain a reserve of in-reservoir cold water, the volume of water in the reservoir at or below the desirable hatching temperature for Chinook salmon (12.8 °C; USBR 2008) was calculated weekly for each calendar year simulation. The elevation of water at or below the cold pool threshold temperature was evaluated at the model segment at the dam face. That elevation was assumed to be representative of the cold pool elevation throughout the reservoir, and the in-reservoir cold pool storage volume was calculated. The volume and Julian day of the maximum cold water pool and the minimum cold water pool were determined. The volume of the May 28th (Julian day 148) and November 1st (Julian day 302) cold water pool were also calculated.

Tradeoff Assessment

Tradeoffs in satisfying the two management objectives of meeting downstream temperature targets and maintaining the in-reservoir cold water pool were examined. The 1-Nov cold water pool reserve was plotted against the degree day exceedances for each scenario for each TCD schedule.

Results

A daily time series of simulated outflow temperature output from W2 is presented for the extreme dry year (*Figure 12*) and the extreme wet year (*Figure 13*). Each figure shows the performance of the TCD schedules in maintaining, or not maintaining, an outflow temperature that is below the chronic, acute and daily temperature target thresholds between May 1 and December 1 (Julian days 121 – 335). Sharp drops in outflow temperature (for example at day 229 for the all-out-the-uppermost TCD schedule for the extreme dry year; *Figure 12*) are due to changes in gate elevation for withdrawals for the all-out-the-uppermost TCD schedule. This drop is a result of moving the gate elevation to avoid a violation in the OCAP submergence criteria. Similar plots for the other W2 scenarios in Appendix C.

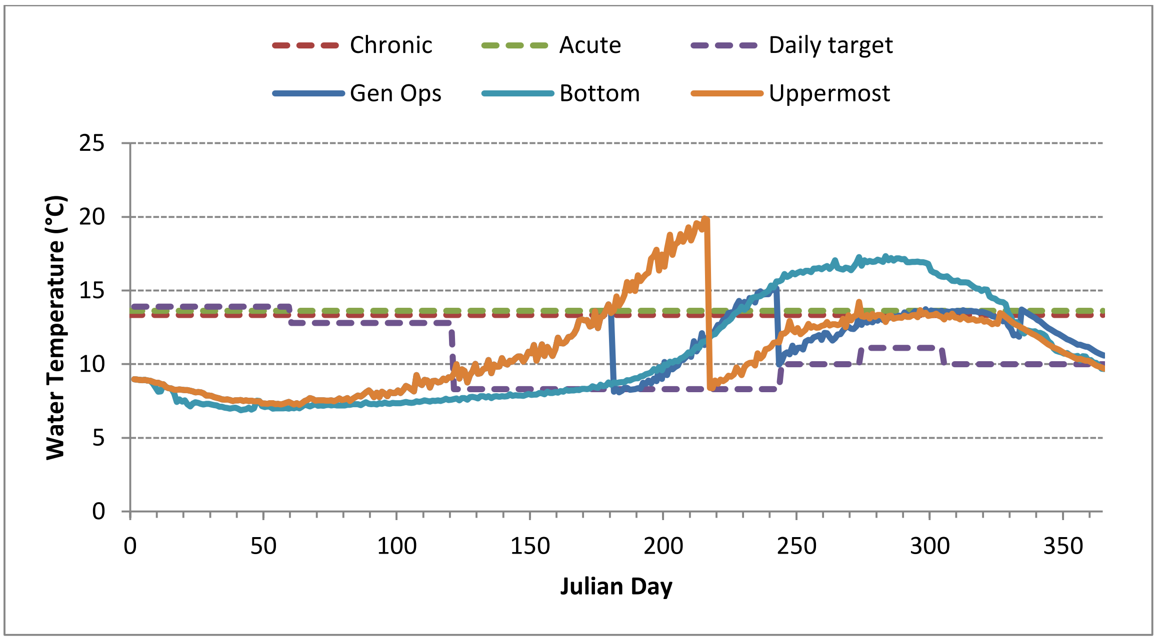

Figure 12. W2 simulated outflow temperatures for the extreme dry year. Solid lines are outflow temperatures for the extreme dry year for each TCD schedule (bottom, uppermost and generalized operations). Dashed lines are the water temperature threshold standards (acute and chronic) and the outlet temperature targets.

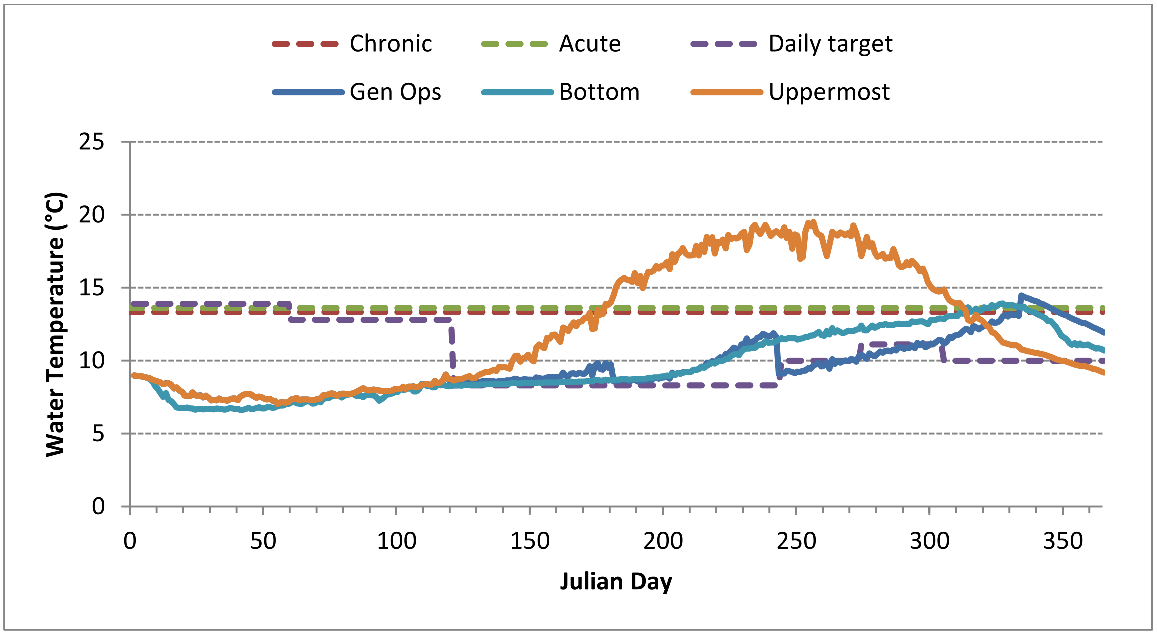

Figure 13. W2 simulated outflow temperatures for the extreme wet year. Solid lines are outflow temperatures for the extreme dry year for each TCD schedule (bottom, uppermost and generalized operations). Dashed lines are the water temperature threshold standards (acute and chronic) and the outlet temperature targets.

Analysis of downstream temperature control of the TCD schedules for the four calendar year non-climate change scenarios (*Table 9*) indicated that the all-out-the-bottom TCD schedule performed best for minimizing degree-day exceedances above the chronic and acute standard for the extreme wet year, wet year with a dry fall and the wet year with a warm fall. The wet year with a dry fall had a larger impact on downstream temperature performance on the all-out-the-uppermost and generalized operations TCD schedules than the wet year with a warm fall when compared to the extreme wet year. However, the wet year with a warm fall had a larger impact on the all-out-the-bottom TCD schedule performance than the wet year with a dry fall. The generalized operations TCD schedule performed best in minimizing degree-day exceedances for the temperature target thresholds for all four scenarios as well as the chronic and acute temperature standards for the extreme dry year. One will notice that the generalized and all out-the-bottom operations for the extreme dry year had degree-day exceedances that were more than two times greater than exceedances for the extreme wet year. The all-out-the-uppermost schedule for the extreme wet year, however, had more exceedances than for the extreme dry year.

*Table 9. Degree-day exceedance results (°C x days) rounded to the nearest integer organized by scenario, temperature threshold standard and TCD operations schedule. The best performing TCD schedule for each temperature standard for each scenario is bolded. "Bottom" is the all-out-the-bottom TCD schedule, "Uppermost" is the all-out-the-uppermost TCD schedule and "Gen Ops" is the generalized operations TCD schedule (*Table 8*).*

Scenario	**Standard**	**TCD Schedule**		
		Bottom	Uppermost	Gen Ops
Extreme Wet Year	Chronic	**8**	517	9
	Acute	**2**	479	5
	Temp Target	304	1223	**205**
Extreme Dry Year	Chronic	266	139	**29**
	Acute	238	127	**16**
	Temp Target	721	761	**572**
Wet Year with Dry Fall	Chronic	**7**	522	27
	Acute	**2**	484	18
	Temp Target	280	1223	**258**
Wet Year with Warm Fall	Chronic	**12**	598	20
	Acute	**5**	558	14
	Temp Target	305	1317	**210**

Degree-day impacts of the addition of a dry fall to the wet year (*Figure 14*) show that the generalized operations schedule was most affected by the addition of a dry fall, and the ability of the all-out-the-bottom schedule was also slightly impacted. The all-out-the-uppermost schedule, on the other hand, was not greatly impacted by the addition of a dry fall. The addition of a warm fall to the extreme wet year also affected degree-day performance compared to the extreme wet year, but in different ways (*Figure 15*). The generalized operations schedule was less affected by the addition of a warm fall, but the all-out-the-uppermost was much more impacted by the addition of a warm fall. The all-out-the-bottom schedule was minimally affected by the addition of a warm fall.

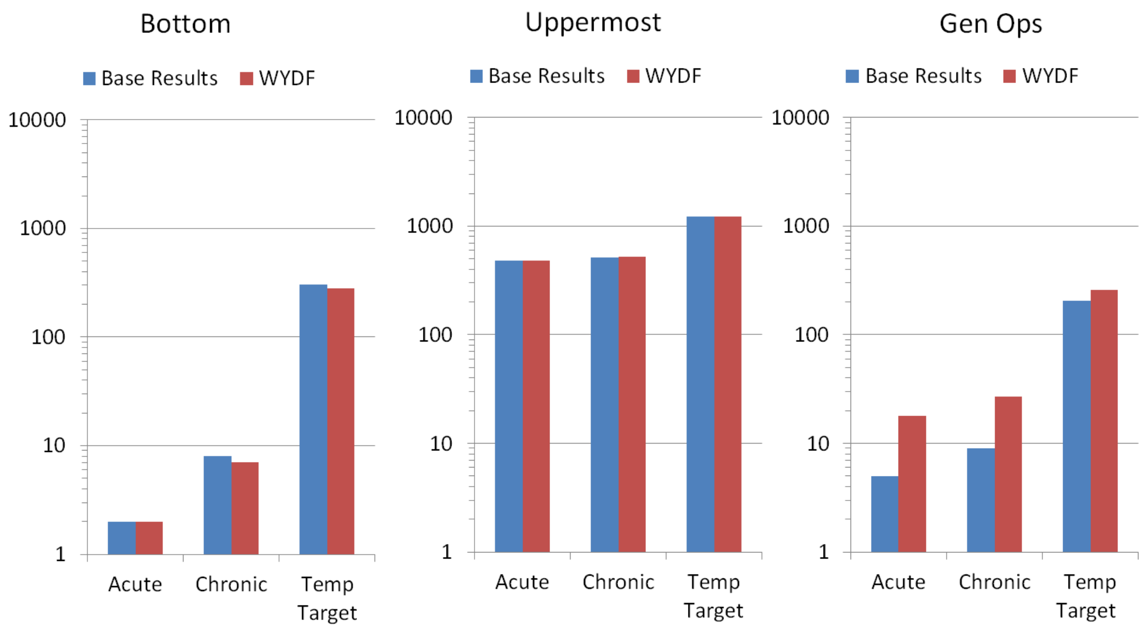

*Figure 14. Degree-day exceedances (°C x days) for the wet year with a dry fall (WYDF) compared to the extreme wet year (Base Results). "Bottom" is the all-out-the-bottom TCD schedule, "Uppermost" is the all-out-the-uppermost TCD schedule and "Gen Ops" is the generalized operations TCD schedule (*Table 8*).*

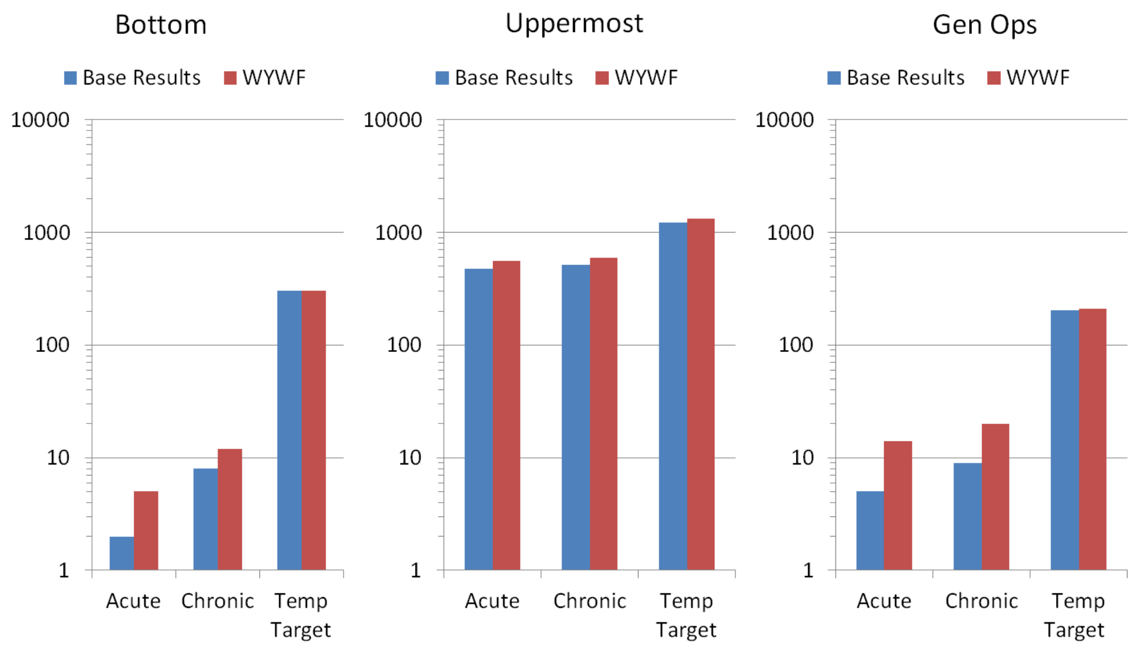

*Figure 15. Degree-day exceedances (°C x days) for the wet year with a warm fall (WYWF) compared to the extreme wet year (Base Results). "Bottom" is the all-out-the-bottom TCD schedule, "Uppermost" is the all-out-the-uppermost TCD schedule and "Gen Ops" is the generalized operations TCD schedule (*Table 8*).*

With climate change, degree day exceedances increased dramatically for both the extreme wet and extreme dry years (Appendix D), and the generalized operations TCD schedule minimized the degree-day exceedances over all three temperature standards for both scenarios. For the extreme wet year when low emissions and high emissions temperature increases are applied to the model, the degree-day exceedances increased more for the all-out-the-uppermost and all-out-the-bottom TCD schedules than for the generalized operations (*Figure 16*). The impacts of low emissions and high emissions temperature increases for the extreme dry year were very similar in the exceedance trends described for the extreme wet year (*Figure 17*). Again, degree-day exceedances were lower for the extreme wet year for the all-out-the-bottom and generalized operations TCD schedules, but were higher for the all-out-the-uppermost TCD schedule than for the wet year without climate change scenarios.

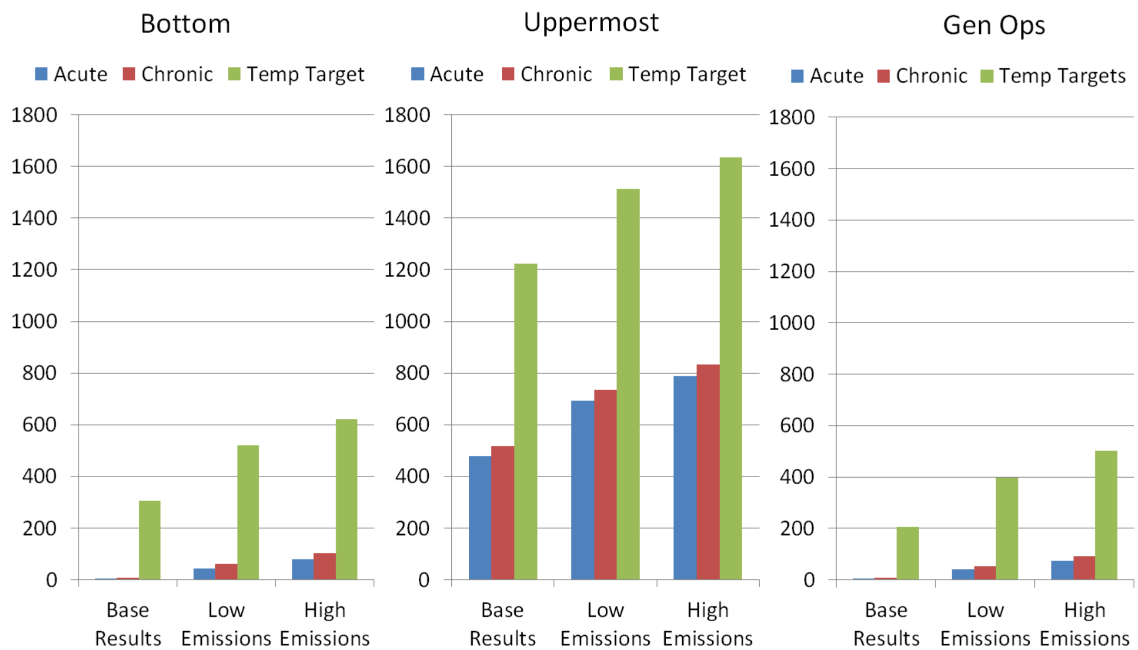

Figure 16. Climate change degree-day exceedances (°C x days) for the wet year "Base Results" in log scale for each TCD schedule compared to model runs where low emissions and high emissions temperature increases are applied, respectively. "Bottom" is the all-out-the-bottom TCD schedule, "Uppermost" is the all-out-the-uppermost TCD schedule and "Gen Ops" is the generalized operations TCD schedule.

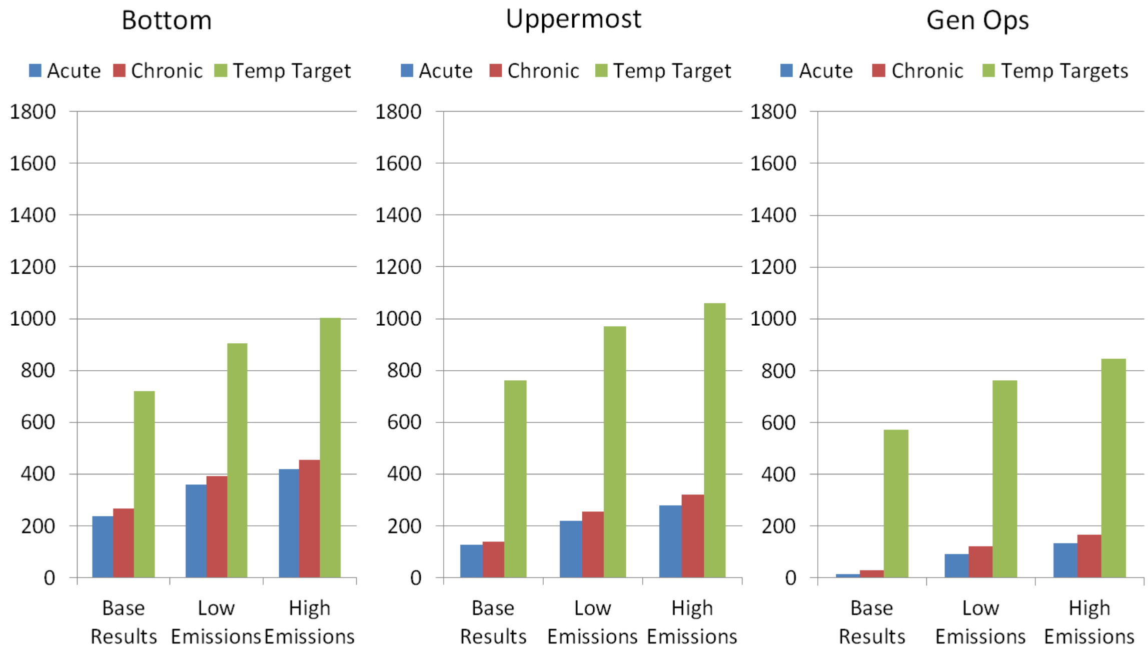

Figure 17. Climate Change degree-day exceedances (°C x days) for the extreme dry year "Base Results" for each TCD schedule compared to model runs where low emissions and high emissions temperature increases are applied, respectively. "Bottom" is the all-out-the-bottom TCD schedule, "Uppermost" is the all-out-the-uppermost TCD schedule and "Gen Ops" is the generalized operations TCD schedule.

Analysis for downstream temperature control of the TCD schedules for each simulation year of the two year drought (*Table 10*) indicates a decrease in downstream temperature control from the first year to the second year. The first simulation year was run with a generalized operations schedule and is the same as the extreme dry year results for that schedule. The generalized operations TCD schedule minimized the degree-day exceedances over all three temperature standards for both simulation years.

Table 10. Two year drought degree-day exceedance results (°C x days) rounded to the nearest integer organized by simulation year, temperature threshold standard and TCD operations schedule. The best performing TCD schedule for each temperature standard for each simulation year is bolded for the second year of simulation. "Bottom" is the all-out-the-bottom TCD schedule, "Uppermost" is the all-out-the-uppermost TCD schedule

and "Gen Ops" is the generalized operations TCD schedule. Results are specific to each year indicated (i.e., not cumulative for both years).

Simulation Year	Standard	TCD Schedule		
		Bottom	Uppermost	Gen Ops
First Year	Chronic	---	---	**29**
	Acute	---	---	**16**
	Temp Target	---	---	**572**
Second Year	Chronic	492	380	**177**
	Acute	459	341	**147**
	Temp Target	1041	1123	**881**

A comparison of the degree-day temperature exceedances for the first year of the two year drought, i.e. generalized operations of the extreme dry year, and the second year of the two year drought (*Figure 18*) indicates that even when the generalized operations are run for a second year, the degree-day exceedances were over an order of magnitude larger for the chronic and acute temperature thresholds compared to the first year, and almost two times larger for the temperature targets compared to the first year. For all temperature thresholds, the generalized operations schedule for the second year outperformed the all-out-the-bottom and the all-out-the-uppermost schedules for the second year.

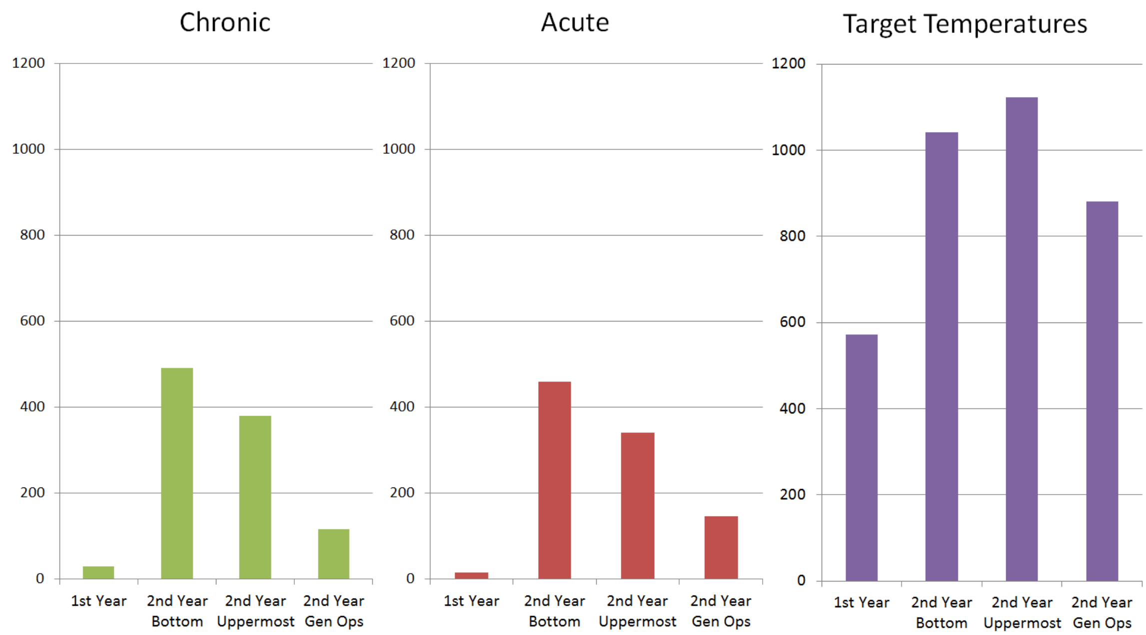

Figure 18. Degree-day exceedances (°C x days) for the first year of the two year drought with generalized operations, and the second year for the two year drought with each TCD schedule for each temperature threshold. "Bottom" is the all-out-the-bottom TCD schedule, "Uppermost" is the all-out-the-uppermost TCD schedule and "Gen Ops" is the generalized operations TCD schedule.

Cold Water Pool Assessment

Weekly time series are presented showing the volume of in-reservoir cold water pool below the cold pool temperature threshold (12.8°C or 55°F) for each TCD schedule for both the extreme wet scenario (*Figure 19*) and the extreme dry scenario (*Figure 20*). Plots for results of other scenarios are available in Appendix E. As expected, the in-reservoir cold water reserve at 1-Nov for the extreme dry year was noticeably lower for all three TCD schedules compared to the extreme wet year. The all-out-the-uppermost schedule was especially impacted in its ability to maintain a late season cold water supply for the extreme dry year when compared to the extreme wet year. Early season in-reservoir cold water reserves were similar for each TCD schedule for both the extreme wet and extreme dry scenarios.

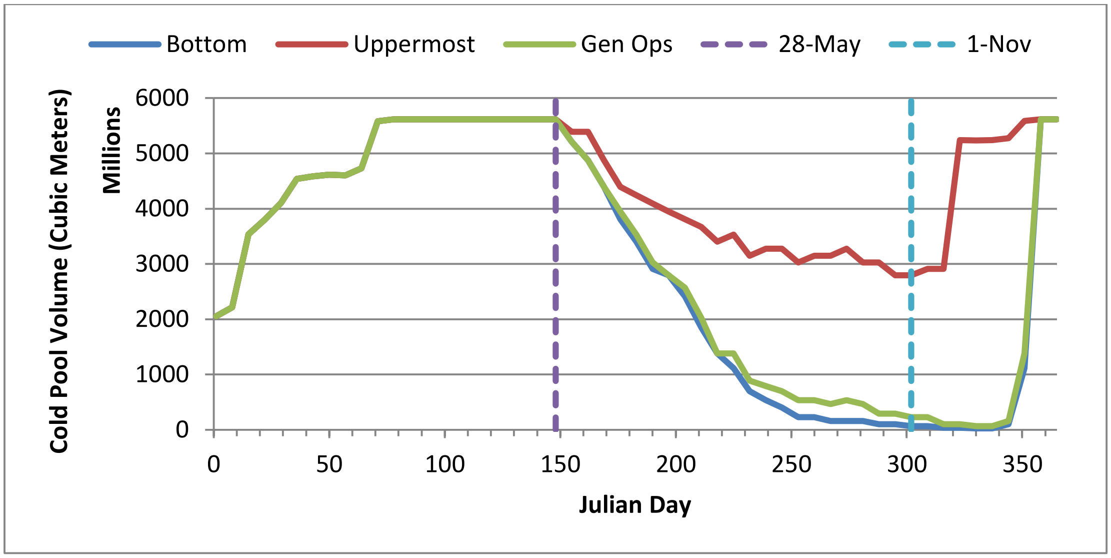

Figure 19. In-reservoir cold pool volume for the extreme wet year, calculated weekly, at or below the cold pool temperature threshold of 12.8°C for each TCD Schedule (bottom, uppermost and generalized operations). "28-May" and "1-Nov" refer to their corresponding calendar dates.

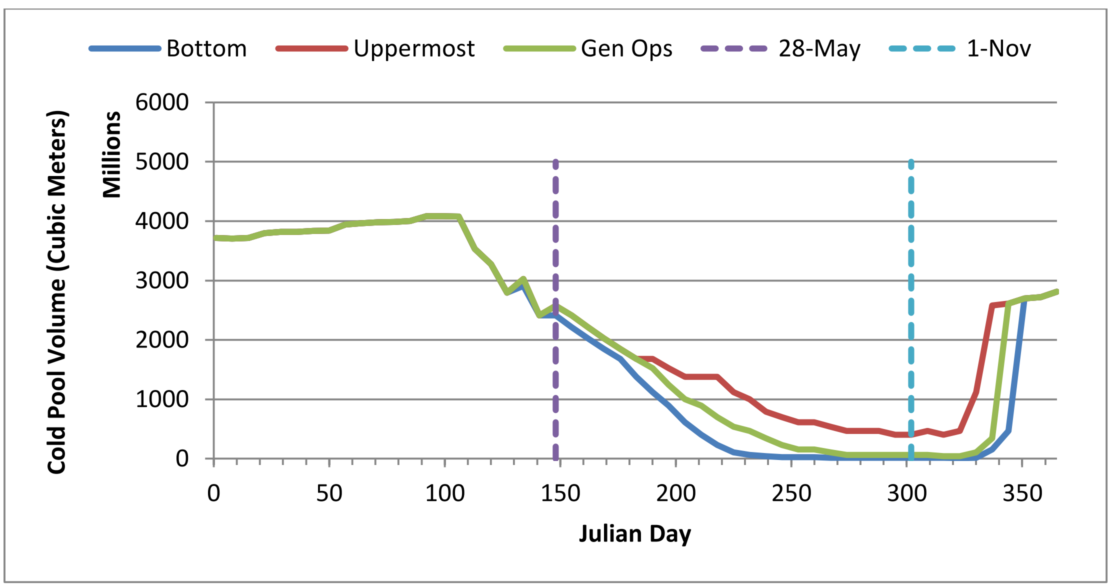

Figure 20. In-reservoir cold pool volume for the extreme dry year, calculated weekly, at or below the cold pool temperature threshold of 12.8°C for each TCD Schedule (bottom, uppermost and generalized operations). "28-May" and "1-Nov" refer to their corresponding calendar dates.

The cold pool reserve for the four calendar year, non-climate change scenarios for 28-May, 1-Nov and 31-Dec for each TCD schedule (*Table 11*) was evaluated to assess which schedule was able to maintain the most in-reservoir cold water pool reserve for spring (28-May), late fall (1-Nov) and end of year (31-Dec). The all-out-the uppermost schedule was the best performing schedule in all scenarios for 28-May, 1-Nov and 31-Dec. Generalized operations 1-Nov cold water pool reserve was always hundreds of millions of cubic meters less than all-out-the-uppermost, but at least tens of millions of cubic meters more than the all-out-the-bottom TCD schedule for the same date.

Table 11. In-reservoir cold water pool volume (million cubic meters) below the cold pool temperature threshold (12.8°C) organized by scenario, date of calculation and TCD operations schedule. The best performing TCD schedule for each date for each scenario is bolded. "Bottom" is the all-out-the-bottom TCD schedule, "Uppermost" is the all-out-the-uppermost TCD schedule and "Gen Ops" is the generalized operations TCD schedule.

Scenario	Standard	TCD Schedule		
		Bottom	**Uppermost**	**Gen Ops**
Extreme Wet Year	28-May	**5615**	**5615**	**5615**
	1-Nov	66	**2794**	228
	31-Dec	**5615**	**5615**	**5615**
Extreme Dry Year	28-May	2415	**2572**	2572
	1-Nov	14	**403**	66
	31-Dec	**2814**	**2814**	**2814**
Wet Year with Dry Fall	28-May	**5569**	5615	**5569**
	1-Nov	66	**2909**	104
	31-Dec	**4928**	**4928**	3527
Wet Year with Warm Fall	28-May	**5615**	**5615**	**5615**
	1-Nov	104	**2909**	294
	31-Dec	**5615**	**5615**	**5615**

Figure 21 compares the in-reservoir cold water pool volumes between the extreme wet year and the wet year with a dry fall. The in-reservoir cold water pool volume was slightly decreased for the early season cold water pool reserve when a dry fall occurred

with a wet spring. The more noticeable impacts, however, were those of the 1-Nov volume and the 31-Dec volume. The 1-Nov cold pool volume was increased for the all-out-the-uppermost schedule with the addition of a dry fall, but reduced for the generalized operations schedule (*Figure 21).* The dry fall also reduced the cold water pool reserve for the end of year more so for the generalized operations schedule than for the all-out-the-bottom or the all-out-the uppermost schedules. The impacts of the addition of a warm fall to a wet year for the cold water pool volumes were compared to the extreme wet year (*Figure 22*) and indicate the addition of a warm fall had no impact on the cold water pool volume for 28-May or 31-Dec. The addition of a warm fall did, however, increase the cold water pool volume for 1-Nov.

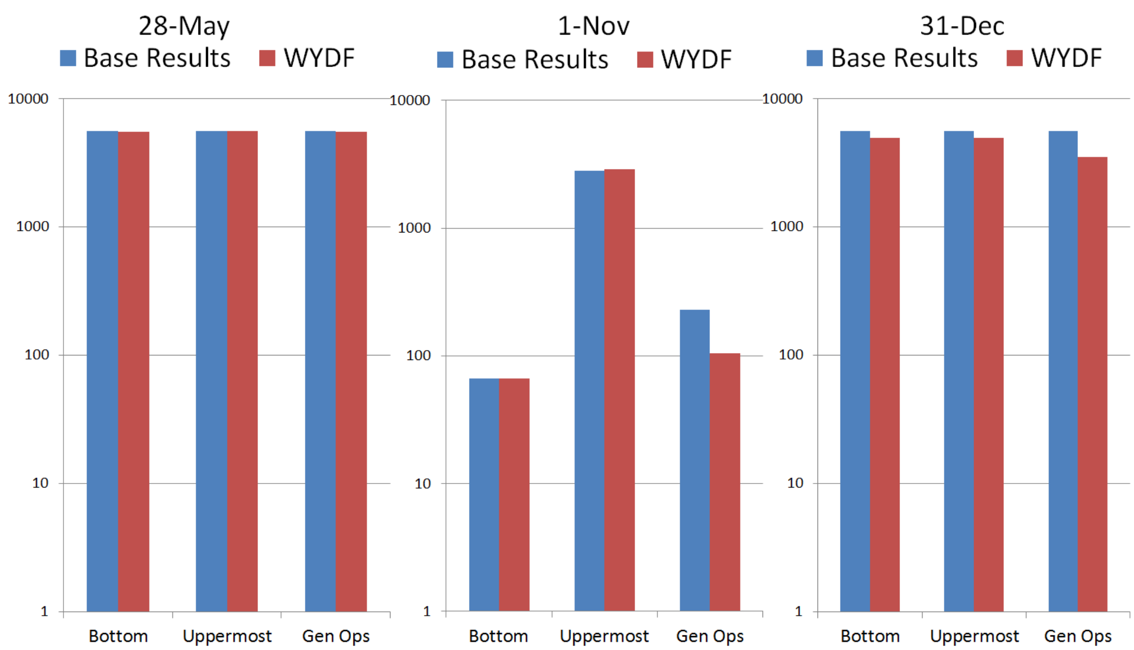

Figure 21. Cold water pool volume (million cubic meters) for the wet year with a dry fall (WYDF) compared to the extreme wet year (Base Results). "Bottom" is the all-out-the-bottom TCD schedule, "Uppermost" is the all-out-the-uppermost TCD schedule and "Gen Ops" is the generalized operations TCD schedule.

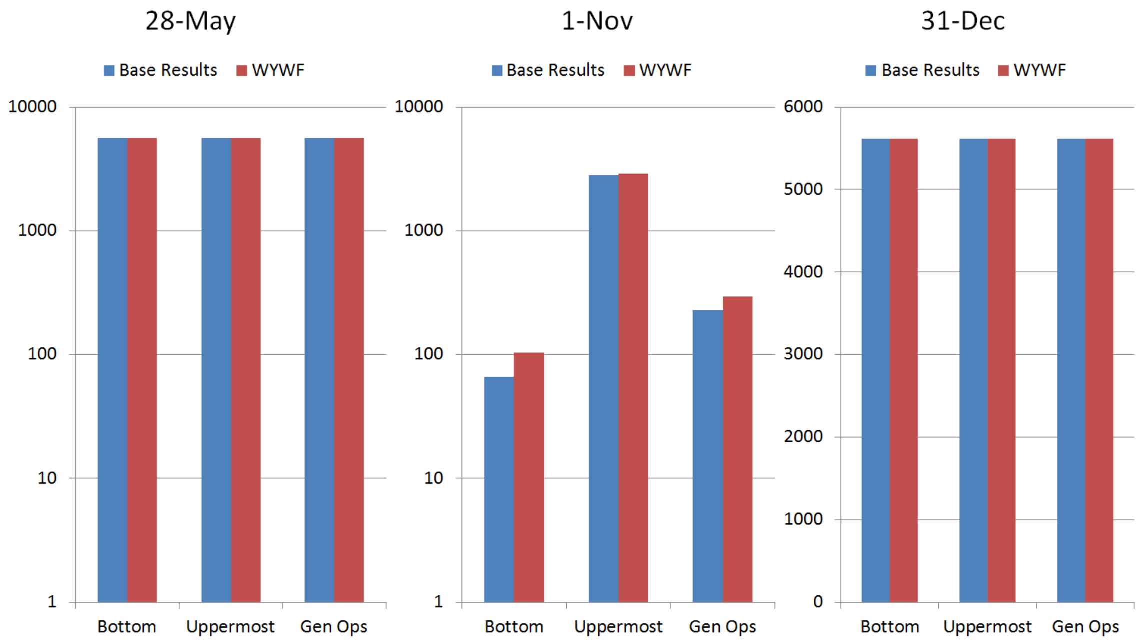

Figure 22. Cold water pool volume (million cubic meters) for the wet year with a warm fall (WYWF) compared to the extreme wet year (Base Results) "Bottom" is the all-out-the-bottom TCD schedule, "Uppermost" is the all-out-the-uppermost TCD schedule and "Gen Ops" is the generalized operations TCD schedule.

The in-reservoir cold water pool volumes for 28-May, 1-Nov and 31-Dec for each TCD schedule for each scenario with the low emissions and high emissions temperature increases (*Figure 23* and *Figure 24*; Appendix D) indicated the all-out-the-uppermost TCD schedule maintained the most in-reservoir cold water pool volume for all dates for both scenarios for both modeled temperature increases. The 28-May all-out-the-bottom and generalized operations TCD schedules for the extreme wet year maintained the same cold water pool volume as the all-out-the-uppermost for the low emissions temperature increase, but were lower for the high emissions temperature increase (*Figure 23*). The end of year cold water pool volume was also negatively affected by the low emissions and high emissions temperature increases, most noticeably in the sharp drop for the 31-Dec all-out-the-bottom extreme dry year cold pool volume between the low emissions temperature increase and the high emissions temperature increase. The 1-Nov cold water pool volumes were hundreds of millions of cubic meters less than the all-out-the-uppermost schedule, but tens of millions of cubic meters more than the all-out-the-bottom schedule for both the low emissions temperature increase and the high emissions temperature increase.

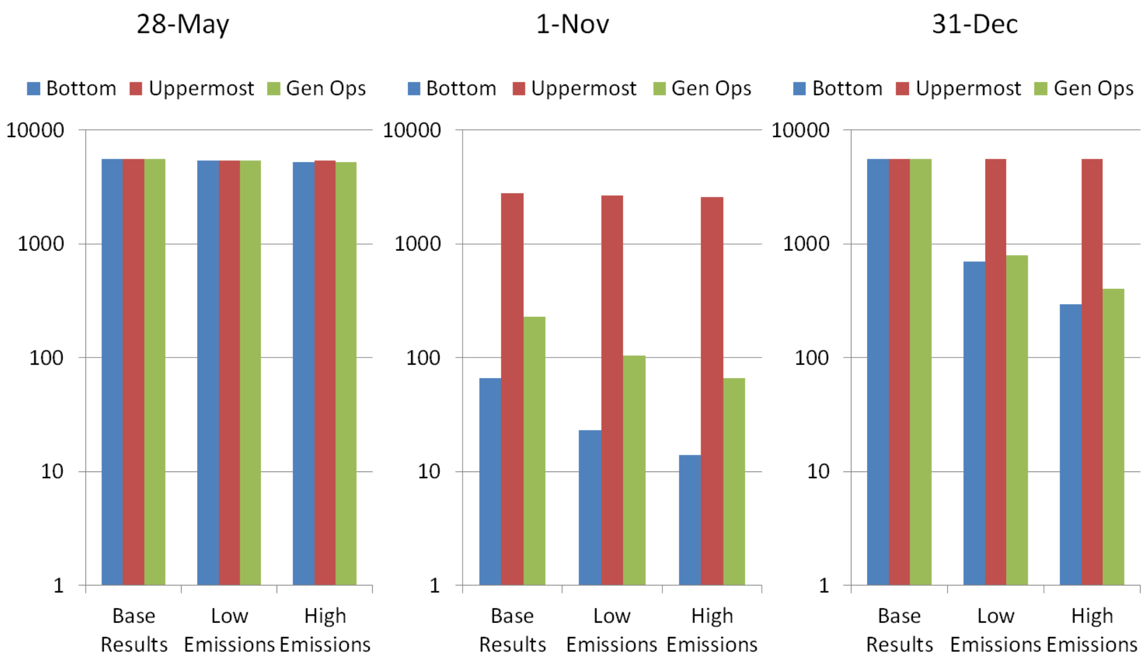

Figure 23. In-reservoir cold water pool volume (million cubic meters) by date for the extreme wet year with climate change. No climate change (Base Results) is compared to results for the low emissions and high emissions temperature increases. "Bottom" is the all-out-the-bottom TCD schedule, "Uppermost" is the all-out-the-uppermost TCD schedule and "Gen Ops" is the generalized operations TCD schedule.

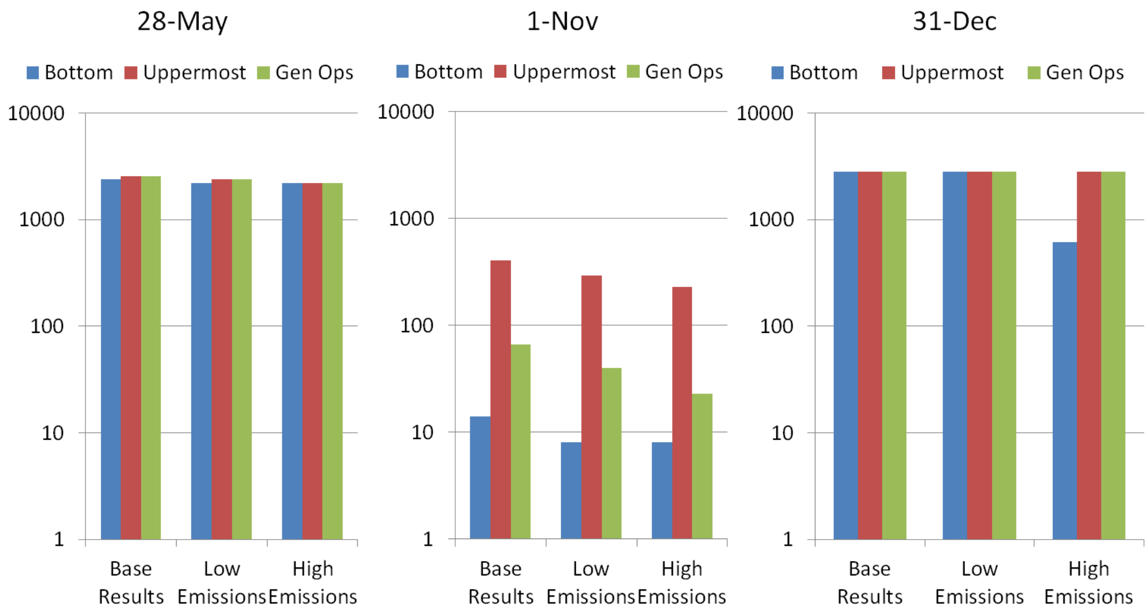

Figure 24. In-reservoir cold water pool volume (million cubic meters) by date for the extreme dry year with climate change. No climate change (Base Results) is compared to results for the low emissions and high emissions temperature increases. "Bottom" is the all-out-the-bottom TCD schedule, "Uppermost" is the all-out-the-uppermost TCD schedule and "Gen Ops" is the generalized operations TCD schedule.

The cold water pool assessment for the first and second year of the two year drought is compared in Figure 25 where the first year was modeled with a generalized operations TCD schedule and the second year was model with each of the three TCD schedules. The generalized operations schedule always underperformed in the second year as compared to the first year. The second year all-out-the-bottom TCD schedule also was unable to maintain a cold water pool reserve similar to that of the first year. The only second year schedule that was able to maintain a greater calculated cold water reserve was the all-out-the-uppermost TCD schedule that maintained over twice the cold water pool in 1-Nov compared to the first year schedule.

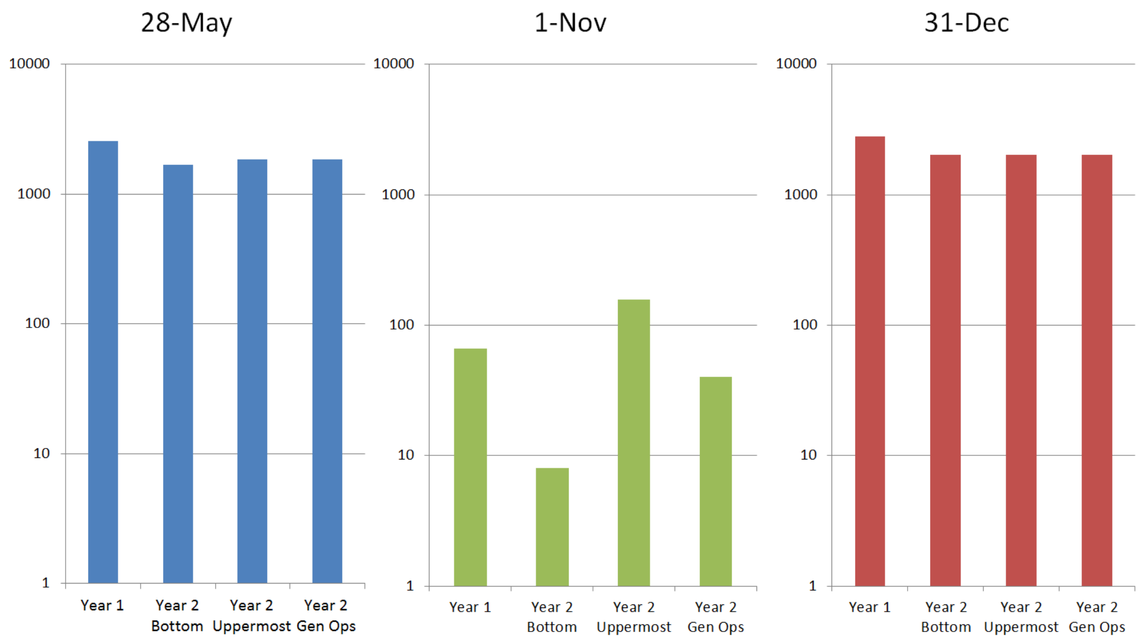

Figure 25. *In-reservoir cold water pool volume (million cubic meters) by date for the two year drought. "Year 1" is the first modeled year of the drought with a generalized operations TCD schedule. "Year 2" is the second modeled year of the drought for each TCD schedule then implemented (Bottom, Uppermost, Generalized Operations).*

Tradeoff Assessment

The tradeoff between downstream temperature control and maintaining the in-reservoir cold water pool for 1-Nov for both the extreme wet year and the extreme dry year (*Figure 26*) showed similar trends at disparate magnitudes. The all-out-the-uppermost TCD schedule did maintain a noticeably larger 1-Nov cold pool volume, but at the expense of more degree-day temperature exceedances for both scenarios. The all-out-the-bottom schedule had both more degree-day exceedances and less 1-Nov cold pool reserve than the generalized operations.

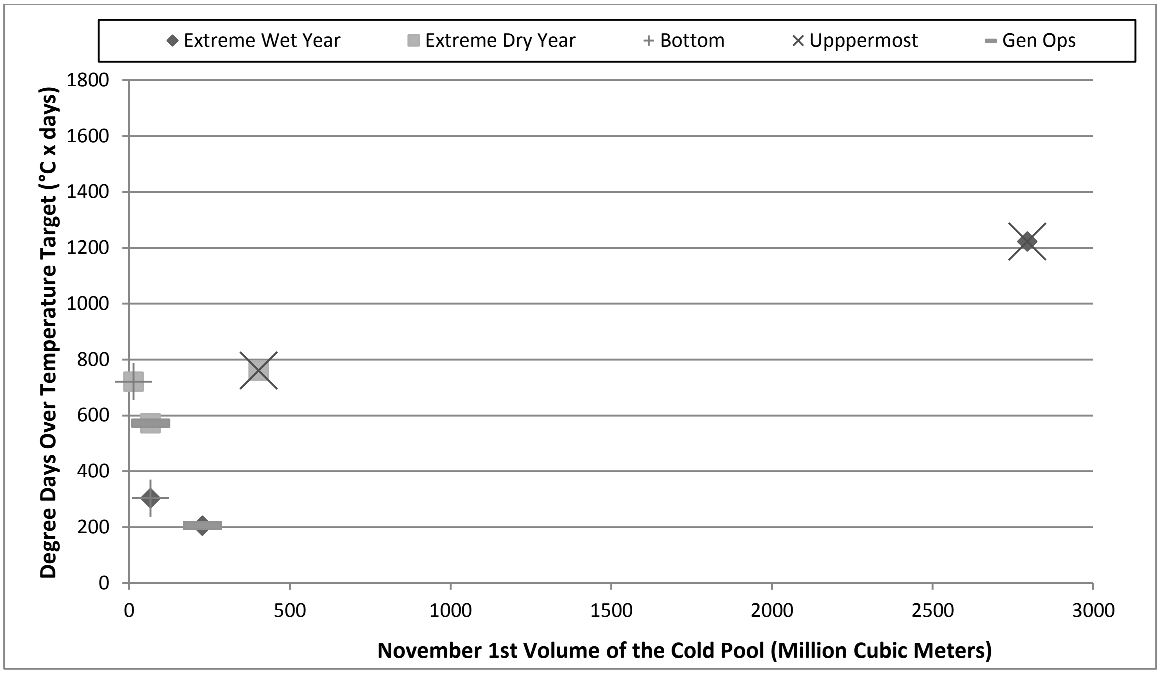

Figure 26. Tradeoff points for the extreme wet year and the extreme dry year for each TCD schedule. "Bottom" is the all-out-the-bottom TCD schedule, "Uppermost" is the all-out-the-uppermost TCD schedule and "Gen Ops" is the generalized operations TCD schedule.

The tradeoff impacts of the addition of a dry fall to an extreme wet year (*Figure 27*) resulted most noticeably in a shift in the generalized operations TCD schedule. A dry fall decreased the calculated cold water reserve and increased the degree-day exceedances as well. The all-out-the-bottom and all-out the uppermost TCD schedules were not noticeably affected. The tradeoff effects of a wet year with a warm fall, however, were more noticeable when compared to an extreme wet year (*Figure 28*). The addition of a warm fall increased the 1-Nov cold pool for the all-out-the-bottom and generalized operations with no obvious tradeoff of degree-day exceedances. The addition of a warm fall for the all-out-the-uppermost schedule, however, had the opposite effect where degree-day exceedances were much greater, but 1-Nov cold water pool was not.

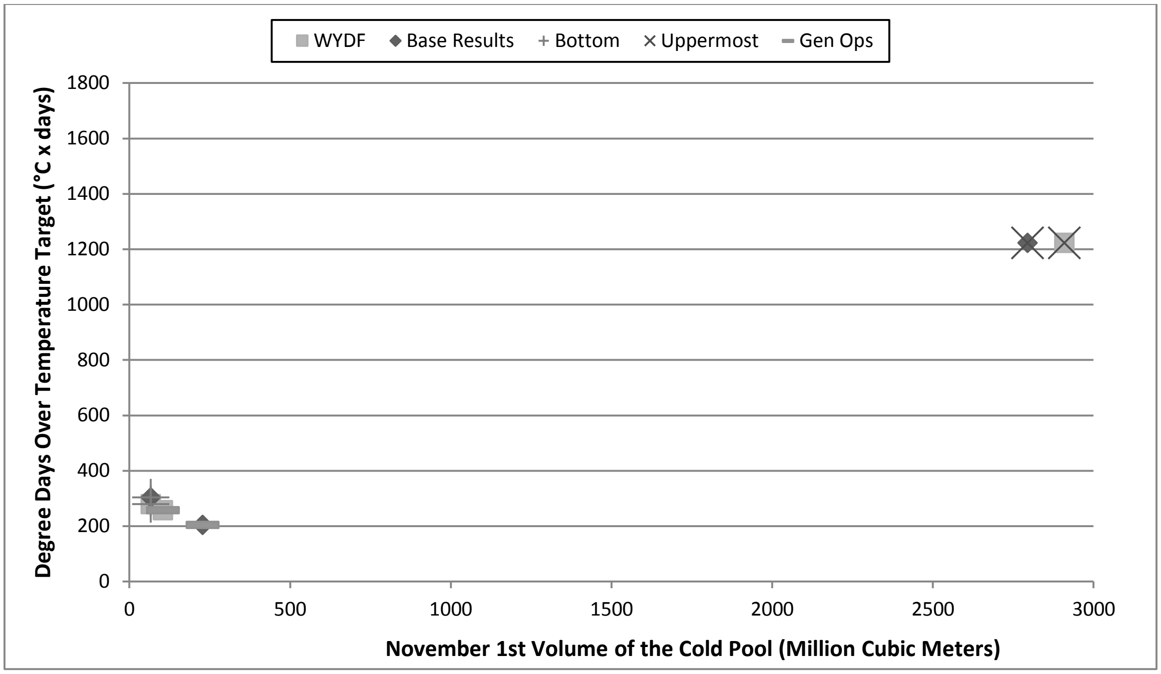

Figure 27. Tradeoff points for the extreme wet year “Base Results” and wet year with a dry fall “WYDF” for each TCD schedule. “Bottom” is the all-out-the-bottom TCD schedule, “Uppermost” is the all-out-the-uppermost TCD schedule and “Gen Ops” is the generalized operations TCD schedule.

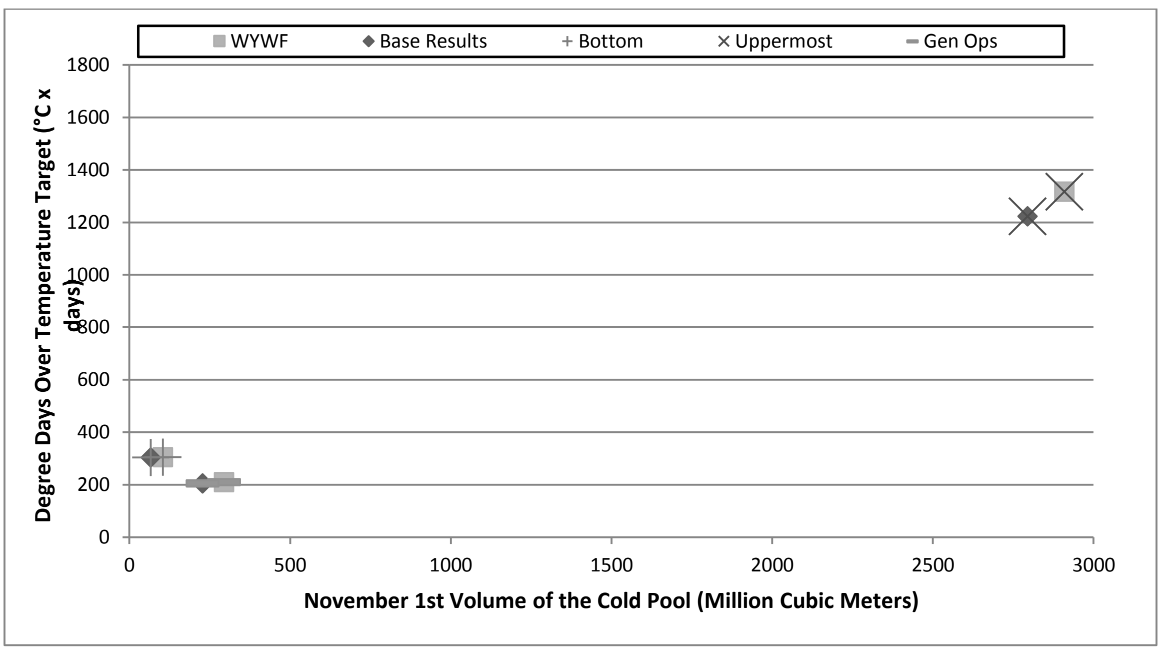

Figure 28. Tradeoff points for the extreme wet year “Base Results” and wet year with a warm fall “WYWF” for each TCD schedule. “Bottom” is the all-out-the-bottom TCD schedule, “Uppermost” is the all-out-the-uppermost TCD schedule and “Gen Ops” is the generalized operations TCD schedule.

The tradeoffs in modeling low emissions and high emissions temperature increases for the extreme wet year were most impacted for the all-out-the-bottom and generalized operations TCD schedule (

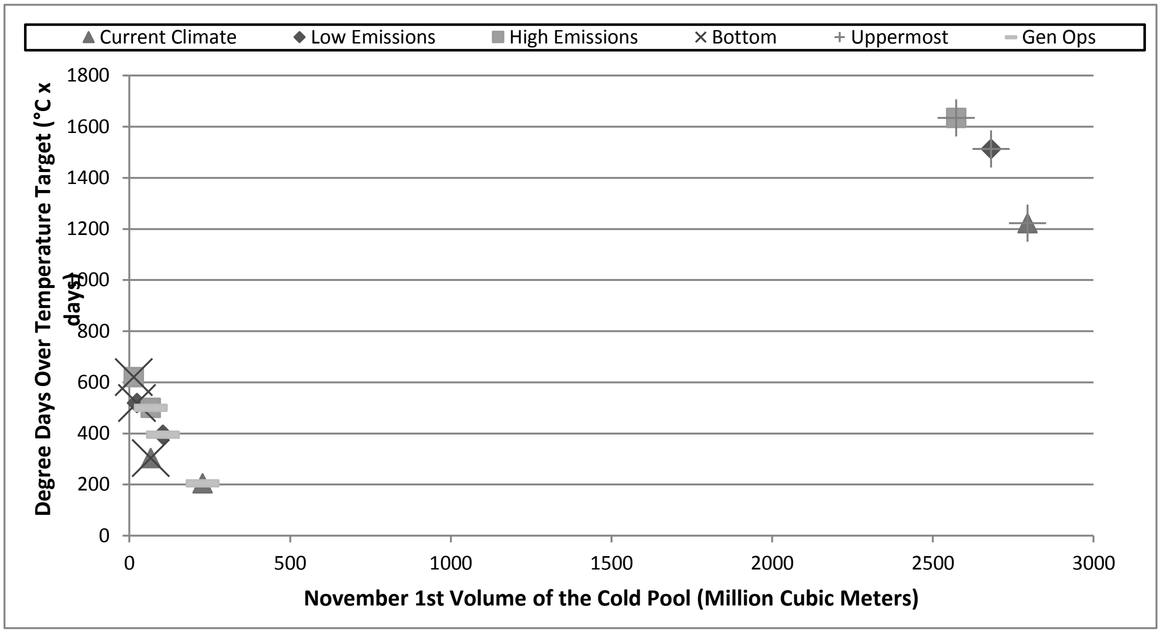

Figure 29). There was a compounding effect of the ability of TCD operations to meet downstream temperature objectives and maintain a late season cold water reserve for both of these schedules. The all-out-the-uppermost schedule, on the other hand, did perform better at maintaining a 1-Nov cold pool as temperature increases were applied, but with consequences in the reduced ability to control downstream temperatures. The tradeoff effects of low emissions and high emissions temperature increases applied to an extreme dry year were similar to those of an extreme wet year with noticeable decreases in performance for both metrics for the TCD schedules (*Figure 30*). The 1-Nov cold water pool volume for the all-out-the-bottom TCD schedule under high emissions

temperature increases, however, was not reduced. Also, the all-out-the-uppermost schedule did have a reduction in 1-Nov cold water reserve that was far more noticeable.

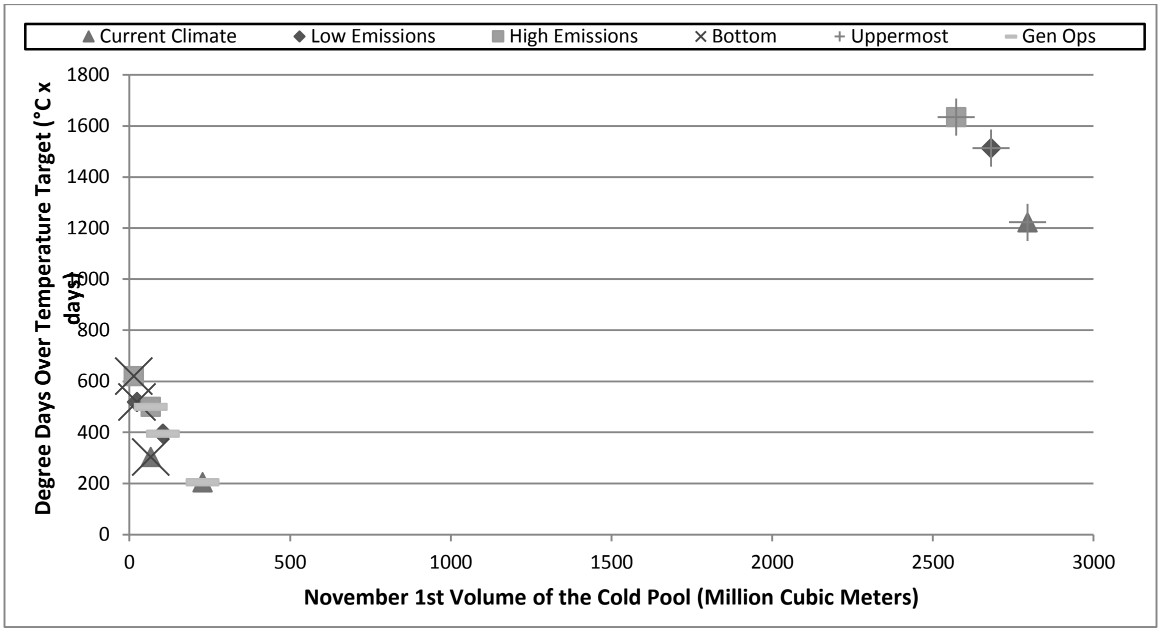

Figure 29. Tradeoff points for the extreme wet year "Current Climate" and the extreme wet year with low emissions and high emissions temperature increases for each TCD schedule. "Bottom" is the all-out-the-bottom TCD schedule, "Uppermost" is the all-out-the-uppermost TCD schedule and "Gen Ops" is the generalized operations TCD schedule.

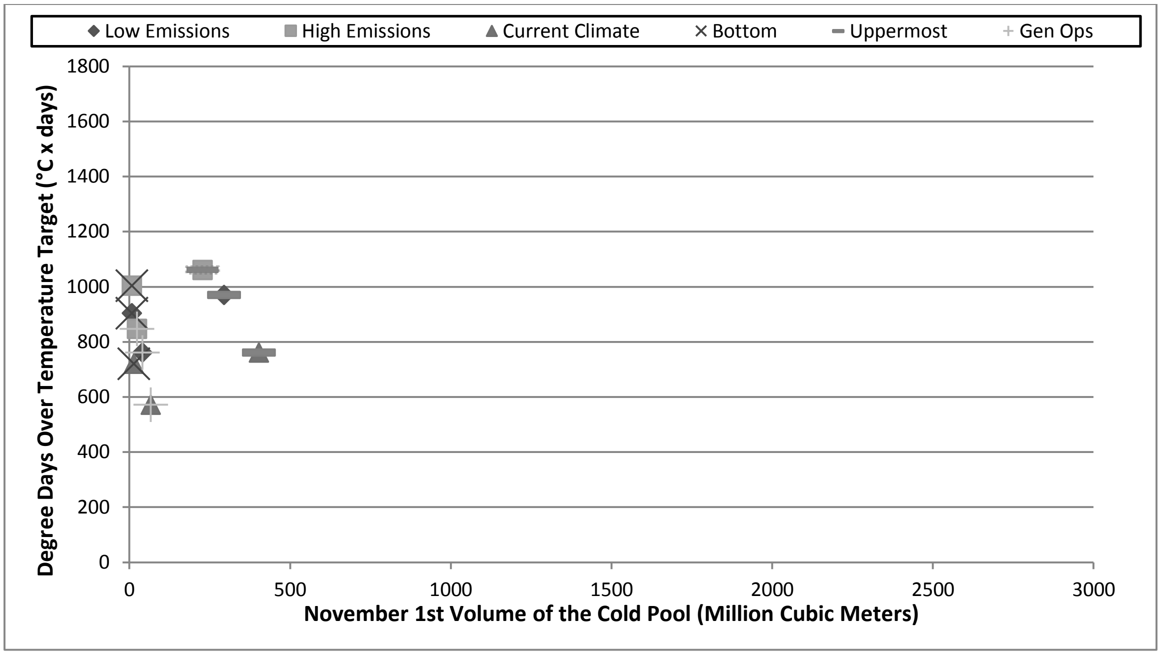

Figure 30. Tradeoff points for the extreme dry year "Current Climate" and the extreme dry year with low emissions and high emissions temperature increases for each TCD schedule. "Bottom" is the all-out-the-bottom TCD schedule, "Uppermost" is the all-out-the-uppermost TCD schedule and "Gen Ops" is the generalized operations TCD schedule.

Two year drought tradeoffs between downstream temperature control and in-reservoir 1-Nov cold water pool (*Figure 31*) show the compounding effect of a second year of dry conditions. The reduction in 1-Nov cold water pool volume was particularly evident for the all-out-the-bottom and generalized operations schedule, yet there was not a noticeable change in degree-day exceedances. The all-out-the-uppermost TCD schedule, on the other hand, did perform worse in the second year for downstream temperature control, but was able to maintain a 1-Nov cold pool volume that was similar to that of the first year of the drought.

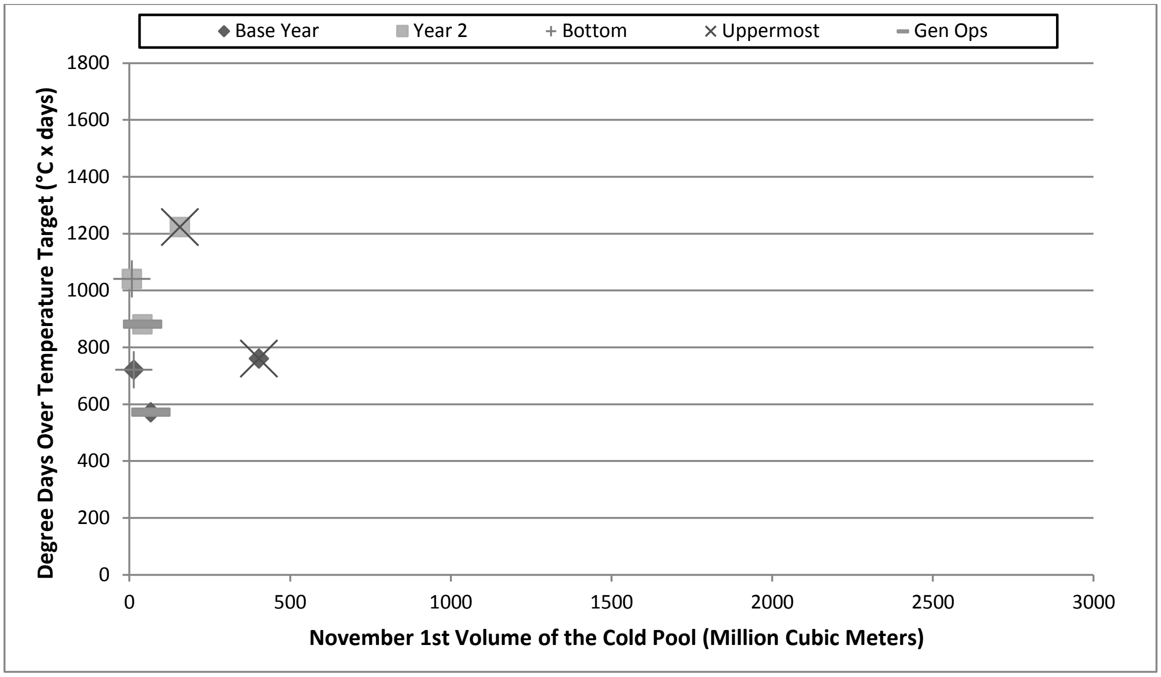

Figure 31. Tradeoff points for the second year of the two year drought "Year 2" and the extreme dry year "Base Year" for each TCD schedule. "Bottom" is the all-out-the-bottom TCD schedule, "Uppermost" is the all-out-the-uppermost TCD schedule and "Gen Ops" is the generalized operations TCD schedule.

Discussion

The generalized operations TCD schedule most often minimized degree-day exceedances over temperature standards. However, the generalized operations TCD schedule was most appropriate in controlling downstream temperatures for the extreme dry year and the two year drought because it minimized the degree-day exceedances for all three temperature thresholds (chronic, acute and temperature targets). For the extreme wet year, wet year with a dry fall, and wet year with a warm fall, the all-out-the-bottom TCD schedule minimized degree-day exceedances over chronic and acute standards.

These results suggest that the in-reservoir cold water pool storage for the extreme wet year was large enough to maintain low elevation cold water releases throughout the calendar year even during continuous depletion whereas the cold pool storage for the extreme dry year was not. The outperformance of the all-out-the-bottom TCD schedule to the generalized operations schedule for the extreme wet year, however, was achieved only by the tradeoff of a massive amount of 1-Nov cold water pool depletion when compared to the generalized operations and all-out-the-uppermost TCD schedules (*Figure 26*).

Seasonal variations to the extreme wet year did impart changes to the tradeoffs seen in meeting multiple objectives for the extreme wet year. Seasonal air temperature increases from projected future climate scenarios (*Figure 28*) were shown to have a more noticeable impact on these tradeoffs than changes in hydrology later in the year (

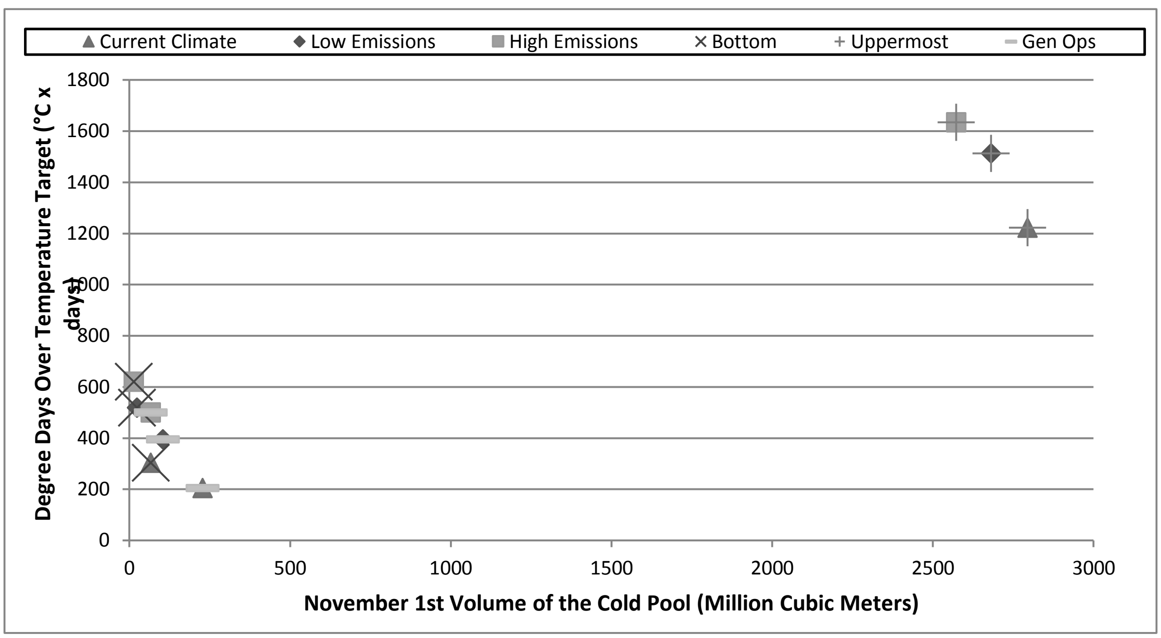

Figure 29) for TCD operations as a whole. This suggests that adjustments in TCD operations would be more concerning for maintaining downstream temperature

objectives and in-reservoir cold water pool during an unseasonably dry fall than an unseasonably warm fall.

Some assumptions were made when developing this model and analysis. One assumption was that the proportion of outflows through the TCD will be distributed equally through all opened TCD gates. This was a necessary assumption for a two dimensional model that assumes consistent conditions across the width of the reservoir. Thus, it was not possible to separate outflows across the face of dam at the same elevations even though the penstocks may differentially pull flow from different gates. Higgs and Vermeyen (1999) noticed a similar discrepancy in development of their FLOW-3D model of Shasta Lake.

The selection of storage curves based on the stochastic method is another limitation in modeling operations realistically. The stochastic method samples the historical operations of Shasta Reservoir from its inception in 1945 to 2010. Shasta Dam has a long history of operations to create hydropower by running as much outflow water through the penstocks as possible. Temperature control was not an operational consideration until 1989, and temperature control with hydropower maximization using the temperature control device was not part of the picture until 1997. Therefore, storage curves that were based on operations prior to 1997 do not reflect operations for the current configuration of Shasta outflows. Storage curves of years selected before 1989 would also not represent operations based on temperature control. Even storage years selected after 1997 would represent operational considerations unique to each year. Another issue with historical storage curves is that depending on starting water surface elevation, the storage output could exceed the storage capacity of the reservoir since W2 does allow storages greater than the capacity of the reservoir. This issue we experienced with our extreme wet year scenario requires revision. Therefore, further input from reservoir managers would likely bring more realistic modeling than revisions to the stochastic approach we used.

Other assumptions involved the calculation of the cold water pool in our analysis. The volume of the cold water pool was calculated at the face of the dam and assumed to be at that elevation throughout the reservoir. This added a great deal of uncertainty to our estimation of cold water availability in the reservoir. This uncertainty has been shown to overpredict the late season availability of cold water in Shasta Lake in the one-dimensional HEC-5Q model that the USBR uses to calculate the cold water pool in Shasta Lake (Russ Yaworsky: personal communication 2014). Calculation of the cold pool reserve by W2 model segment would have most likely improved the estimate of cold water pool but was not conducted due to time constraints. Future analysis should include a segment-by-segment calculation of the cold water pool to investigate the degree of uncertainty imparted by this assumption.

The resolution of the cold water pool calculation based on the way the model was originally configured could be improved upon for future analysis. The lowest vertical layers of the reservoir were originally developed at 6m intervals since cold water reserve calculation was not the original intent of the model. The uncertainty in a 6m resolution of the cold water pool reservoir calculation, when assumed to be at that elevation throughout the reservoir, could be hundreds of millions of cubic meters. For example, the difference in storage for vertical model segments at 297.81 m and 302.31 m is 364,973,149 m^3 according to the storage elevation curve for Shasta. Future configuration of the model if intended to be used for cold water pool reserve calculation would benefit from finer vertical layer resolution of the reservoir, which would require compiling W2 again and recalibrating the model.

An interesting future analysis would be to examine the impact of the sharp temperature drops in the reservoir outflows when transition from TCD gates at different elevations are applied. When the submergence criteria was violated for the all-out-the-top scenario at Julian day 229, for example, the temperature change when gates were closed at elevation 281.3 and opened up at elevation 249.3 dropped a dramatic 11.6°C (Figure *32*). Abrupt temperature changes have been shown to affect the development of Chinook salmon (Donaldson et al. 2008, Steel et al. 2012). Steel et al. (2012) observed that high daily variability in water temperature almost halved the probability that Chinook salmon would emerge from their eggs fully developed, compared with salmon under a stable temperature regime. Temperature shifts at the Shasta Dam outfall, however, will become less severe at downstream compliance points with transport and mixing with other inputs into the Sacramento River.

There are also limitations in the method of storage selection for the calendar year runs. The predetermined storage drives the outflows and creates some counter-intuitive results. For example, the 1-Nov cold water pool was greater for the all-out-the-uppermost TCD schedule when comparing a wet year with a dry fall to an extreme wet year (*Figure 21*). Both scenarios use the same storage curve for the method, so these results indicate that lower streamflow inputs later in the year for the wet year with a dry fall reduces total outflow to achieve these same storage objectives, which acts as a conservation strategy and reduces the withdrawal of water above temperature thresholds. Predetermined storage curves are most realistic for operations of flood control, but it would be interesting to investigate storage curves that included seasonal flow variability.

The winter-run Chinook salmon are most susceptible to temperature shifts during the months of September and October (Kilgour et al. 1985). Generalized operations was preferable for creating a favorable temperature regime for the salmon than all-out-the-bottom and all-out-the-uppermost schedules in the majority of cases presented. Modeling showed that salmon could be more impacted by an extreme dry year than an extreme wet year in terms of overall degree day exceedances. It also illustrated how air temperature increases from climate change could increase stress on salmon survival because TCD operations become less effective at maintaining an adequate downstream temperature environment during the critical late fall period. The cold water pool did have a direct impact on salmon thermal habitat when considering the two year drought because decreased water availability exacerbated the impact of late season degree day exceedances. The ability of the TCD to provide cold water habitat downstream could help alleviate ecological changes predicted by others for Pacific salmon resulting from climate change shifts in thermal regimes (Crozier et al. 2008, Steel et al. 2012).

The only aspect of climate change that was modeled for this study was the effect of temperature increase on the in-reservoir cold water pool and downstream temperature control of TCD operations. Other probable consequences of climate change such as altered precipitation, snowmelt and seasonal shifts in hydroclimate patterns were not modeled. These addition changes would likely compound the ability of TCD operations to control downstream temperatures for the salmon, and would be useful inclusions into the generation of inputs for future models.

Future work will also include pseudo-optimized operations with blended releases from different elevations similar to Hanna et al. (1999) were an optimal solution would be sought only by trial and error instead of a search algorithm. Allowing blended releases could prove to perform better than TCD schedules modeled here in terms of both metrics analyzed for tradeoff in this study. The pseudo-optimized operations are likely to vary from the generalized operations schedule. A sensitivity analysis of the generalized operations of the extreme dry year revealed that shifting the generalized operations dropdown schedule one month later increased degree-day exceedances at the beginning of the summer, but dramatically reduced them in the late fall (Appendix F). The one month later shift in the generalized operations also decreased the cold pool volume tradeoff necessary for temperature control for the extreme dry year. This suggests that pseudo-optimized operations dropdowns will likely be later in the year compared to the generalized operations schedule. It is likely therefore that pseudo-optimized operations for an extreme wet year will resemble more closely the generalized operations than they will for the extreme dry year.

Conclusions

Stochastically generated scenarios of hydrologic and climatic uncertainty both outside the range of the historical record with implications for climate change, as well as variations to them of interest to reservoir managers, were modeled in W2 with various operations release schedules to analyze the ability of the TCD to maintain downstream temperature control and in-reservoir cold water pool in extreme yet plausible future conditions. Active operation of the TCD by a generalized operations schedule was more effective at controlling downstream temperatures for salmon propagation than either an all-out-the-bottom or all-out-the-uppermost operating scheme in most cases. In the few cases for the extreme wet year where the all-out-the-bottom schedule outperformed generalized operations in downstream temperature control, it came at the cost of a greatly depleted late fall cold water pool. Future work should address limitations in the method such as the resolution and calculation of the cold water pool, and a more complete picture of likely changes caused by climate change. A pseudo-optimized operations schedule will also be developed that is likely to be more different from the generalized operations schedule for an extreme dry year than it will be for an extreme wet year.

Acknowledgements

Funding for this project was provided by the National Oceanic and Atmospheric Administration (NOAA SARP Award Number NA12OAR4310093). Workshops for interaction with reservoir managers were organized and administered by Derek Kauneckis of the University of Nevada Reno. Assistance with model output assessment was provided by Joel Hupp, Alexes Garrett and Helaine Berris, all of the University of Nevada Reno. Recommendations for scenario development and simulated operations were provided by Russ Yaworsky, Kristin White, Paul Fujitani and Tom Morstein-Marx of the USBR.

References

Bartholow J, Hanna RB, Saito L, Lieberman D, Horn M. 2001. Simulated Limnological Effects of the Shasta Lake Temperature Control Device. Environmental Management. 27(4):609-626.

California Climate Change Center. 2012. Our Changing Climate: Vulnerability and Adaptation to the increasing Risks from Climate Change in California. A Summary Report on the Third Assessment from the California Climate Change Center. CEC-500-2012-007.

Cayan DR, Kammerdiener SA, Dettinger MD, Caprio JM, and Peterson DH. 2001. Changes in the onset of spring in the western United States. Bull. Amer. Meteor. Soc., 82:399–415.

Cole T, Wells S. 2011. CE-QUAL-W2: A two-dimensional, laterally averaged, hydrodynamic and water quality model, version 3.7. User Manual. Washington DC: US Army Corps of Engineers. 759 p.

Crozier LG, Hendry AP, Lawson PW, Quinn TP, Mantua NJ, Battin J, Shaw RG, Huey RB. 2008. Potential responses to climate change for organisms with complex life histories: evolution and plasticity in Pacific salmon. Evolutionary Applications, 1:252–270.

Donaldson MR, Cooke SJ, Patterson DA, MacDonald JS. 2008. Cold shock and fish. Journal of Fish Biology, 73:1491-1530.

Hanna RB, Saito L, Bartholow JM, Sandelin J. 1999. Results of simulated temperature control device operations on in-reservoir and discharge water temperatures using CEQUAL-W2. Lake Reserv Manage 15(2):87-102.

Higgs, JA and Vermeyen TB. 1999. Shasta Temperature Control Device CFD Modeling Study. US Bureau of Reclamation Technical Services Center, Water Resources Research Laboratory.

Kilgour DM, McCauley RW, Kwain W. 1985. Modeling the lethal effects of high temperature on fish. Can J Fish Aquat Sci, 42:947-951.

McGinnis SM. 1984. Freshwater fishes of California. Berkeley: University of California Press. 316 p.

Mote PW, Hamlet AF, Clark MP, Lettenmaier DP. 2005. Declining mountain snowpack in western north America. American Meteorlogical Society, 86(1):39-49.

Nowak K, Prairie J, Rajagopalan B, and Lall U. 2010. A nonparametric stochastic approach for multisite disaggregation of annual to daily streamflow, Water Resour. Res. 46, W08529.

Saito L, Johnson BM, Bartholow J, Hanna RB. 2001. Assessing ecosystem effects of reservoir operations using food web-energy transfer and water quality models. Ecosystems, 4:105-125.

Steel, EA., Tillotson A, Larsen DA, Fullerton AH. Denton KP, Beckman BR. 2012. Beyond the mean: The role of variability in predicting ecological effects of stream temperature on salmon. Ecosphere, 3(11):104.

Stewart IT, Cayan DR, Dettinger MD. 2004. Changes in snowmelt runoff timing in western north American under a 'business as usual' climate change scenario. Climate Change, 62:217-232.

[USBR] US Department of the Interior, Bureau of Reclamation. 1997. Biological Assessment on the Continued Long-term Operations of the Central Valley Project and the State Water Project. US Department of the Interior, Bureau of Reclamation, Mid-Pacific Region, Sacramento CA.

[USBR] US Department of the Interior, Bureau of Reclamation. 2008. Biological Assessment on the Continued Long-term Operations of the Central Valley Project and the State Water Project. US Department of the Interior, Bureau of Reclamation, Mid-Pacific Region, Sacramento CA.

[USBR] US Department of the Interior, Bureau of Reclamation. 2011a. Fisheries and Aquatic Ecosystems Technical Report. Shasta Lake Water Resources Investigation. US Department of the Interior, Bureau of Reclamation, Mid-Pacific Region, Sacramento CA.

[USBR] US Department of the Interior, Bureau of Reclamation. 2011b. Reclamation, SECURE Water Act Section 9503(c) – Reclamation Climate Change and Water, Report to Congress. US Department of the Interior, Bureau of Reclamation, Policy and Administration, Denver CO.

[USBR] US Department of the Interior, Bureau of Reclamation. 2012. Facilities Description, Shasta Dam and Shasta Lake. Shasta Division, Central Valley Project. US Department of the Interior, Bureau of Reclamation, Mid-Pacific Region, Sacramento CA.http://www.usbr.gov/projects/Project.jsp?proj_Name=Shasta/Trinity+River+Division+Project [accessed 3/27/14].

Yates D, Gallbraith H, Purkey D, Huber-Lee A, Sieber J, West J, Herrod-Julius S, Joyce B. 2008. Climate warming, water storage, and Chinook salmon in California's Sacramento Valley. Climatic Change 91:335-350.

Yaworksy, R. 2014. US Department of the Interior, Bureau of Reclamation, Mid-Pacific Region, Sacramento CA. Personal communication in May and June, 2014.

Yoshiyama RM, Fisher FW and Moyle, PB. 1998. Historical Abundance and Decline of Chinook Salmon in the Central Valley Region, North American Journal of Fisheries Management, 18(3):487-521.

Chapter 4: Recommendations Based on Feedback from Second Workshop

Introduction

On May 28, 2014, a workshop was held at the US Bureau of Reclamation Sacramento office to present the results of chapters two and three, and obtain feedback for refinement of modeling methods. Many of the limitations and assumptions of the methods of chapters two and three were discussed and suggestions were made by the reservoir managers for improvements that could be implemented to model more realistic operating conditions. These suggestions primarily concerned adjustments to outflows, storage objectives, temperature target calculation, and cold pool volume calculation. Chapter four presents revisions recommended by the reservoir managers and how some of these revisions have been and will be implemented. Some revisions apply to all scenarios while others are specific to individual scenarios developed in chapters two and three. Some of these changes are ongoing. Therefore, discussions in chapter four should be considered as first steps in the process, and not finalized method revisions.

Recommended Revisions for All Scenarios

Starting Water Surface Elevation

Starting water surface elevation was originally the January 1 water surface elevation of the stochastically selected year of the proportion vector used for temporal disaggregation in the methods of chapter two. Reservoir managers suggested that January 1 starting surface elevation be based instead on CALSIM II model results (Appendix G). CALSIM II is a model of the Central Valley Project that estimates water availability and reservoir storage in the system under different conditions (CADWR 2009). The "Sac River Index" of the CALSIM II model designates types of water years, including "critically dry" and "wet" to the historical record of the Sacramento River from 1922 to 2003. Storage values from years prior to the construction of Shasta Dam are estimates made by US Bureau of Reclamation modelers of what the storage would have likely been had Shasta Dam been in place at that time. Workshop participants recommended that average of January 1 storage for "critically dry" years be used for the extreme dry year starting storage and the two year drought, whereas the average of January 1 storage for "wet" years be used as starting storage for the extreme wet year, wet year with a dry fall and wet year with a warm fall. Resulting starting water surface elevations were obtained with the USBR storage regression curve based on the Jan-1 storage (Equation 1; Table 12).

Equation 1. USBR storage regression curve

$$Storage\ (AF) = -1.094 * 10^{7} + 1.686 * 10^{-6}(elevation)^{4} + 0.0435(elevation)^{3} - 84.127(elevation)^{2} + 52676.71(elevation)$$

Table 12. Adjustments made to starting surface elevation

Scenario	January 1 Storage (m^3)		January 1 Water Surface Elevation (m)	
	Original	Revised	Original	Revised
Extreme Wet Year	2179	3859	287.6	308.9
Extreme Dry Year	3832	1747	308.6	280.2

Temperature Target Adjustments

Reservoir managers informed us that temperature targets used in Hanna et al. (1999) were outdated and are no longer used. A better representation would be to base temperature targets on modeled end of May storage values as is done for current operations. Reservoir managers provided target temperatures from Future No Action CALSIM II simulations that included four to five transition dates for target temperatures each year (Table 13; USBR 2008). Extreme dry year model runs have an end of May storage of 2163 million m^3 (1754 TAF) and therefore fell into temperature targets for Tier I, and extreme wet year model runs will likely use temperature targets for Tier IV.

Table 13. Temperature targets based on Future No Action CALSIM II simulation

Tier	End of May Shasta Storage (TAF)	Target Temperatures	
		Date	Temperature (Deg C)
Tier I	< 3100	1-Jan	16
		7-Apr	12
		31-Jul	9
		7-Dec	16
Tier II	< 3500	1-Jan	16
		7-Apr	12
		7-Jul	9
		7-Dec	16
Tier III	< 4100	1-Jan	16
		7-Apr	12
		14-Jun	9
		15-Sep	7
		7-Dec	16
Tier IV	> 4100	1-Jan	16
		7-Apr	12
		10-May	9
		15-Sep	5
		7-Dec	16

Generalized Operations Schedule Adjustments

The generalized operations schedule was adjusted from that developed by Hanna et al. (1999) to correspond better with the new temperature targets. First, historical TCD operations were examined to gain insight about which gates at which elevations were being used on average at different times of the year (Appendix H). These were compared to the generalized operations of Hanna et al. (1999) and appropriate adjustments were made based on the historical operations. The dates for gate elevation transitions were then adjusted to also match transition dates in the new temperature targets for the extreme wet year (Table 14).

Table 14. Adjusted generalized operations schedule (JD=Julian day)

Start Day	End Day	Start JD	End JD	Gate elevation (ft)	Gate elevation (m)
1-Jan	6-May	1	126	1022	311.5
7-May	30-Jun	127	181	923	281.3
1-Jul	15-Sep	182	258	818	249.3
16-Sep	7-Dec	259	341	720	219.5
8-Dec	31-Dec	342	365	1022	311.5

TCD Gate Elevation Transitions

Initially, gate adjustments (i.e., changing outflows from one gate elevation to the next adjacent elevation) were simulated as occurring within one day. After meeting with reservoir managers, gate adjustments were changed to be carried out over a six day simulated period because managers noted that full transitions from one elevation to the next over a single day were unrealistic. The adjustments were made between gates at different elevations one gate per day at a time with an equal proportion of outflows assumed to be distributed through each gate. So if there were 5 gates open, each gate passes 20% of the total flow; with 4 gates open, each gate passes 25% of the total flow; and so on. An example of six day gate transitions between both equal and unequal numbers of gates is shown in Table 15. In addition, application of the six day transitions to the generalized operations schedule is shown in *Table 16*. The six day transition period was also implemented for the all-out-the-uppermost TCD operations which assume *a priori* knowledge of drops in water surface elevations.

Table 15. Example of proportional outflow transitions from the lowest elevation gate (Side) to the next higher elevation (Lower) and the next higher elevation (Middle) over the six day transition period. There are two side gates and five gates at all other outflow elevations.

Day	Proportion (%) of flow through Gates			Number of Gates Open		
	Side	Lower	Middle	Side	Lower	Middle
1	100	0	0	2	0	0
2	67	33	0	2	1	0
3	50	50	0	2	2	0
4	25	75	0	1	3	0
5	20	80	0	1	4	0
6	0	100	0	0	5	0
7	0	80	20	0	4	1
8	0	60	40	0	3	2
9	0	40	60	0	2	3
10	0	20	80	0	1	4
11	0	0	100	0	0	5

Table 16. Revised generalized operations TCD schedule showing release distribution by elevation with six day incremental gate elevation changes.

Julian Day	Percent Outflow by Release Elevation			
	219.5m	249.3m	281.3m	311.5m
1	0	0	0	100
123	0	0	20	80
124	0	0	40	60
125	0	0	60	40
126	0	0	80	20
127	0	0	100	0
178	0	20	80	0
179	0	40	60	0
180	0	60	40	0
181	0	80	20	0
182	0	100	0	0
255	20	80	0	0
256	25	75	0	0
257	50	50	0	0
258	67	33	0	0
259	100	0	0	0
328	80	20	0	0
329	75	25	0	0
330	50	50	0	0
331	33	67	0	0
332	0	100	0	0
333	0	80	20	0
334	0	60	40	0
335	0	40	60	0
336	0	20	80	0
337	0	0	100	0
338	0	0	80	20
339	0	0	60	40
340	0	0	40	60
341	0	0	20	80
342	0	0	0	100

Cold Pool Threshold

The original cold pool threshold temperature was 12.8°C which is the desirable hatching temperature for Chinook salmon (USBR 2008). Reservoir managers informed us that a cold pool threshold of 9°C is more useful for Shasta Lake. 9°C is the desirable temperature for reaching the 13.3°C mandated threshold at downstream temperature locations. We therefore used 9°C when calculating the cold water pool in revised modeling of Shasta Lake.

Recommended Revisions for Extreme Dry Year

Outflow Adjustments

Initially, outflows were based on the storage of the stochastically selected year for daily streamflow values from the historical record, where the outflows were the difference of incoming streamflow from that storage curve. Reservoir operators provided a general monthly schedule of outflows for a critically dry water year (*Table 17*) which was used for establishing outflows for the extreme dry year and two year drought scenarios. The OCAP ramping criteria of maximum daily outflow change was also applied to flow transitions between months.

Table 17. Outflow schedule for critically dry years in cubic meters per second and cubic feet per second

Month	Jan	Feb	Mar	Apr	May	Jun	Jul	Aug	Sep	Oct	Nov	Dec
m^3/s	92	92	92	142	227	255	283	227	142	113	92	92
ft^3/s	3250	3250	3250	5000	8000	9000	10000	8000	5000	4000	3250	3250

Recommended Revisions for Extreme Wet Year

Flood Control Curve

The extreme wet year storage was originally based on the stochastically chosen year for the proportion vector from the temporal disaggregation for the stochastic methods of chapter two. Managers suggested operating the extreme wet year for flood control until May or June of each year. Therefore, storage for the extreme wet year will be based on the USBR flood control storage curve (Appendix I). The flood control curve uses seasonal predictions to determine how much space reserved for flood storage on any given day. For the extreme wet year we will use the most conservative flood control curve that requires flood storage from 1-Jan until 15-Jun. Outflows will initially be adjusted for reservoir storage that exceeds the flood control curve. Outflow will be run through the TCD up to penstock capacity of 495.5 m^3 /s (17,500 ft^3/s), with additional outflow run through the bypass outlets on the dam up to the downstream channel capacity 2,237 m^3/s (79,000 ft^3/s). The goal after 15-Jun will be to get outflows down to (5,000 ft^3/s) by 1-Oct. The flood storage curve will also be applied to reservoir storage from 1-Sept to 31-Dec (Appendix I). All OCAP criteria from chapter three will apply.

Fall X2 Requirements

In the fall for an above normal wet year, reservoir managers are mandated to make adjustments to fall outflows in an effort to improve downstream delta smelt habitat (USBR 2008). Shasta Lake managers are obligated to release all inflow for the month of

October without any addition to reservoir storage in an above normal wet year. Therefore, outflows for the month of October will be set to at least the volume of inflow for an extreme wet year.

Recommended Revisions for Extreme Wet Year with a Dry Fall

Managers informed us that the transition from high inflow conditions to low inflow conditions for a wet year with a dry fall would be more problematic if it occurred later than we originally modeled. Initially, Julian day 151 (30-May) was used as the transition from high to low inflows since it was a crossover point in the hydrographs of the extreme wet and the extreme dry years. After additional analysis of the hydrographs, Julian day 225 (12-Aug) was found to be a reasonable alternative because the aggregate inflows between Julian day 224 for the extreme wet year and Julian day 225 for the extreme dry year were within the variance of the historical record. The wet year with a dry fall will be reconstructed by making the transition from high to low inflows on Julian day 225 (12-Aug) instead of 151 (30-May).

Preliminary Results

Preliminary Results for Extreme Dry Year

The simulated outflows for the revised extreme dry year in relation to the revised temperature targets (also the chronic and acute standards) show a large increase in the temperature of the simulated outflow overall (Figure 33). While the generalized operations schedule for the original simulated outflows was able to keep the outflow temperatures below the chronic and acute temperature standards (*Figure 12*), the revised generalized operations schedule did not. The six day transition in the revised results also shows a more graduate decrease in outflow temperatures for days where a transition was made between gates at different elevations. Another interesting change in the results was that the new all-out-the-uppermost schedule had the coldest water released on 1-Nov (Julian day 302) whereas before the generalized operations schedule had the coldest 1-Nov outflow temperatures.

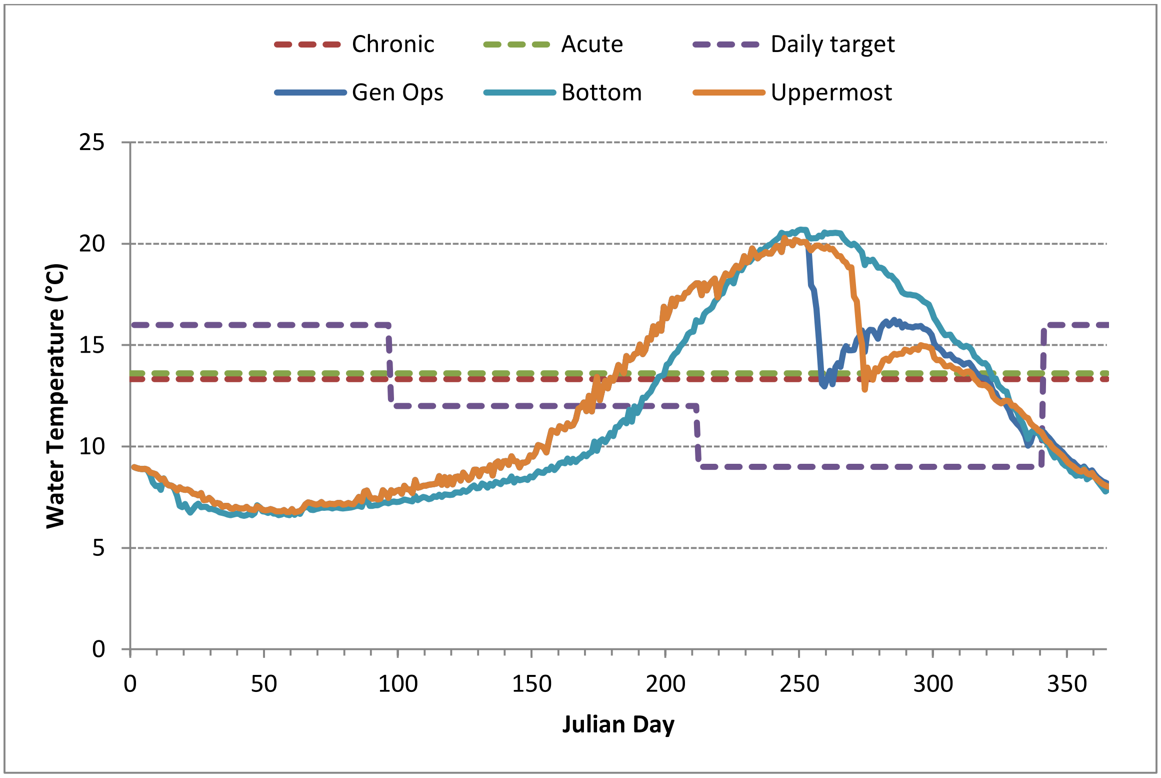

Figure 33. Revised W2 simulated outflow temperatures for the extreme dry year. Solid lines are simulated outflow temperatures for the extreme dry year for each TCD schedule (bottom, uppermost and generalized operations). Dashed lines are the water temperature threshold standards (acute and chronic) and the outlet temperature targets.

Changes to the starting water surface elevation, outflow schedule, generalized operations schedule and temperature target schedule for the extreme dry year did result in greatly decreased performance in downstream temperature control (Table 18).

The percent change between original and revised degree-day exceedance results indicated that the generalized operations schedule was impacted more than either the all-out-the-bottom or the all-out-the-uppermost schedules (Table 19). This could suggest that although the decrease in starting water surface elevation, outflow schedule and temperature target schedule had a major impact on degree-day exceedances, the change in the generalized operations schedule itself had a large impact on downstream temperature performance.

Table 18. Original and revised degree-day exceedance results (°C x days) organized by scenario, temperature threshold standard and TCD operations schedule. The best performing TCD schedule for each temperature standard for each scenario is bolded. "Bottom" is the all-out-the-bottom TCD schedule, "Uppermost" is the all-out-the-uppermost TCD schedule and "Gen Ops" is the generalized operations TCD schedule. Parentheses indicate number of days of calculation for each standard.

Scenario	*Standard*	*TCD Schedule*		
		Bottom	**Uppermost**	**Gen Ops**
Extreme Dry Year (Original)	Chronic (365)	266	139	**29**
	Acute (365)	238	127	**16**
	Temp Target (214)	721	761	**572**
Extreme Dry Year (Revised)	Chronic (365)	556	468	**433**
	Acute (365)	521	432	**396**
	Temp Target (244)	1108	1044	**1003**

Table 19. Percent difference between the original and revised degree-day exceedance results. "Bottom" is the all-out-the-bottom TCD schedule, "Uppermost" is the all-out-the-uppermost TCD schedule and "Gen Ops" is the generalized operations TCD schedule. Positive differences indicate increased degree day exceedances.

Scenario	*Standard*	*TCD Schedule*		
		Bottom	***Uppermost***	***Gen Ops***
Extreme Dry Year	Chronic	109%	237%	1393%
	Acute	119%	240%	2375%
	Temp Target	54%	37%	75%

Revisions to the extreme dry year also changed in-reservoir cold water pool volume by a large margin (Figure 34; Table 20). The cold water pool was decreased almost 75% for all scenarios on each date with the exception of the 1-Nov generalized operations. The percent decrease for the early spring and end of year cold water pool was almost the same for all three schedules (Table 21), with the magnitude of the decrease highlighting the sensitivity of the system to changes in the starting water surface elevation. Changes in the 1-Nov cold water pool volume were most impacted by the all-out-the-uppermost operation and least impacted by the all-out-the-bottom-schedule. Because the 28-May cold water pool differed between original and revised simulations and the decrease was transmitted to later times in the year, the change in the starting surface elevation appeared to have the largest impact on the volume of the cold pool of the revisions made for dry year simulations based on manager input. This sensitivity of starting water surface elevation is consistent with the findings of Bartholow et al. (2001) that hydrology controlled the reservoir's internal dynamics to a far higher degree than TCD operations. The change in starting surface elevation also caused the all-out-the-uppermost schedule and the generalized operations schedule to basically mimic each other with only 25 days of release elevation differences. This combined with the lowered cold pool threshold also resulted in the same cold pool volume results for the two schedules within the resolution of a million cubic meters.

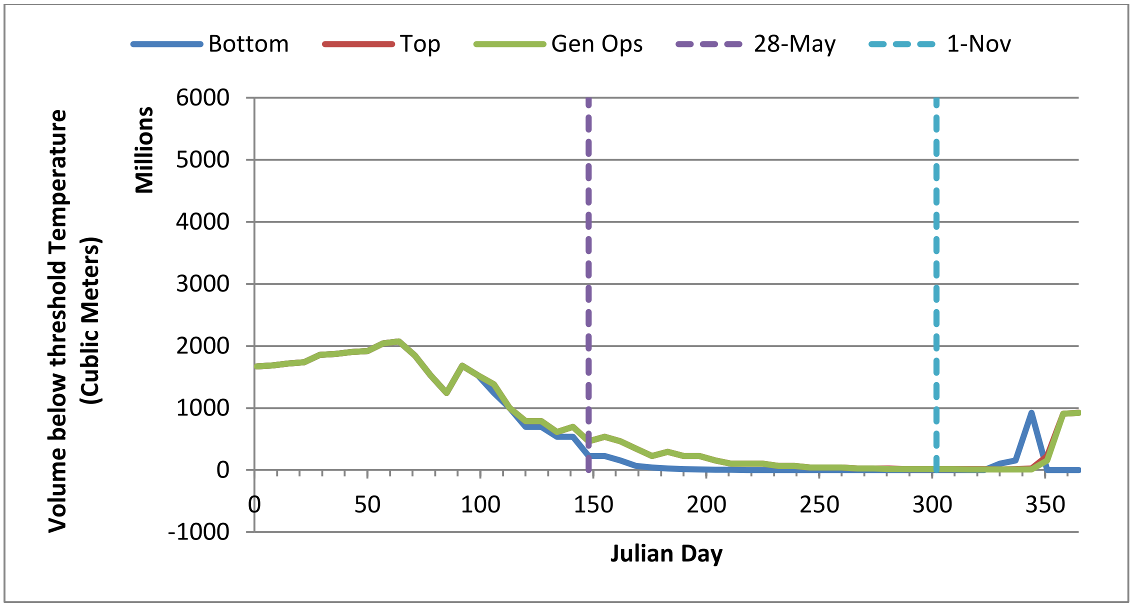

Figure 34. Revised in-reservoir cold pool volume for the extreme dry year, calculated weekly, at or below the cold pool temperature threshold of 9°C for each TCD Schedule (bottom, uppermost and generalized operations). "28-May" and "1-Nov" refer to their corresponding calendar dates.

Table 20. In-reservoir cold water pool reserve for original and revised extreme dry year (million cubic meters) below the cold pool temperature threshold (12.8°C for original and 9°C for revised) organized by scenario, date of calculation and TCD operations schedule. The best performing TCD schedule for each calculation date for each scenario is bolded. "Bottom" is the all-out-the-bottom TCD schedule, "Uppermost" is the all-out-the-uppermost TCD schedule and "Gen Ops" is the generalized operations TCD schedule.

Scenario	Standard	TCD Schedule		
		Bottom	Uppermost	Gen Ops
Extreme Dry Year (Original)	28-May	2415	**2572**	**2572**
	1-Nov	14	**403**	66
	31-Dec	**2814**	**2814**	**2814**
Extreme Dry Year (Revised)	28-May	228	**467**	**467**
	1-Nov	0	**14**	**14**
	31-Dec	0	**925**	**925**

Table 21. Percent difference between the pre-revision and post revision in-reservoir cold water pool volume. "Bottom" is the all-out-the-bottom TCD schedule, "Uppermost" is the all-out-the-uppermost TCD schedule and "Gen Ops" is the generalized operations TCD schedule. Positive changes indicate an increase in the cold pool volume.

Scenario	Standard	TCD Schedule		
		Bottom	Uppermost	Gen Ops
Extreme Dry Year	28-May	-91%	-82%	-82%
	1-Nov	-100%	-97%	-79%
	31-Dec	-100%	-67%	-67%

Expectations for Revision to Extreme Wet Year

The revisions to the extreme wet year are likely to have a significant impact on both the degree-day exceedances and the in-reservoir cold water pool throughout the year. It is expected that there will be a decrease in the performance of all schedules for both metrics because the storage at 28-May should decrease due to increased outflows in the early part of the year to match the flood storage curve. The in-reservoir cold water pool will likely suffer the most from decrease in early season storage and lower cold pool temperature threshold, although with a larger storage it is expected that the generalized operations schedule will be able to differentiate more from the all-out-the-uppermost schedule. Adherence to the flood storage curve is also likely to negatively impact the volume of cold pool available. The change in the degree-day exceedances, however, is harder to predict since revisions also involve relaxing temperature standards for part of the year and making them stricter at other times. The change in the length of calculation for the degree-days and the change in the generalized operations schedule may likely have a negative impact on the degree-day exceedances. The fall X2 requirement is also likely to have a negative impact on the end of year in-reservoir cold water pool volume and possibly the 1-Nov degree-day exceedances. To what extent these negative consequences will have on downstream temperature control is unclear.

Discussion

Revisions to the methods for all simulations will likely result in large shifts in TCD schedule performance for maintaining downstream temperature control and in-reservoir cold water pool. This has already been shown in preliminary results for the extreme dry year. Even though summer outflows were reduced during the simulated summer period, degree-day exceedances increased and cold water pool volumes decreased under all TCD schedules (Figure 35). The change in starting water surface elevation appeared to be the biggest factor in the dramatic decrease of in-reservoir cold water reserve (Table 21) whereas changes in the generalized operations schedule itself played a major role in decreasing downstream temperature performance. The revision to the extreme wet year of matching the flood storage curve in the early part of the year is expected to increase in-reservoir cold water pool reserve, although other factors such as the Fall X2 requirement could confound this increase. Changes to the generalized operations schedule and the calculation of degree-days may also have a negative impact on the results for downstream temperature control for the extreme wet year.

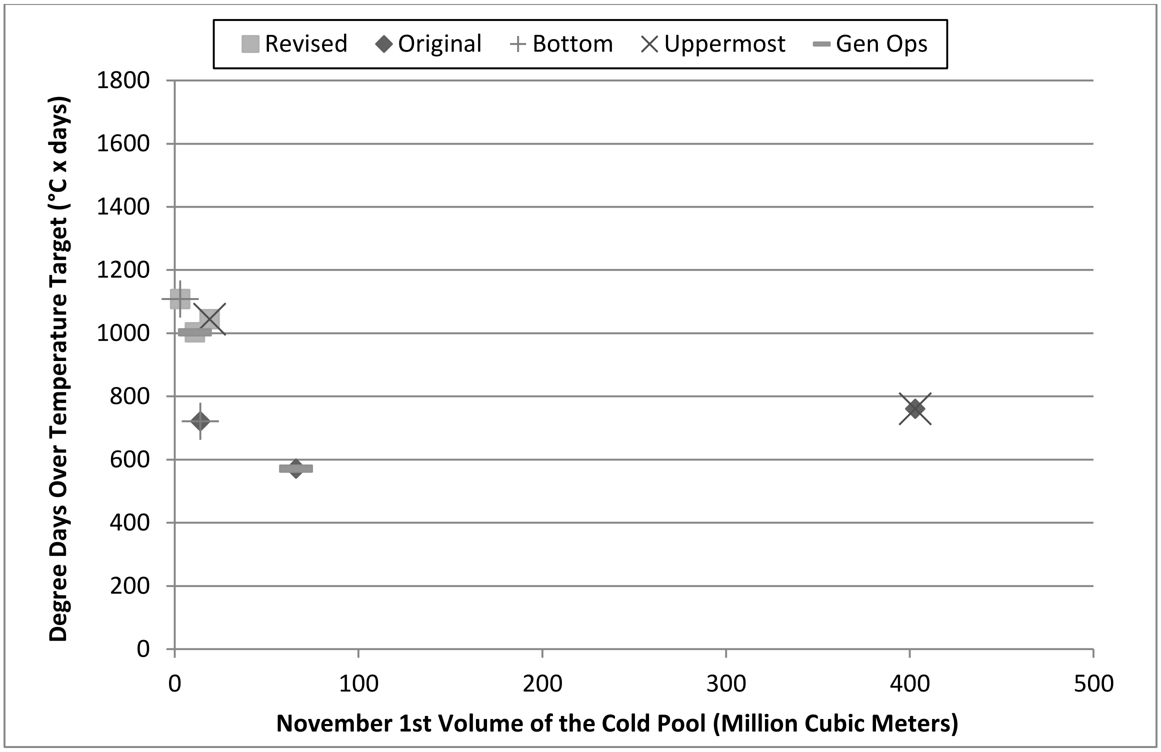

Figure 35. Tradeoff points for the original and revised results for the extreme dry year for each TCD schedule. "Bottom" is the all-out-the-bottom TCD schedule, "Uppermost" is the all-out-the-uppermost TCD schedule and "Gen Ops" is the generalized operations TCD schedule.

Revisions included a six day transition period for gate elevation transitions. Whether real operations have the *a priori* knowledge of a six day transition period before the TCD gate submergence criteria is violated is questionable. Managers did indicate they use weather forecasts of up to seven days when making operational decisions. If a dry forecast is predicted and outflow demand is high, or a storm is predicted to be a flood risk, it may be possible to make a six day transition. A smooth elevation transition between gates on the TCD, however, is not a priority in operational decisions, and the six day transition is therefore likely an idealized operational adjustment.

Strict adherence to the storage curve may also be of questionable realism to simulate. In order to maintain storage strictly below the flood storage curve during periods of extremely high inflow it may be necessary to simulate outflows at or near the channel capacity for extended periods of time. In reality, reservoir managers would likely only increase outflows to the channel capacity as a last resort. Maintaining the proper flood control elevation in the reservoir would be a priority, but so would the needs and safety of downstream stakeholders. Therefore, it is unclear whether using high outflows at or near the channel capacity of the Sacramento River would be realistic in order to maintain strict adherence to the flood control storage curve.

References

Bartholow J, Hanna RB, Saito L, Lieberman D, Horn M. 2001. Simulated Limnological Effects of the Shasta Lake Temperature Control Device. Environmental Management. 27(4):609-626.

[CADWR] California Department of Water Resources. 2009. State Water Project Delivery Reliability Report. 139p.

Hanna RB, Saito L, Bartholow JM, Sandelin J. 1999. Results of simulated temperature control device operations on in-reservoir and discharge water temperatures using CEQUAL-W2. Lake Reserv Manage 15(2):87-102.

[USBR] US Department of the Interior, Bureau of Reclamation. 2008. Biological Assessment on the Continued Long-term Operations of the Central Valley Project and the State Water Project. US Department of the Interior, Bureau of Reclamation, Mid-Pacific Region, Sacramento CA.

Chapter 5: Additional Work and Summary

Chapter five provides additional information not included in previous chapters and a conclusion to the thesis.

Additional Information

Originally, stream temperature was going to be generated based on a regression curve to some corollary dataset. A correlation analysis of stream temperature to datasets of air temperature and streamflow, however, revealed that no correlation was strong enough to develop a regression relationship (Appendix J). Therefore, it was decided that stream temperature would be chosen based on an additional k nearest neighbor selection based on streamflow because streamflow had the best correlation with stream temperature.

Conclusions to Thesis

Reservoir managers on the Sacramento River are faced with difficult choices regarding efficient management of a limited supply of cold water to satisfy fishery obligations while also meeting delivery obligations and flood control. Managers have a mandated obligation to provide artificial cold water habitat to endangered winter-run Chinook salmon (USBR 2008). These managers must also operate the reservoir to generate hydropower and provide water for agriculture, recreation, navigation, and municipal and industrial use. During the springtime period there is also the obligation to manage the storage of the reservoir to prepare for extreme hydrologic events such as flooding. Foreseeing how to work this balance in the face of climate change and unprecedented hydrologic events exacerbates pressure faced by managers in their decision-making.

By combining stochastic hydrologic and meteorological input generation with two dimensional hydrodynamic modeling of Shasta Lake, we were able to generate information of how release operations could impact the ability of meeting downstream temperature target objectives under uncertain and unprecedented hydrologic events. Operating the TCD using a generalized operations schedule was shown to be more effective at balancing the tradeoff of conserving the cold water pool later into the year versus minimizing temperature exceedances than release schedules of all-out-the-bottom or all-out-the-uppermost elevations. Seasonal variations for extreme wet years such as the addition of a dry fall or the addition of a warm fall were shown to decrease the ability of generalized TCD operations to both maintain an in-reservoir cold water pool and provide artificial cold water habitat for salmon propagation. Droughts lasting multiple years decreased the TCD's ability to meet these objectives to an even greater extent. Temperature increases due to climate change will negatively impact the ability of operations to meet downstream temperature objectives and decrease in-reservoir cold water pool reserve for generalized operations and all-out-the-bottom schedules.

The project also demonstrated the effectiveness of modelers and reservoir managers working together to investigate operations schemes for uncertain and extreme hydrologic events in real world grounded and meaningful ways. Feedback from the first workshop allowed us to make adjustments to stochastically generated extreme events to model situations that were of interest to the reservoir managers. In the second workshop, presenting results of modeling gave managers and modelers a means to communicate better about how operations would likely proceed under the synthetic conditions generated for W2 and improve the modeling. By incorporating the input of reservoir managers into the simulations of reservoir operations under extreme conditions we are able to generate information that managers could potentially incorporate into their decision making regarding operation rules for the TCD and release times. Reservoir managers could use the results to complement their own modeling and anticipate circumstances when TCD operations of Shasta Lake may be insufficient for enabling Central Valley Project operations to meet regulatory requirements on the Sacramento River.

Future work will include making adjustments to the methods of simulating operations based on the feedback of the second workshop. Reducing limitations in the model such as the spatial resolution and methods of the cold water pool calculation would be useful in future investigations of cold water management tradeoffs. Additions of seasonal variations to the stochastic method would also be a useful addition to the methods of the project and would allow for the creation of events such as a wet year with a dry fall and a wet year with a warm fall without having to force the trends onto other stochastically generated datasets.

References

[USBR] US Department of the Interior, Bureau of Reclamation. 2008. Biological Assessment on the Continued Long-term Operations of the Central Valley Project and the State Water Project. US Department of the Interior, Bureau of Reclamation, Mid-Pacific Region, Sacramento CA.

Appendix A: Additional Statistics of Stochastic Method

Table 22. Synthetic monthly mean inflow from temporal and spatial disaggregations in $1x10^3$ m^3 from 50 simulations of 61 year ensembles using random annual inflow selection.

Disaggregation	JAN	FEB	MAR	APR	MAY	JUN	JUL	AUG	SEPT	OCT	NOV	DEC
Temporal	419634	410584	453303	362129	283894	174359	126661	113440	111674	131460	182635	287558
Squaw Creek	9509	9867	10081	7978	5364	3135	2201	1910	1839	2284	3284	5834
Sacramento River	61999	64756	72050	63274	57310	26255	10918	7574	7094	10627	22890	41178
Pit River	188990	185435	219088	192125	163121	113472	94422	89031	86721	98695	111088	138845
McCloud River	52233	51051	54516	44523	35029	22708	18104	16215	15452	17369	23589	36665

Table 23. Synthetic monthly inflow skew from temporal and spatial disaggregations from 50 simulations of 61 year ensembles using random annual inflow selection.

Disaggregation	JAN	FEB	MAR	APR	MAY	JUN	JUL	AUG	SEPT	OCT	NOV	DEC
Temporal	1.93	1.84	1.51	1.50	0.76	1.17	0.93	0.75	0.66	3.14	3.71	1.26
Squaw Creek	2.31	3.04	1.20	2.89	1.11	0.81	-0.14	-0.37	-0.47	1.65	2.88	4.62
Sacramento River	1.55	2.39	1.27	1.49	1.07	1.73	2.11	1.07	2.27	3.74	4.22	1.14
Pit River	2.43	1.53	1.08	1.13	0.91	0.97	0.69	0.76	0.53	1.25	2.32	1.15
McCloud River	1.65	2.16	1.27	1.49	0.87	1.18	1.22	1.17	1.15	1.49	2.89	2.41

Table 24. Synthetic monthly inflow variance from temporal and spatial disaggregations in $1x10^5$ $(m^3)^2$ from 50 simulations of 61 year ensembles using random annual inflow selection.

Disaggregation	JAN	FEB	MAR	APR	MAY	JUN	JUL	AUG	SEPT	OCT	NOV	DEC
Temporal	1070457	615761	428472	356956	131391	34496	6321	3505	3076	13875	156324	350586
Squaw Creek	954	957	290	466	63	14	7	8	8	17	57	493
Sacramento River	30412	22723	14314	10158	8450	2991	213	34	41	701	9269	13424
Pit River	166809	81405	81672	74855	41909	12412	4693	3756	3553	6837	19575	32841
McCloud River	21658	14603	9083	11886	5725	2600	1634	1351	1118	1578	4604	9430

Table 25. Synthetic daily mean inflow from temporal disaggregation in $1x10^3m^3$ from 50 simulations of 61 year ensembles using random annual inflow selection.

AVG	1	2	3	4	5	6	7	8	9	10	11	12	13	14	15	
JAN	12114	11013	9744	9953	9651	9233	10165	10496	13547	11695	11631	13528	15298	15991	16179	
	16	17	18	19	20	21	22	23	24	25	26	27	28	29	30	31
	20967	17426	16375	15593	16012	16167	15573	16418	14594	12576	13428	13258	12616	13240	12060	13094
FEB	1	2	3	4	5	6	7	8	9	10	11	12	13	14	15	
	12870	11906	11852	12160	12694	13699	14268	13798	14477	13525	13576	14823	15559	15438	15444	
	16	17	18	19	20	21	22	23	24	25	26	27	28			
	16331	18116	17700	17414	16748	16314	15307	14659	15050	14179	14171	13960	14545			
MAR	1	2	3	4	5	6	7	8	9	10	11	12	13	14	15	
	15155	15543	14889	13983	14618	14124	13850	14758	16008	15958	15360	15241	14204	14108	14167	
	16	17	18	19	20	21	22	23	24	25	26	27	28	29	30	31
	14841	14770	14804	14755	13822	13639	13527	14064	14251	14797	14444	13863	14069	15028	16026	14638
APR	1	2	3	4	5	6	7	8	9	10	11	12	13	14	15	
	14158	13847	13168	12892	13094	13862	13457	12901	12517	12300	12661	13161	13142	13549	12828	
	16	17	18	19	20	21	22	23	24	25	26	27	28	29	30	
	12228	11855	11633	11044	11192	10961	10729	10746	10789	10791	10413	10700	10572	10599	10340	
MAY	1	2	3	4	5	6	7	8	9	10	11	12	13	14	15	
	10083	10126	10003	10089	9973	9774	10048	10054	9742	9734	9366	9104	8972	8838	9078	
	16	17	18	19	20	21	22	23	24	25	26	27	28	29	30	31
	10203	8915	9991	9869	9295	8840	8799	8496	8417	8321	8198	8454	8299	7843	7406	7564
JUN	1	2	3	4	5	6	7	8	9	10	11	12	13	14	15	
	7405	7358	7050	6945	6976	6762	6657	6682	6311	6186	6327	6184	6118	5843	5769	
	16	17	18	19	20	21	22	23	24	25	26	27	28	29	30	
	5537	5505	5579	5440	5211	5216	5228	4932	4790	5004	4791	4460	4609	4835	4647	
JUL	1	2	3	4	5	6	7	8	9	10	11	12	13	14	15	
	4436	4572	4631	4203	4236	4354	4270	4265	4459	4520	4237	4016	4006	4084	4084	
	16	17	18	19	20	21	22	23	24	25	26	27	28	29	30	31
	4055	4104	3969	3994	3874	3969	3965	3956	3729	3690	3859	3642	3780	3862	3891	3949
AUG	1	2	3	4	5	6	7	8	9	10	11	12	13	14	15	
	3659	3726	3889	3794	3735	3819	3644	3575	3591	3703	3671	3621	3659	3614	3740	
	16	17	18	19	20	21	22	23	24	25	26	27	28	29	30	31
	3619	3646	3608	3530	3744	3675	3538	3503	3570	3484	3669	3722	3834	3559	3570	3729
SEPT	1	2	3	4	5	6	7	8	9	10	11	12	13	14	15	
	3457	3613	3635	3784	3789	3552	3628	3698	3694	3580	3870	3694	3656	3658	3519	
	16	17	18	19	20	21	22	23	24	25	26	27	28	29	30	31
	3696	3668	4185	3848	4045	3824	3653	3644	3787	3801	3832	3905	3697	3719	3547	
OCT	1	2	3	4	5	6	7	8	9	10	11	12	13	14	15	
	3687	3589	3716	3674	3761	3854	3962	3810	4091	4205	4383	4749	4581	4440	4375	
	16	17	18	19	20	21	22	23	24	25	26	27	28	29	30	31
	4234	4280	4139	4038	4086	4059	4307	4928	4546	4349	4285	4318	4799	5022	4824	4372
NOV	1	2	3	4	5	6	7	8	9	10	11	12	13	14	15	
	4070	4295	4465	4463	4666	5004	4985	5074	5863	5972	7099	6771	6348	6828	6872	
	16	17	18	19	20	21	22	23	24	25	26	27	28	29	30	31
	7749	7190	6349	6564	6472	5914	6079	6725	6711	6187	6369	6351	6644	6526	8029	
DEC	1	2	3	4	5	6	7	8	9	10	11	12	13	14	15	
	8876	9324	8955	8231	7985	8219	7730	7741	8323	8869	9089	8123	7746	8527	8460	
	16	17	18	19	20	21	22	23	24	25	26	27	28	29	30	31
	9006	8328	8243	9830	10460	12152	11631	10488	9004	8240	8684	9738	11176	10698	11099	12585

Table 26. Synthetic daily inflow skew from temporal disaggregation in from 50 simulations of 61 year ensembles using random annual inflow selection.

SKEW	1	2	3	4	5	6	7	8	9	10	11	12	13	14	15	
JAN	6.9	4.6	3.6	2.9	2.4	2.5	3.2	2.4	3.4	3.0	2.7	2.5	2.2	2.5	2.8	
	16	17	18	19	20	21	22	23	24	25	26	27	28	29	30	31
	4.1	2.7	2.4	2.4	1.8	2.7	3.8	5.1	5.1	4.4	3.4	3.8	2.5	2.9	2.1	1.8
FEB	1	2	3	4	5	6	7	8	9	10	11	12	13	14	15	
	1.9	1.9	2.6	1.8	2.0	1.9	2.9	2.5	1.8	1.7	2.2	1.6	2.0	2.3	2.6	
	16	17	18	19	20	21	22	23	24	25	26	27	28			
	2.7	3.5	3.0	3.0	2.6	2.6	2.6	1.9	3.4	3.1	2.7	2.0	1.4			
MAR	1	2	3	4	5	6	7	8	9	10	11	12	13	14	15	
	2.3	2.5	2.6	1.1	1.8	1.0	1.2	1.6	2.9	3.2	3.4	2.3	3.3	5.1	3.4	
	16	17	18	19	20	21	22	23	24	25	26	27	28	29	30	31
	2.1	3.6	2.6	2.4	1.7	2.6	2.1	2.8	2.9	1.5	2.9	1.2	1.8	4.6	5.6	3.4
APR	1	2	3	4	5	6	7	8	9	10	11	12	13	14	15	
	3.9	3.2	2.5	2.0	2.2	1.8	2.4	2.1	1.8	1.9	2.4	3.0	2.8	3.2	2.7	
	16	17	18	19	20	21	22	23	24	25	26	27	28	29	30	
	2.2	1.5	1.4	1.3	1.1	1.2	1.0	1.0	0.8	0.8	0.8	0.9	1.4	1.6	1.6	
MAY	1	2	3	4	5	6	7	8	9	10	11	12	13	14	15	
	2.5	2.1	1.7	1.5	1.3	0.9	0.7	1.0	2.6	1.5	0.8	0.7	0.6	0.7	0.8	
	16	17	18	19	20	21	22	23	24	25	26	27	28	29	30	31
	1.3	0.8	2.3	2.6	1.7	1.2	1.1	0.9	0.6	0.5	0.4	2.4	2.8	1.9	1.6	2.0
JUN	1	2	3	4	5	6	7	8	9	10	11	12	13	14	15	
	1.1	1.4	1.0	1.1	0.8	0.6	0.6	0.6	0.8	0.9	0.8	0.9	0.9	1.0	1.8	
	16	17	18	19	20	21	22	23	24	25	26	27	28	29	30	
	1.1	1.0	1.1	1.0	0.9	0.6	1.2	0.7	0.4	1.0	0.3	0.4	-0.2	0.7	0.3	
JUL	1	2	3	4	5	6	7	8	9	10	11	12	13	14	15	
	0.1	0.2	0.3	0.2	0.0	0.0	0.3	1.3	1.0	0.1	0.3	-0.3	-0.4	-0.1	0.0	
	16	17	18	19	20	21	22	23	24	25	26	27	28	29	30	31
	-0.1	-0.2	0.1	-0.1	0.5	0.1	0.2	0.1	0.2	-0.1	-0.1	-0.5	0.2	0.1	0.1	-0.1
AUG	1	2	3	4	5	6	7	8	9	10	11	12	13	14	15	
	-0.2	-0.1	0.3	0.2	0.4	0.7	0.2	-0.3	-0.3	-0.1	-0.2	-0.1	-0.2	-0.3	-0.3	
	16	17	18	19	20	21	22	23	24	25	26	27	28	29	30	31
	-0.3	0.0	0.7	0.1	0.1	-0.2	-0.3	-0.2	-0.4	0.6	0.5	0.2	-0.2	-0.2	0.1	0.7
SEPT	1	2	3	4	5	6	7	8	9	10	11	12	13	14	15	
	0.8	0.7	0.2	0.4	-0.2	-0.2	0.5	0.4	0.1	-0.5	0.4	0.3	0.5	-0.2	-0.2	
	16	17	18	19	20	21	22	23	24	25	26	27	28	29	30	31
	0.4	0.5	3.8	1.0	0.9	-0.1	0.4	0.9	1.6	1.5	0.8	4.7	0.7	0.9	-0.1	
OCT	1	2	3	4	5	6	7	8	9	10	11	12	13	14	15	
	0.6	0.1	0.5	-0.1	-0.5	0.1	0.8	1.4	0.8	3.3	5.1	7.2	6.1	4.7	5.3	
	16	17	18	19	20	21	22	23	24	25	26	27	28	29	30	31
	5.0	4.1	3.8	2.9	1.6	0.9	2.7	3.3	1.9	3.5	1.3	2.5	7.7	8.1	7.3	3.1
NOV	1	2	3	4	5	6	7	8	9	10	11	12	13	14	15	
	2.5	1.6	1.0	1.6	2.5	2.4	2.3	3.0	3.8	5.2	5.8	5.6	4.1	2.8	3.7	
	16	17	18	19	20	21	22	23	24	25	26	27	28	29	30	31
	4.3	4.1	4.3	2.6	2.8	2.2	2.0	2.4	2.6	2.3	2.0	3.7	4.0	2.7	3.6	
DEC	1	2	3	4	5	6	7	8	9	10	11	12	13	14	15	
	3.2	1.7	1.6	2.9	3.4	2.1	2.1	2.6	2.4	4.1	3.7	2.4	1.9	1.8	2.0	
	16	17	18	19	20	21	22	23	24	25	26	27	28	29	30	31
	2.7	2.3	2.1	4.4	4.3	4.2	5.5	4.7	2.8	2.7	2.7	3.5	3.5	2.0	3.2	3.5

Table 27. Synthetic daily inflow variance from temporal disaggregation in $1x10^5$ $(m^3)^2$ from 50 simulations of 61 year ensembles using random annual inflow selection

VAR	1	2	3	4	5	6	7	8	9	10	11	12	13	14	15	
JAN	6331	2670	1220	1030	828	742	1010	943	3410	1390	1040	2030	3190	3730	4130	
	16	17	18	19	20	21	22	23	24	25	26	27	28	29	30	31
	12000	4840	3380	2910	2880	3670	3890	7980	4750	1920	2200	2280	1250	1700	943	1320
FEB	1	2	3	4	5	6	7	8	9	10	11	12	13	14	15	
	1280	909	1070	914	1170	1340	1890	1580	1540	1060	1090	1490	1770	1680	1920	
	16	17	18	19	20	21	22	23	24	25	26	27	28			
	2450	4830	4070	3600	2530	2480	1680	1320	2170	1430	1240	978	975			
MAR	1	2	3	4	5	6	7	8	9	10	11	12	13	14	15	
	1410	1210	966	579	805	615	572	947	1880	1740	1550	1170	1270	1320	952	
	16	17	18	19	20	21	22	23	24	25	26	27	28	29	30	31
	884	1200	1180	1010	543	599	580	679	850	815	962	576	694	1820	3520	1240
APR	1	2	3	4	5	6	7	8	9	10	11	12	13	14	15	
	1440	1220	929	682	770	845	940	654	551	568	793	1090	1010	1420	954	
	16	17	18	19	20	21	22	23	24	25	26	27	28	29	30	
	592	427	390	330	250	247	234	197	205	207	171	246	278	315	290	
MAY	1	2	3	4	5	6	7	8	9	10	11	12	13	14	15	
	318	263	251	210	237	192	184	216	376	254	189	173	141	135	135	
	16	17	18	19	20	21	22	23	24	25	26	27	28	29	30	31
	190	155	453	502	270	167	193	191	130	116	121	205	214	135	126	149
JUN	1	2	3	4	5	6	7	8	9	10	11	12	13	14	15	
	108	91	74	71	81	81	87	85	78	61	61	66	60	62	62	
	16	17	18	19	20	21	22	23	24	25	26	27	28	29	30	
	57	46	59	42	38	32	34	40	33	28	30	34	30	25	27	
JUL	1	2	3	4	5	6	7	8	9	10	11	12	13	14	15	
	26	16	20	20	19	14	18	29	22	17	17	21	13	14	15	
	16	17	18	19	20	21	22	23	24	25	26	27	28	29	30	31
	12	16	15	18	15	14	24	17	17	20	16	14	15	18	14	15
AUG	1	2	3	4	5	6	7	8	9	10	11	12	13	14	15	
	15	16	18	19	16	18	17	16	14	13	11	12	12	14	16	
	16	17	18	19	20	21	22	23	24	25	26	27	28	29	30	31
	10	9	16	17	14	16	19	11	8	14	15	12	14	10	9	9
SEPT	1	2	3	4	5	6	7	8	9	10	11	12	13	14	15	
	11	15	12	15	17	14	14	12	15	12	15	11	12	11	12	
	16	17	18	19	20	21	22	23	24	25	26	27	28	29	30	
	13	11	42	16	13	12	11	14	14	12	10	32	13	14	9	
OCT	1	2	3	4	5	6	7	8	9	10	11	12	13	14	15	
	9	10	12	9	12	12	16	14	17	43	71	259	142	108	58	
	16	17	18	19	20	21	22	23	24	25	26	27	28	29	30	31
	61	44	32	15	22	13	33	85	48	49	20	30	195	303	177	39
NOV	1	2	3	4	5	6	7	8	9	10	11	12	13	14	15	
	21	12	17	23	53	76	91	86	272	530	1750	1140	405	377	558	
	16	17	18	19	20	21	22	23	24	25	26	27	28	29	30	
	1280	865	510	249	269	180	152	279	243	146	160	238	334	219	1030	
DEC	1	2	3	4	5	6	7	8	9	10	11	12	13	14	15	
	1230	838	595	561	463	428	320	371	555	1120	1170	519	321	545	521	
	16	17	18	19	20	21	22	23	24	25	26	27	28	29	30	31
	746	395	347	1490	1820	3050	3160	1740	617	484	637	1210	2240	1190	1950	3540

Table 28. Synthetic daily mean inflow from spatial disaggregation for Squaw Creek in1x10^3 m^3 from 50 simulations of 61 year ensembles using random annual inflow selection.

AVG	1	2	3	4	5	6	7	8	9	10	11	12	13	14	15
JAN	216	207	199	226	243	236	274	306	429	287	278	348	412	339	322
	16	17	18	19	20	21	22	23	24	25	26	27	28	29	30
	413	388	360	345	360	329	310	352	292	262	274	274	278	328	276
FEB	1	2	3	4	5	6	7	8	9	10	11	12	13	14	15
	361	311	287	281	330	312	329	395	405	362	356	369	391	371	370
	16	17	18	19	20	21	22	23	24	25	26	27	28		
	421	416	397	376	355	389	363	323	361	337	316	301	280		
MAR	1	2	3	4	5	6	7	8	9	10	11	12	13	14	15
	282	297	311	280	282	307	307	316	393	394	341	322	301	283	285
	16	17	18	19	20	21	22	23	24	25	26	27	28	29	30
	294	297	294	330	317	316	315	322	354	344	327	323	372	401	416
APR	1	2	3	4	5	6	7	8	9	10	11	12	13	14	15
	329	322	303	300	328	385	348	298	283	290	288	287	280	296	287
	16	17	18	19	20	21	22	23	24	25	26	27	28	29	30
	267	248	240	230	231	232	226	217	212	207	205	210	206	212	211
MAY	1	2	3	4	5	6	7	8	9	10	11	12	13	14	15
	212	207	201	197	194	190	186	192	189	183	187	178	173	170	165
	16	17	18	19	20	21	22	23	24	25	26	27	28	29	30
	165	161	178	179	171	162	161	161	154	159	158	159	155	145	136
JUN	1	2	3	4	5	6	7	8	9	10	11	12	13	14	15
	133	132	127	123	126	123	120	124	120	112	115	115	109	104	104
	16	17	18	19	20	21	22	23	24	25	26	27	28	29	30
	100	98	101	97	93	93	93	87	85	88	84	79	82	84	82
JUL	1	2	3	4	5	6	7	8	9	10	11	12	13	14	15
	76	81	82	76	75	78	75	71	75	78	74	71	72	73	69
	16	17	18	19	20	21	22	23	24	25	26	27	28	29	30
	69	71	70	70	67	68	66	68	65	65	66	61	66	67	68
AUG	1	2	3	4	5	6	7	8	9	10	11	12	13	14	15
	63	65	65	66	62	62	63	61	62	63	61	58	62	61	63
	16	17	18	19	20	21	22	23	24	25	26	27	28	29	30
	63	61	61	59	61	61	58	58	61	60	61	62	63	60	59
SEPT	1	2	3	4	5	6	7	8	9	10	11	12	13	14	15
	58	59	61	63	62	57	60	62	59	61	65	63	62	60	57
	16	17	18	19	20	21	22	23	24	25	26	27	28	29	30
	60	59	74	69	67	63	59	60	62	62	59	59	60	60	57
OCT	1	2	3	4	5	6	7	8	9	10	11	12	13	14	15
	61	60	61	62	63	62	66	65	65	73	77	87	82	71	70
	16	17	18	19	20	21	22	23	24	25	26	27	28	29	30
	71	71	67	66	67	65	71	79	76	74	77	78	98	102	113
NOV	1	2	3	4	5	6	7	8	9	10	11	12	13	14	15
	77	78	79	81	81	91	83	85	104	100	114	111	105	118	121
	16	17	18	19	20	21	22	23	24	25	26	27	28	29	30
	142	140	127	125	125	108	118	131	127	119	122	114	112	110	137
DEC	1	2	3	4	5	6	7	8	9	10	11	12	13	14	15
	185	184	168	161	149	160	154	158	160	159	157	147	133	143	161
	16	17	18	19	20	21	22	23	24	25	26	27	28	29	30
	168	168	194	241	254	334	328	251	178	155	169	224	212	187	182

Table 29. Synthetic daily inflow skew from spatial disaggregation for Squaw Creek from 50 simulations of 61 year ensembles using random annual inflow selection.

SKEW	1	2	3	4	5	6	7	8	9	10	11	12	13	14	15	
JAN	4.99	3.34	3.44	3.23	3.74	4.49	4.13	3.60	4.64	3.44	3.34	4.27	4.56	3.35	4.02	
	16	17	18	19	20	21	22	23	24	25	26	27	28	29	30	31
	3.98	5.57	2.40	3.31	4.29	3.00	2.42	3.20	3.55	3.00	2.34	2.38	2.19	6.80	5.31	3.51
FEB	1	2	3	4	5	6	7	8	9	10	11	12	13	14	15	
	4.28	4.43	3.15	2.93	3.64	3.51	4.18	4.42	3.92	4.14	4.96	2.89	4.35	4.14	3.57	
	16	17	18	19	20	21	22	23	24	25	26	27	28			
	4.21	2.66	2.73	2.79	2.57	8.65	8.81	5.41	5.12	5.15	6.21	4.82	2.26			
MAR	1	2	3	4	5	6	7	8	9	10	11	12	13	14	15	
	1.51	1.36	5.70	3.33	1.37	3.52	4.67	4.52	4.82	4.01	2.27	2.85	2.03	2.92	2.21	
	16	17	18	19	20	21	22	23	24	25	26	27	28	29	30	31
	1.82	3.00	3.76	2.63	2.39	5.15	4.32	3.51	3.79	3.68	2.91	2.02	4.71	4.66	3.83	3.11
APR	1	2	3	4	5	6	7	8	9	10	11	12	13	14	15	
	3.75	5.52	5.94	3.99	5.73	3.99	4.23	3.44	3.54	3.82	3.25	3.36	3.56	4.47	4.50	
	16	17	18	19	20	21	22	23	24	25	26	27	28	29	30	31
	3.60	3.28	3.01	2.93	2.51	4.02	4.35	3.07	2.50	2.27	2.29	1.70	1.55	3.00	4.11	
MAY	1	2	3	4	5	6	7	8	9	10	11	12	13	14	15	
	5.26	4.95	3.97	3.50	2.87	2.28	2.03	1.35	1.25	0.93	0.99	1.02	0.75	0.80	0.77	
	16	17	18	19	20	21	22	23	24	25	26	27	28	29	30	31
	0.83	0.90	1.85	2.23	1.79	1.47	1.33	0.95	0.78	1.05	2.44	1.76	1.54	1.16	1.07	1.29
JUN	1	2	3	4	5	6	7	8	9	10	11	12	13	14	15	
	0.87	1.00	0.80	0.87	0.84	0.56	0.85	1.63	1.46	0.92	0.66	0.81	0.87	1.09	1.04	
	16	17	18	19	20	21	22	23	24	25	26	27	28	29	30	31
	1.03	0.87	1.24	1.00	0.83	0.62	1.16	0.78	0.56	1.04	0.42	0.53	0.23	0.51	0.68	
JUL	1	2	3	4	5	6	7	8	9	10	11	12	13	14	15	
	0.73	0.24	0.25	0.32	0.34	0.18	0.25	0.36	0.46	0.08	0.29	0.22	0.80	0.60	0.23	
	16	17	18	19	20	21	22	23	24	25	26	27	28	29	30	31
	0.27	0.22	0.16	0.24	0.49	0.12	0.54	0.23	0.61	0.26	0.26	0.14	0.35	0.33	0.25	0.14
AUG	1	2	3	4	5	6	7	8	9	10	11	12	13	14	15	
	0.21	0.18	0.59	0.32	0.59	0.94	0.48	0.20	0.05	0.16	0.10	0.11	0.31	0.22	0.20	
	16	17	18	19	20	21	22	23	24	25	26	27	28	29	30	31
	-0.02	0.16	0.58	0.37	0.43	0.13	0.32	0.08	-0.21	0.44	0.34	0.27	0.03	0.06	0.17	0.30
SEPT	1	2	3	4	5	6	7	8	9	10	11	12	13	14	15	
	0.71	0.46	0.09	0.21	0.21	0.16	0.22	-0.04	0.08	-0.05	0.09	0.11	0.19	-0.03	0.11	
	16	17	18	19	20	21	22	23	24	25	26	27	28	29	30	31

	0.27	0.06	4.30	3.20	0.21	0.06	0.26	0.56	0.70	0.46	-0.21	0.66	-0.05	-0.02	0.11	
OCT	1	2	3	4	5	6	7	8	9	10	11	12	13	14	15	
	0.09	0.03	0.30	-0.05	0.03	-0.02	0.30	0.69	0.24	4.06	5.74	7.30	6.67	3.89	1.52	
	16	17	18	19	20	21	22	23	24	25	26	27	28	29	30	31
	3.16	0.36	-0.02	-0.09	0.24	0.13	1.01	1.91	0.86	1.23	1.19	2.38	8.09	7.77	8.36	5.03
NOV	1	2	3	4	5	6	7	8	9	10	11	12	13	14	15	
	3.06	2.39	1.98	1.83	1.75	2.02	0.96	1.66	2.52	4.26	5.48	5.28	3.38	2.35	2.45	
	16	17	18	19	20	21	22	23	24	25	26	27	28	29	30	31
	4.75	6.08	7.00	5.62	3.70	4.59	3.37	2.60	1.91	4.16	3.29	1.59	2.07	2.29	4.21	
DEC	1	2	3	4	5	6	7	8	9	10	11	12	13	14	15	
	6.85	3.73	2.76	4.39	4.24	4.08	3.55	6.02	5.47	3.83	3.02	3.03	2.64	3.98	7.21	
	16	17	18	19	20	21	22	23	24	25	26	27	28	29	30	31
	4.69	3.35	3.62	7.29	7.38	7.44	8.22	8.10	6.83	5.57	4.91	8.38	5.64	3.47	2.75	3.34

Table 30. Synthetic daily inflow variance from spatial disaggregation for in $1x10^5$ $(m^3)^2$ from 50 simulations of 61 year ensembles using random annual inflow selection

VAR	1	2	3	4	5	6	7	8	9	10	11	12	13	14	15	
JAN	1.26	0.75	0.70	1.12	1.88	1.92	2.60	3.22	12.48	2.28	1.66	4.69	8.41	2.73	2.19	
	16	17	18	19	20	21	22	23	24	25	26	27	28	29	30	31
	5.49	5.63	2.36	2.48	3.76	1.96	1.36	3.14	1.60	0.82	0.84	0.88	0.91	4.91	1.51	
FEB	1	2	3	4	5	6	7	8	9	10	11	12	13	14	15	
	3.94	2.13	1.46	1.15	2.19	1.77	2.07	5.99	5.56	3.48	3.26	2.55	4.01	2.60	2.54	
	16	17	18	19	20	21	22	23	24	25	26	27	28			
	4.88	3.23	2.73	2.12	1.51	5.84	4.32	1.27	3.53	2.72	2.12	1.29	0.40			
MAR	1	2	3	4	5	6	7	8	9	10	11	12	13	14	15	
	0.36	0.37	1.18	0.41	0.26	0.82	1.11	1.17	3.57	2.84	0.99	0.77	0.50	0.44	0.36	
	16	17	18	19	20	21	22	23	24	25	26	27	28	29	30	31
	0.35	0.56	0.61	0.90	0.67	1.19	0.97	0.70	1.37	1.08	0.74	0.61	2.60	3.81	3.90	
APR	1	2	3	4	5	6	7	8	9	10	11	12	13	14	15	
	1.16	1.63	1.38	0.94	2.55	4.01	2.73	1.04	0.85	1.15	1.00	1.00	0.91	1.52	1.56	
	16	17	18	19	20	21	22	23	24	25	26	27	28	29	30	31
	0.92	0.53	0.40	0.36	0.30	0.45	0.42	0.26	0.20	0.16	0.15	0.16	0.15	0.22	0.28	
MAY	1	2	3	4	5	6	7	8	9	10	11	12	13	14	15	
	0.43	0.34	0.22	0.18	0.14	0.12	0.10	0.11	0.11	0.09	0.10	0.09	0.08	0.07	0.06	
	16	17	18	19	20	21	22	23	24	25	26	27	28	29	30	31
	0.068	0.062	0.136	0.183	0.116	0.080	0.082	0.075	0.057	0.066	0.103	0.092	0.077	0.055	0.047	0.053
JUN	1	2	3	4	5	6	7	8	9	10	11	12	13	14	15	
	0.042	0.037	0.031	0.029	0.029	0.031	0.037	0.047	0.042	0.029	0.025	0.025	0.025	0.022	0.020	
	16	17	18	19	20	21	22	23	24	25	26	27	28	29	30	31
	0.021	0.017	0.022	0.016	0.015	0.015	0.016	0.018	0.014	0.014	0.013	0.013	0.014	0.013	0.015	
JUL	1	2	3	4	5	6	7	8	9	10	11	12	13	14	15	
	0.013	0.011	0.011	0.010	0.010	0.010	0.010	0.010	0.012	0.012	0.010	0.012	0.013	0.013	0.010	
	16	17	18	19	20	21	22	23	24	25	26	27	28	29	30	31

	0.010	0.011	0.011	0.012	0.010	0.011	0.014	0.011	0.011	0.011	0.011	0.009	0.012	0.013	0.012	0.012
AUG	1	2	3	4	5	6	7	8	9	10	11	12	13	14	15	
	0.010	0.012	0.014	0.013	0.012	0.013	0.013	0.011	0.011	0.011	0.010	0.010	0.012	0.011	0.012	
	16	17	18	19	20	21	22	23	24	25	26	27	28	29	30	31
	0.011	0.011	0.014	0.013	0.013	0.012	0.013	0.010	0.010	0.013	0.012	0.013	0.012	0.010	0.010	0.013
SEPT	1	2	3	4	5	6	7	8	9	10	11	12	13	14	15	
	0.011968	0.012689	0.011868	0.014077	0.013693	0.011431	0.012849	0.011662	0.012233	0.011624	0.014492	0.012763	0.013417	0.012258	0.011187	
	16	17	18	19	20	21	22	23	24	25	26	27	28	29	30	31
	0.013	0.011	0.055	0.032	0.014	0.013	0.012	0.013	0.014	0.013	0.010	0.013	0.010	0.011	0.010	
OCT	1	2	3	4	5	6	7	8	9	10	11	12	13	14	15	
	0.011	0.011	0.013	0.012	0.013	0.012	0.014	0.014	0.012	0.038	0.063	0.260	0.132	0.036	0.018	
	16	17	18	19	20	21	22	23	24	25	26	27	28	29	30	31
	0.025	0.016	0.011	0.010	0.013	0.011	0.017	0.031	0.023	0.021	0.024	0.036	0.487	0.417	1.109	0.084
NOV	1	2	3	4	5	6	7	8	9	10	11	12	13	14	15	
	0.040	0.030	0.028	0.028	0.029	0.050	0.028	0.034	0.092	0.116	0.359	0.273	0.110	0.119	0.138	
	16	17	18	19	20	21	22	23	24	25	26	27	28	29	30	31
	0.548	0.686	0.618	0.235	0.205	0.128	0.129	0.179	0.117	0.129	0.116	0.057	0.056	0.062	0.361	
DEC	1	2	3	4	5	6	7	8	9	10	11	12	13	14	15	
	0.37	0.83	3.75	4.17	11.91	16.81	6.29	0.80	0.33	0.61	4.34	1.57	0.52	0.45	0.92	
	16	17	18	19	20	21	22	23	24	25	26	27	28	29	30	31
	2.19	0.82	0.42	0.43	0.29	0.33	0.22	0.55	0.43	0.33	0.30	0.19	0.11	0.20	0.79	0.52

Table 31. Synthetic daily mean inflow from spatial disaggregation for Sacramento River in 1x10^3 m^3 from 50 simulations of 61 year ensembles using random annual inflow selection.

AVG	1	2	3	4	5	6	7	8	9	10	11	12	13	14	15	
JAN	1805	1553	1246	1230	1284	1341	1502	1616	2257	1829	1663	2107	2334	2567	2683	
	16	17	18	19	20	21	22	23	24	25	26	27	28	29	30	31
	3826	2495	2355	2301	2319	2197	2178	2320	2000	1669	1920	1863	1808	1909	1778	2044
FEB	1	2	3	4	5	6	7	8	9	10	11	12	13	14	15	
	2037	1846	1916	1994	2211	2089	2306	2297	2208	2061	2085	2345	2468	2486	2539	
	16	17	18	19	20	21	22	23	24	25	26	27	28			
	2542	2951	2861	2653	2417	2428	2228	2249	2440	2335	2219	2172	2373			
MAR	1	2	3	4	5	6	7	8	9	10	11	12	13	14	15	
	2544	2644	2360	2135	2326	2198	2136	2491	2718	2653	2371	2370	2185	2093	2167	
	16	17	18	19	20	21	22	23	24	25	26	27	28	29	30	31
	2279	2334	2280	2176	2068	2075	2120	2300	2360	2463	2287	2279	2293	2416	2608	2321
APR	1	2	3	4	5	6	7	8	9	10	11	12	13	14	15	
	2231	2163	2024	2013	2076	2163	2138	2063	2038	2009	2179	2403	2410	2589	2364	
	16	17	18	19	20	21	22	23	24	25	26	27	28	29	30	31
	2173	2167	2154	2026	1983	1991	1973	1970	1990	1984	1950	2034	2034	2028	1955	
MAY	1	2	3	4	5	6	7	8	9	10	11	12	13	14	15	
	1932	1948	1999	1983	2092	2037	2017	2116	2124	1990	1897	1821	1787	1793	1792	
	16	17	18	19	20	21	22	23	24	25	26	27	28	29	30	31
	1801	1807	2100	1994	1888	1757	1857	1835	1676	1610	1596	1823	1731	1537	1460	1511
JUN	1	2	3	4	5	6	7	8	9	10	11	12	13	14	15	
	1385	1322	1258	1256	1228	1207	1174	1130	1062	993	952	907	869	858	843	
	16	17	18	19	20	21	22	23	24	25	26	27	28	29	30	31
	812	792	843	783	718	674	646	624	603	582	569	576	547	530	515	
JUL	1	2	3	4	5	6	7	8	9	10	11	12	13	14	15	
	495	472	456	445	436	424	415	405	397	385	373	363	358	351	344	
	16	17	18	19	20	21	22	23	24	25	26	27	28	29	30	31
	338	333	326	320	313	307	303	299	299	291	287	283	279	275	274	273
AUG	1	2	3	4	5	6	7	8	9	10	11	12	13	14	15	
	269	267	265	262	260	258	257	255	253	250	246	244	241	240	240	
	16	17	18	19	20	21	22	23	24	25	26	27	28	29	30	31
	242	238	236	234	238	236	234	233	232	230	233	233	243	238	233	233
SEPT	1	2	3	4	5	6	7	8	9	10	11	12	13	14	15	
	229	227	226	239	238	226	226	229	248	251	240	236	223	223	226	
	16	17	18	19	20	21	22	23	24	25	26	27	28	29	30	31
	241	249	247	255	239	231	225	228	225	227	229	301	244	237	233	
OCT	1	2	3	4	5	6	7	8	9	10	11	12	13	14	15	
	229	234	233	234	235	239	249	243	263	320	365	471	392	328	301	
	16	17	18	19	20	21	22	23	24	25	26	27	28	29	30	31
	323	285	283	271	285	309	438	585	443	426	379	365	467	579	474	382
NOV	1	2	3	4	5	6	7	8	9	10	11	12	13	14	15	
	361	335	343	361	398	477	500	593	831	897	1140	1076	830	1076	1002	
	16	17	18	19	20	21	22	23	24	25	26	27	28	29	30	31
	1196	1009	764	755	840	720	701	815	838	743	814	728	746	794	1209	
DEC	1	2	3	4	5	6	7	8	9	10	11	12	13	14	15	
	1263	1302	1172	1083	1055	1242	1082	1033	1282	1532	1553	1174	1044	1287	1235	
	16	17	18	19	20	21	22	23	24	25	26	27	28	29	30	31
	1429	1158	1117	1458	1496	1926	1745	1446	1186	1069	1152	1301	1676	1398	1501	1781

Table 32. Synthetic daily inflow variance from spatial disaggregation for Sacramento River in 1x10^5 (m^3)^2 from 50 simulations of 61 year ensembles using random annual inflow selection.

VAR	1	2	3	4	5	6	7	8	9	10	11	12	13	14	15	
JAN	277	100	35	24	29	48	70	46	207	93	43	96	96	141	208	
	16	17	18	19	20	21	22	23	24	25	26	27	28	29	30	31
	838	123	84	85	75	70	98	165	100	34	59	65	35	61	34	62
FEB	1	2	3	4	5	6	7	8	9	10	11	12	13	14	15	
	61.0	46.4	60.5	49.5	58.7	51.4	86.5	73.6	49.9	35.0	46.2	55.5	57.8	84.9	136.8	
	16	17	18	19	20	21	22	23	24	25	26	27	28			
	79.3	167.5	153.7	106.1	54.6	58.3	37.9	50.9	135.5	87.8	56.3	44.3	43.7			
MAR	1	2	3	4	5	6	7	8	9	10	11	12	13	14	15	
	66.3	104.0	41.3	21.6	40.7	22.1	20.2	60.1	113.7	121.3	61.4	36.4	34.5	47.2	41.6	
	16	17	18	19	20	21	22	23	24	25	26	27	28	29	30	31
	33.7	47.7	40.3	26.2	16.6	27.1	26.0	44.3	43.3	33.2	24.7	18.5	21.2	42.6	112.0	32.0
APR	1	2	3	4	5	6	7	8	9	10	11	12	13	14	15	
	31.8	30.3	17.5	16.5	19.5	15.5	20.8	14.4	12.2	10.8	26.3	50.9	46.7	85.7	45.0	
	16	17	18	19	20	21	22	23	24	25	26	27	28	29	30	31
	23.1	16.6	20.9	13.0	9.1	8.7	8.8	8.6	8.8	8.4	8.2	13.9	13.0	17.3	13.2	
MAY	1	2	3	4	5	6	7	8	9	10	11	12	13	14	15	
	11.0	9.8	10.2	8.8	12.5	10.7	10.7	16.8	21.9	12.3	10.6	9.0	8.1	8.9	10.0	
	16	17	18	19	20	21	22	23	24	25	26	27	28	29	30	31
	11.1	12.4	32.5	21.1	17.9	13.0	22.6	21.7	11.7	9.7	9.0	46.2	31.4	12.8	10.6	23.7
JUN	1	2	3	4	5	6	7	8	9	10	11	12	13	14	15	
	10.2	8.5	7.8	9.4	9.0	7.7	7.6	7.5	5.8	4.8	4.1	3.8	3.5	3.6	3.7	
	16	17	18	19	20	21	22	23	24	25	26	27	28	29	30	31
	3.26	3.04	7.80	4.80	2.91	2.24	1.90	1.82	1.64	1.46	1.37	1.28	1.08	1.04	0.93	
JUL	1	2	3	4	5	6	7	8	9	10	11	12	13	14	15	
	0.811	0.740	0.643	0.580	0.557	0.527	0.481	0.437	0.421	0.357	0.290	0.245	0.256	0.228	0.202	
	16	17	18	19	20	21	22	23	24	25	26	27	28	29	30	31
	0.182	0.163	0.149	0.131	0.110	0.101	0.100	0.102	0.133	0.095	0.082	0.075	0.070	0.067	0.068	0.060
AUG	1	2	3	4	5	6	7	8	9	10	11	12	13	14	15	
	0.057	0.055	0.055	0.053	0.051	0.052	0.046	0.046	0.047	0.043	0.041	0.038	0.036	0.035	0.033	
	16	17	18	19	20	21	22	23	24	25	26	27	28	29	30	31
	0.037	0.031	0.029	0.029	0.031	0.029	0.030	0.032	0.028	0.027	0.030	0.032	0.168	0.047	0.031	0.032
SEPT	1	2	3	4	5	6	7	8	9	10	11	12	13	14	15	
	0.027	0.026	0.027	0.198	0.187	0.036	0.029	0.047	0.263	0.310	0.186	0.160	0.028	0.025	0.031	
	16	17	18	19	20	21	22	23	24	25	26	27	28	29	30	31
	0.148	0.161	0.078	0.162	0.044	0.027	0.024	0.034	0.026	0.023	0.033	4.854	0.202	0.085	0.050	
OCT	1	2	3	4	5	6	7	8	9	10	11	12	13	14	15	
	0.036	0.041	0.036	0.035	0.037	0.046	0.065	0.035	0.245	1.769	3.208	23.270	5.691	1.411	0.560	
	16	17	18	19	20	21	22	23	24	25	26	27	28	29	30	31
	1.58	0.26	0.19	0.11	0.28	0.28	5.53	13.89	3.55	2.65	1.70	1.33	13.52	46.33	12.60	1.86
NOV	1	2	3	4	5	6	7	8	9	10	11	12	13	14	15	
	1.4	0.5	0.4	0.5	1.2	4.1	3.5	9.5	34.5	63.9	163.5	91.2	25.8	32.5	27.9	
	16	17	18	19	20	21	22	23	24	25	26	27	28	29	30	31
	81.3	46.8	18.2	9.3	21.3	6.9	5.6	8.5	8.6	5.3	8.8	5.4	7.1	9.6	70.5	
DEC	1	2	3	4	5	6	7	8	9	10	11	12	13	14	15	
	56.9	37.4	22.8	21.0	19.9	30.6	18.7	14.7	44.3	129.2	118.8	26.9	13.7	31.0	23.8	
	16	17	18	19	20	21	22	23	24	25	26	27	28	29	30	31
	56.0	23.4	14.2	60.3	50.8	118.8	118.5	48.8	18.9	13.7	21.7	33.3	129.0	40.1	65.0	128.1

Table 33. Synthetic daily inflow skew from spatial disaggregation for Sacramento River from 50 simulations of 61 year ensembles using random annual inflow selection.

SKEW	1	2	3	4	5	6	7	8	9	10	11	12	13	14	15	
JAN	7.45	4.40	3.37	2.44	2.86	4.34	4.98	2.74	4.46	4.68	3.20	2.95	2.17	2.57	3.79	
	16	17	18	19	20	21	22	23	24	25	26	27	28	29	30	31
	5.35	2.81	2.20	2.15	1.68	2.28	3.99	4.83	4.62	3.42	3.23	3.62	1.82	3.30	2.10	2.48
FEB	1	2	3	4	5	6	7	8	9	10	11	12	13	14	15	
	2.57	2.86	3.05	2.74	2.02	2.70	3.54	2.68	1.96	1.62	2.57	1.74	1.75	3.26	4.66	
	16	17	18	19	20	21	22	23	24	25	26	27	28			
	2.84	3.60	2.92	3.06	2.16	2.27	2.22	2.67	4.83	3.80	3.00	2.68	1.61			
MAR	1	2	3	4	5	6	7	8	9	10	11	12	13	14	15	
	2.81	4.12	2.87	1.50	2.43	1.45	1.28	2.54	3.46	4.40	4.15	1.95	3.40	6.54	4.00	
	16	17	18	19	20	21	22	23	24	25	26	27	28	29	30	31
	2.33	3.39	2.82	2.43	2.18	4.17	3.34	4.95	3.62	1.58	1.81	1.24	1.67	4.04	5.55	2.82
APR	1	2	3	4	5	6	7	8	9	10	11	12	13	14	15	
	2.87	3.34	2.51	2.29	2.81	1.28	3.11	2.12	1.81	1.38	3.29	3.31	2.71	3.77	3.10	
	16	17	18	19	20	21	22	23	24	25	26	27	28	29	30	31
	1.93	1.40	2.70	1.51	0.99	0.85	0.90	1.04	0.84	0.57	0.62	1.41	1.49	2.62	2.36	
MAY	1	2	3	4	5	6	7	8	9	10	11	12	13	14	15	
	1.92	1.71	1.37	0.84	1.16	0.85	0.75	1.71	2.62	1.29	1.27	1.18	1.01	0.99	1.14	
	16	17	18	19	20	21	22	23	24	25	26	27	28	29	30	31
	1.32	1.54	2.91	1.45	2.08	1.63	2.53	2.35	1.36	1.19	1.02	4.80	4.05	2.07	1.77	4.59
JUN	1	2	3	4	5	6	7	8	9	10	11	12	13	14	15	
	2.00	1.41	1.57	2.11	1.99	1.59	1.61	1.89	1.84	2.09	1.91	2.01	2.19	2.20	2.22	
	16	17	18	19	20	21	22	23	24	25	26	27	28	29	30	31
	2.01	1.74	3.85	2.98	2.21	2.06	2.10	2.39	2.36	2.35	2.38	1.94	2.12	2.14	2.27	
JUL	1	2	3	4	5	6	7	8	9	10	11	12	13	14	15	
	2.41	2.74	2.69	2.63	2.71	2.99	2.91	2.68	2.51	2.47	2.17	2.00	2.43	2.33	2.07	
	16	17	18	19	20	21	22	23	24	25	26	27	28	29	30	31
	1.98	1.73	1.72	1.62	1.34	1.36	1.40	1.70	2.53	1.64	1.47	1.39	1.27	1.27	1.35	1.31
AUG	1	2	3	4	5	6	7	8	9	10	11	12	13	14	15	
	1.39	1.29	1.33	1.17	1.27	1.34	1.23	1.15	1.13	1.15	1.15	1.05	1.03	1.04	1.03	
	16	17	18	19	20	21	22	23	24	25	26	27	28	29	30	31
	1.10	1.05	0.94	0.99	0.97	0.92	1.11	1.46	1.02	1.07	0.98	0.96	6.23	1.81	0.95	0.93
SEPT	1	2	3	4	5	6	7	8	9	10	11	12	13	14	15	
	0.78	0.82	0.90	6.45	6.41	1.85	1.11	2.19	4.82	4.82	5.43	5.77	1.33	1.15	1.51	
	16	17	18	19	20	21	22	23	24	25	26	27	28	29	30	31
	5.73	4.41	2.19	5.47	1.75	0.51	0.62	1.31	0.95	0.79	2.18	9.25	7.39	5.14	3.79	
OCT	1	2	3	4	5	6	7	8	9	10	11	12	13	14	15	
	3.04	2.15	1.96	1.73	1.74	2.15	2.38	1.59	6.47	5.92	5.35	7.62	6.43	4.87	4.46	
	16	17	18	19	20	21	22	23	24	25	26	27	28	29	30	31
	6.54	3.35	2.64	2.78	5.23	2.55	5.04	3.92	3.74	3.33	4.33	4.98	8.27	8.58	8.36	6.83
NOV	1	2	3	4	5	6	7	8	9	10	11	12	13	14	15	
	2.80	2.23	3.40	3.78	2.82	2.82	2.61	3.44	5.34	5.01	3.10	2.25	2.74	2.14	3.75	
	16	17	18	19	20	21	22	23	24	25	26	27	28	29	30	31
	3.70	1.90	4.50	3.78	3.50	5.51	3.98	2.48	2.37	2.85	2.86	4.82	3.16	3.57	3.81	
DEC	1	2	3	4	5	6	7	8	9	10	11	12	13	14	15	
	5.64	4.77	3.70	2.57	3.08	4.00	3.62	5.19	4.88	5.57	5.92	5.68	4.32	2.49	3.20	
	16	17	18	19	20	21	22	23	24	25	26	27	28	29	30	31
	4.71	4.85	4.38	3.25	5.79	3.00	2.15	2.18	1.91	1.97	2.54	2.14	2.84	2.65	4.37	3.98

Table 34. Synthetic daily mean inflow from spatial disaggregation for Pit River in1x10^3 m^3 from 50 simulations of 61 year ensembles using random annual inflow selection.

AVG	1	2	3	4	5	6	7	8	9	10	11	12	13	14	15	
JAN	5060	5351	5209	5128	4860	4679	4765	4811	5148	5095	5261	5498	5909	6286	6462	
	16	17	18	19	20	21	22	23	24	25	26	27	28	29	30	31
	7319	7581	7453	7271	6940	7431	7392	7356	7080	6711	6592	6386	6013	6249	5843	5850
FEB	1	2	3	4	5	6	7	8	9	10	11	12	13	14	15	
	5919	5889	5737	5643	5820	5846	6050	5988	6334	6316	6344	6219	6426	6664	6572	
	16	17	18	19	20	21	22	23	24	25	26	27	28			
	6906	7266	7555	7798	7716	7630	7397	7173	7050	6831	6795	6724	6830			
MAR	1	2	3	4	5	6	7	8	9	10	11	12	13	14	15	
	6793	7084	6932	6835	6907	6644	6760	6817	7156	7535	7578	7342	7281	7019	7061	
	16	17	18	19	20	21	22	23	24	25	26	27	28	29	30	31
	7191	7038	7070	7160	6985	6837	6691	6786	6802	6911	7222	7005	7190	7441	7489	7525
APR	1	2	3	4	5	6	7	8	9	10	11	12	13	14	15	
	7299	7250	6877	6875	6703	7098	6946	6911	6709	6605	6539	6537	6577	6827	6519	
	16	17	18	19	20	21	22	23	24	25	26	27	28	29	30	31
	6514	6360	6322	6018	6152	6015	5923	5917	5961	5909	5783	5780	5672	5787	5738	
MAY	1	2	3	4	5	6	7	8	9	10	11	12	13	14	15	
	5645	5647	5596	5651	5609	5623	5533	5621	5474	5437	5717	5442	5361	5350	5254	
	16	17	18	19	20	21	22	23	24	25	26	27	28	29	30	31
	5320	5254	5523	5497	5403	5212	5108	5123	4985	5074	4859	4776	4757	4583	4276	4407
JUN	1	2	3	4	5	6	7	8	9	10	11	12	13	14	15	
	4462	4367	4364	4189	4309	4119	4038	4180	3975	3893	4123	4153	4026	3843	3786	
	16	17	18	19	20	21	22	23	24	25	26	27	28	29	30	31
	3628	3617	3725	3620	3480	3624	3626	3335	3337	3511	3319	3003	3236	3306	3278	
JUL	1	2	3	4	5	6	7	8	9	10	11	12	13	14	15	
	3058	3306	3390	2947	2997	3222	3073	3036	3263	3337	3111	2967	3057	3120	3045	
	16	17	18	19	20	21	22	23	24	25	26	27	28	29	30	31
	2999	3080	2995	3049	2900	2960	2947	3028	2845	2868	2919	2747	2934	3066	3093	3064
AUG	1	2	3	4	5	6	7	8	9	10	11	12	13	14	15	
	2783	2927	2950	3027	2874	2910	2889	2738	2819	2927	2879	2765	2894	2809	2886	
	16	17	18	19	20	21	22	23	24	25	26	27	28	29	30	31
	2921	2901	2856	2836	2871	2843	2784	2811	2812	2785	2897	2995	2980	2846	2798	3020
SEPT	1	2	3	4	5	6	7	8	9	10	11	12	13	14	15	
	2707	2798	2905	3021	2969	2700	2843	2908	2862	2905	3074	2944	2890	2839	2719	
	16	17	18	19	20	21	22	23	24	25	26	27	28	29	30	31
	2840	2798	3044	2908	3201	3042	2819	2885	2950	2982	2942	2827	2851	2822	2725	
OCT	1	2	3	4	5	6	7	8	9	10	11	12	13	14	15	
	2870	2841	2936	2922	3000	2990	3063	3060	3055	3120	3158	3278	3292	3160	3294	
	16	17	18	19	20	21	22	23	24	25	26	27	28	29	30	31
	3236	3255	3155	3142	3111	3060	3129	3342	3364	3197	3369	3370	3433	3644	3406	3443
NOV	1	2	3	4	5	6	7	8	9	10	11	12	13	14	15	
	3255	3433	3480	3525	3427	3497	3314	3302	3563	3589	3868	3706	3688	3783	3845	
	16	17	18	19	20	21	22	23	24	25	26	27	28	29	30	31
	4053	4020	3832	3972	3848	3526	3838	3785	3918	3769	3832	3910	3890	3799	3822	
DEC	1	2	3	4	5	6	7	8	9	10	11	12	13	14	15	
	3969	4197	4248	4180	4061	3991	4107	4028	4162	4288	4240	4305	4037	4112	4118	
	16	17	18	19	20	21	22	23	24	25	26	27	28	29	30	31
	4301	4487	4337	4577	4592	4933	5056	5109	4882	4593	4504	4610	4854	5222	5195	5551

Table 35. Synthetic daily inflow skew from spatial disaggregation for Pit River from 50 simulations of 61 year ensembles using random annual inflow selection.

SKEW	1	2	3	4	5	6	7	8	9	10	11	12	13	14	15	
JAN	4.27	4.42	4.84	4.01	3.38	2.69	1.86	1.13	1.90	1.54	1.47	1.92	2.89	2.59	2.81	
	16	17	18	19	20	21	22	23	24	25	26	27	28	29	30	31
	3.53	3.02	3.21	3.52	2.62	2.67	3.41	4.55	4.92	4.79	4.41	4.49	3.76	2.73	2.32	1.82
FEB	1	2	3	4	5	6	7	8	9	10	11	12	13	14	15	
	1.15	1.16	1.19	1.17	1.15	1.02	1.20	1.08	1.57	0.95	0.86	1.02	0.82	0.88	1.07	
	16	17	18	19	20	21	22	23	24	25	26	27	28			
	2.13	3.72	3.52	3.78	4.11	3.48	3.00	2.44	1.97	1.69	1.42	1.41	0.90			
MAR	1	2	3	4	5	6	7	8	9	10	11	12	13	14	15	
	0.95	0.96	1.04	1.03	1.02	0.90	0.87	0.92	1.52	1.90	2.32	2.07	2.29	2.51	2.07	
	16	17	18	19	20	21	22	23	24	25	26	27	28	29	30	31
	1.50	3.00	3.07	2.17	1.74	1.58	1.41	1.55	1.33	0.79	2.79	1.76	1.93	2.46	4.41	3.89
APR	1	2	3	4	5	6	7	8	9	10	11	12	13	14	15	
	3.80	4.04	2.04	2.03	1.70	1.50	1.73	1.92	1.86	1.39	1.08	1.30	1.75	2.58	1.80	
	16	17	18	19	20	21	22	23	24	25	26	27	28	29	30	31
	1.61	0.97	0.77	0.99	0.95	1.01	0.68	0.88	0.58	0.52	0.58	0.35	0.43	0.66	0.94	
MAY	1	2	3	4	5	6	7	8	9	10	11	12	13	14	15	
	2.28	2.18	2.73	2.27	1.74	1.28	1.32	1.19	1.14	0.87	0.80	0.83	0.66	0.94	0.89	
	16	17	18	19	20	21	22	23	24	25	26	27	28	29	30	31
	0.77	0.78	1.34	1.81	1.04	0.88	0.81	0.47	0.46	0.47	0.39	0.29	0.49	0.46	0.53	0.25
JUN	1	2	3	4	5	6	7	8	9	10	11	12	13	14	15	
	0.48	0.22	0.38	0.59	0.44	0.13	0.58	0.43	0.42	0.57	0.24	0.43	0.34	0.76	0.71	
	16	17	18	19	20	21	22	23	24	25	26	27	28	29	30	31
	0.45	0.40	0.75	0.46	0.22	0.35	1.29	0.42	0.17	1.23	-0.12	0.01	-0.20	0.54	0.55	
JUL	1	2	3	4	5	6	7	8	9	10	11	12	13	14	15	
	0.43	-0.08	0.22	0.04	-0.01	0.14	-0.03	-0.19	-0.18	-0.23	0.19	-0.16	0.92	0.62	-0.04	
	16	17	18	19	20	21	22	23	24	25	26	27	28	29	30	31
	0.09	0.01	0.02	0.00	0.70	-0.07	0.32	0.06	0.53	0.05	0.06	-0.30	0.31	0.22	0.19	0.03
AUG	1	2	3	4	5	6	7	8	9	10	11	12	13	14	15	
	0.03	0.01	0.83	0.36	0.47	1.06	0.30	0.04	-0.29	0.20	0.10	-0.25	0.29	0.12	0.12	
	16	17	18	19	20	21	22	23	24	25	26	27	28	29	30	31
	-0.02	0.39	0.85	0.25	0.59	0.10	0.01	-0.01	-0.25	0.82	0.51	0.39	0.10	0.20	0.46	1.28
SEPT	1	2	3	4	5	6	7	8	9	10	11	12	13	14	15	
	1.34	0.77	0.27	0.29	0.02	0.02	0.43	0.04	-0.11	0.13	0.26	0.18	0.31	-0.21	-0.04	
	16	17	18	19	20	21	22	23	24	25	26	27	28	29	30	31
	0.30	0.13	0.93	0.53	0.95	0.18	0.53	1.23	1.56	1.31	-0.23	-0.22	0.09	0.01	0.24	
OCT	1	2	3	4	5	6	7	8	9	10	11	12	13	14	15	
	0.81	0.37	0.76	0.24	0.08	0.31	0.83	1.56	0.84	1.02	0.82	2.61	3.45	4.35	4.89	
	16	17	18	19	20	21	22	23	24	25	26	27	28	29	30	31
	5.57	3.57	3.32	1.44	0.53	0.89	0.26	0.52	1.67	1.38	1.84	3.32	3.68	4.28	3.74	3.56
NOV	1	2	3	4	5	6	7	8	9	10	11	12	13	14	15	
	3.99	4.59	3.79	3.44	3.75	2.60	2.45	2.05	1.65	1.84	3.41	3.57	2.01	1.97	2.08	
	16	17	18	19	20	21	22	23	24	25	26	27	28	29	30	31
	3.70	2.93	2.66	1.97	1.63	1.53	1.55	2.49	2.77	2.72	2.28	1.84	1.46	1.82	2.04	
DEC	1	2	3	4	5	6	7	8	9	10	11	12	13	14	15	
	2.17	1.14	1.71	1.42	1.26	1.03	1.09	1.84	2.39	2.21	1.43	1.06	1.14	0.73	0.81	
	16	17	18	19	20	21	22	23	24	25	26	27	28	29	30	31
	0.59	0.94	0.62	2.41	3.07	2.75	3.51	4.01	3.06	2.62	2.83	2.52	2.47	1.68	2.01	3.29

Table 36. Synthetic daily inflow variance from spatial disaggregation for Pit River in $1x10^5$ $(m^3)^2$ from 50 simulations of 61 year ensembles using random annual inflow selection.

VAR	1	2	3	4	5	6	7	8	9	10	11	12	13	14	15	
JAN	262	285	261	169	124	95	84	57	96	85	76	112	239	286	381	
	16	17	18	19	20	21	22	23	24	25	26	27	28	29	30	31
	668	694	589	567	412	556	602	900	822	607	480	403	238	188	137	127
FEB	1	2	3	4	5	6	7	8	9	10	11	12	13	14	15	
	123	129	137	115	101	98	114	107	145	114	95	104	111	112	111	
	16	17	18	19	20	21	22	23	24	25	26	27	28			
	186	345	384	468	514	415	336	255	211	170	135	121	126			
MAR	1	2	3	4	5	6	7	8	9	10	11	12	13	14	15	
	130	120	112	114	99	99	96	108	160	163	192	192	192	174	153	
	16	17	18	19	20	21	22	23	24	25	26	27	28	29	30	31
	127.3	167.2	167.9	146.4	116.4	90.5	87.1	77.9	88.0	97.4	163.1	120.5	132.7	178.7	256.0	245.4
APR	1	2	3	4	5	6	7	8	9	10	11	12	13	14	15	
	249	269	163	154	128	131	147	148	145	133	117	123	114	156	116	
	16	17	18	19	20	21	22	23	24	25	26	27	28	29	30	31
	94.1	78.6	81.8	84.4	69.9	66.9	68.3	56.2	57.9	56.8	52.4	56.7	54.1	58.9	59.3	
MAY	1	2	3	4	5	6	7	8	9	10	11	12	13	14	15	
	74.5	76.5	75.2	71.0	61.8	64.7	52.1	58.8	63.1	65.3	61.6	57.8	56.8	54.2	51.8	
	16	17	18	19	20	21	22	23	24	25	26	27	28	29	30	31
	58.1	50.2	82.3	107.7	71.3	53.2	61.7	63.8	45.1	38.5	44.6	36.1	31.6	34.0	34.6	34.8
JUN	1	2	3	4	5	6	7	8	9	10	11	12	13	14	15	
	32.6	22.3	25.4	24.1	26.8	29.7	31.6	32.8	33.8	28.4	27.2	30.7	31.5	26.2	24.6	
	16	17	18	19	20	21	22	23	24	25	26	27	28	29	30	31
	28.5	20.6	27.0	18.0	19.4	18.2	22.0	26.7	19.2	19.8	19.0	18.5	18.9	16.7	22.5	
JUL	1	2	3	4	5	6	7	8	9	10	11	12	13	14	15	
	19.3	16.0	15.6	16.1	15.5	12.6	13.4	13.5	14.8	15.4	14.0	19.6	18.3	19.4	12.2	
	16	17	18	19	20	21	22	23	24	25	26	27	28	29	30	31
	12.0	14.8	14.4	16.7	13.5	14.4	20.2	15.2	16.2	15.2	14.1	11.9	16.2	17.3	14.3	14.5
AUG	1	2	3	4	5	6	7	8	9	10	11	12	13	14	15	
	13.4	15.7	18.5	17.2	16.1	16.9	17.1	14.3	12.9	12.4	10.8	10.3	13.8	12.9	15.5	
	16	17	18	19	20	21	22	23	24	25	26	27	28	29	30	31
	12.1	11.9	17.9	16.8	14.7	14.1	16.4	10.1	10.0	16.0	14.2	14.1	13.0	10.5	9.8	11.8
SEPT	1	2	3	4	5	6	7	8	9	10	11	12	13	14	15	
	14.3	14.6	11.9	14.5	14.2	12.9	14.0	11.4	11.8	10.2	15.1	12.4	15.1	12.4	11.4	
	16	17	18	19	20	21	22	23	24	25	26	27	28	29	30	31
	14.1	9.4	13.0	12.7	14.1	12.6	12.1	13.6	15.8	13.0	6.5	10.1	8.7	10.3	9.6	
OCT	1	2	3	4	5	6	7	8	9	10	11	12	13	14	15	
	9.56	9.58	12.24	10.88	13.11	9.71	14.94	16.10	12.42	10.34	13.72	13.93	25.00	30.15	32.13	
	16	17	18	19	20	21	22	23	24	25	26	27	28	29	30	31
	34.2	28.5	23.0	11.0	14.9	10.7	8.7	13.5	22.6	21.4	20.0	40.2	30.7	37.2	39.8	37.9
NOV	1	2	3	4	5	6	7	8	9	10	11	12	13	14	15	
	37.1	32.3	34.5	37.7	35.5	31.2	28.5	22.9	22.5	28.1	59.2	57.5	35.4	37.2	40.5	
	16	17	18	19	20	21	22	23	24	25	26	27	28	29	30	31
	74.8	70.5	47.9	32.8	31.0	27.3	26.8	33.7	42.6	30.5	27.0	25.6	27.2	23.4	33.0	
DEC	1	2	3	4	5	6	7	8	9	10	11	12	13	14	15	
	49.1	39.1	38.5	33.2	33.6	31.4	34.7	32.2	42.0	39.1	43.1	45.4	34.7	43.5	43.0	
	16	17	18	19	20	21	22	23	24	25	26	27	28	29	30	31
	39.4	44.6	27.1	65.2	92.9	107.8	157.9	179.6	106.1	97.1	89.7	90.0	125.9	125.9	132.6	251.9

Table 37. Synthetic daily mean inflow from spatial disaggregation for McCould River in1x10^3 m^3 from 50 simulations of 61 year ensembles using random annual inflow selection.

AVG	1	2	3	4	5	6	7	8	9	10	11	12	13	14	15	
JAN	1730	1445	1198	1128	1142	1128	1220	1294	1768	1474	1425	1663	1989	2078	2025	
	16	17	18	19	20	21	22	23	24	25	26	27	28	29	30	31
		2884	2225	1946	1866	2001	1934	1815	2212	1968	1492	1551	1632	1489	1555	1439
FEB	1	2	3	4	5	6	7	8	9	10	11	12	13	14	15	
	1581	1453	1431	1468	1715	1652	1774	1837	1825	1739	1659	1853	2020	1935	1922	
	16	17	18	19	20	21	22	23	24	25	26	27	28			
	2006	2303	2322	2188	2003	1994	1794	1794	1848	1805	1747	1661	1722			
MAR	1	2	3	4	5	6	7	8	9	10	11	12	13	14	15	
	1943	1951	1829	1664	1693	1644	1588	1728	1997	1926	1898	1876	1768	1655	1688	
	16	17	18	19	20	21	22	23	24	25	26	27	28	29	30	31
	1797	1788	1737	1720	1599	1584	1565	1624	1734	1743	1691	1601	1695	1791	2175	1824
APR	1	2	3	4	5	6	7	8	9	10	11	12	13	14	15	
	1709	1639	1558	1534	1594	1642	1748	1591	1517	1498	1526	1643	1652	1746	1669	
	16	17	18	19	20	21	22	23	24	25	26	27	28	29	30	31
	1570	1489	1445	1378	1342	1328	1317	1308	1309	1300	1276	1296	1304	1305	1291	
MAY	1	2	3	4	5	6	7	8	9	10	11	12	13	14	15	
	1256	1241	1239	1218	1227	1196	1194	1231	1275	1233	1179	1142	1114	1090	1063	
	16	17	18	19	20	21	22	23	24	25	26	27	28	29	30	31
	1065	1052	1214	1293	1179	1109	1086	1084	1038	1013	1012	1035	1046	984	964	958
JUN	1	2	3	4	5	6	7	8	9	10	11	12	13	14	15	
	939	932	887	871	869	861	853	862	834	801	786	773	757	744	739	
	16	17	18	19	20	21	22	23	24	25	26	27	28	29	30	31
	728	724	718	711	699	689	679	673	668	660	657	655	649	645	643	
JUL	1	2	3	4	5	6	7	8	9	10	11	12	13	14	15	
	642	634	626	620	615	612	608	606	611	600	595	592	590	586	584	
	16	17	18	19	20	21	22	23	24	25	26	27	28	29	30	31
	581	578	575	572	569	567	564	562	559	557	556	552	550	549	547	545
AUG	1	2	3	4	5	6	7	8	9	10	11	12	13	14	15	
	542	540	538	537	536	535	533	532	530	527	526	523	523	521	521	
	16	17	18	19	20	21	22	23	24	25	26	27	28	29	30	31
	523	518	518	518	519	517	516	515	514	513	513	512	515	516	512	511
SEPT	1	2	3	4	5	6	7	8	9	10	11	12	13	14	15	
	513	517	516	515	515	514	514	518	518	517	513	512	512	512	512	
	16	17	18	19	20	21	22	23	24	25	26	27	28	29	30	31
	513	519	526	526	519	512	510	510	510	511	511	525	518	515	511	
OCT	1	2	3	4	5	6	7	8	9	10	11	12	13	14	15	
	510	511	509	508	509	511	516	511	519	552	568	641	609	615	570	
	16	17	18	19	20	21	22	23	24	25	26	27	28	29	30	31
	560	541	540	530	531	536	559	607	573	570	561	563	622	667	662	588
NOV	1	2	3	4	5	6	7	8	9	10	11	12	13	14	15	
	559	552	552	568	596	643	649	671	706	785	1013	1013	852	891	924	
	16	17	18	19	20	21	22	23	24	25	26	27	28	29	30	31
	1056	982	847	813	825	792	761	823	842	793	788	758	757	771	1006	
DEC	1	2	3	4	5	6	7	8	9	10	11	12	13	14	15	
	1187	1187	1082	1001	968	1037	960	961	1018	1088	1154	1025	932	1041	1129	
	16	17	18	19	20	21	22	23	24	25	26	27	28	29	30	31
	1182	1067	1005	1204	1477	1859	1692	1398	1144	1010	1071	1201	1415	1320	1310	1540

Table 38. Synthetic daily inflow variance from spatial disaggregation for McCloud River in 1x10^5 (m^3)^2 from 50 simulations of 61 year ensembles using random annual inflow selection.

VAR	1	2	3	4	5	6	7	8	9	10	11	12	13	14	15	
JAN	261.7	82.7	27.8	16.8	15.1	18.0	29.6	21.9	101.0	37.4	29.6	61.4	75.2	86.5	75.7	
	16	17	18	19	20	21	22	23	24	25	26	27	28	29	30	31
	386.8	112.9	56.4	50.5	60.7	60.5	64.8	253.0	180.3	39.8	32.4	52.2	21.8	33.3	19.8	20.2
FEB	1	2	3	4	5	6	7	8	9	10	11	12	13	14	15	
	26.8	19.4	22.8	20.3	30.4	25.2	41.3	50.7	39.9	35.8	24.4	33.2	46.1	35.6	44.9	
	16	17	18	19	20	21	22	23	24	25	26	27	28			
	60.4	102.2	115.0	81.5	46.2	51.6	35.5	31.1	55.5	58.4	40.0	25.4	19.6			
MAR	1	2	3	4	5	6	7	8	9	10	11	12	13	14	15	
	31.7	31.4	20.3	12.3	18.2	12.7	9.9	18.0	44.8	41.0	44.1	24.4	24.2	27.5	24.2	
	16	17	18	19	20	21	22	23	24	25	26	27	28	29	30	31
	19.7	21.1	18.9	19.1	11.1	16.6	12.7	14.3	28.2	16.4	14.5	9.8	18.2	35.9	172.3	41.9
APR	1	2	3	4	5	6	7	8	9	10	11	12	13	14	15	
	29.0	24.7	18.1	17.1	28.0	23.9	36.3	21.2	15.3	13.9	15.4	30.1	31.2	46.4	37.2	
	16	17	18	19	20	21	22	23	24	25	26	27	28	29	30	31
	26.7	18.6	15.0	12.3	10.3	9.8	9.5	8.9	8.4	8.0	7.8	9.0	9.5	9.7	10.0	
MAY	1	2	3	4	5	6	7	8	9	10	11	12	13	14	15	
	9.0	8.6	7.9	7.6	8.2	7.8	7.8	8.7	10.0	8.6	7.5	7.1	6.5	6.3	5.9	
	16	17	18	19	20	21	22	23	24	25	26	27	28	29	30	31
	5.8	5.7	11.4	17.4	9.0	7.0	6.3	6.2	5.6	5.2	5.1	5.6	6.2	5.1	4.8	4.7
JUN	1	2	3	4	5	6	7	8	9	10	11	12	13	14	15	
	4.3	4.5	4.0	3.7	3.7	3.8	3.9	5.0	4.5	3.7	3.4	3.4	3.1	2.9	2.8	
	16	17	18	19	20	21	22	23	24	25	26	27	28	29	30	31
	2.8	2.7	2.6	2.6	2.5	2.5	2.4	2.4	2.3	2.2	2.2	2.1	2.1	2.1	2.0	
JUL	1	2	3	4	5	6	7	8	9	10	11	12	13	14	15	
	2.0	1.9	1.9	1.9	1.9	1.8	1.8	1.8	1.8	1.8	1.7	1.7	1.7	1.7	1.7	
	16	17	18	19	20	21	22	23	24	25	26	27	28	29	30	31
	1.7	1.7	1.7	1.6	1.6	1.6	1.6	1.6	1.6	1.6	1.6	1.6	1.6	1.6	1.5	1.5
AUG	1	2	3	4	5	6	7	8	9	10	11	12	13	14	15	
	1.5	1.5	1.5	1.5	1.5	1.5	1.5	1.5	1.5	1.4	1.4	1.4	1.4	1.4	1.4	
	16	17	18	19	20	21	22	23	24	25	26	27	28	29	30	31
	1.4	1.4	1.4	1.4	1.4	1.4	1.4	1.4	1.3	1.3	1.4	1.4	1.4	1.4	1.4	1.3
SEPT	1	2	3	4	5	6	7	8	9	10	11	12	13	14	15	
	1.3	1.3	1.3	1.3	1.3	1.2	1.2	1.3	1.3	1.2	1.2	1.2	1.3	1.2	1.2	
	16	17	18	19	20	21	22	23	24	25	26	27	28	29	30	31
	1.2	1.2	1.4	1.3	1.2	1.2	1.2	1.2	1.2	1.2	1.2	1.5	1.3	1.2	1.2	
OCT	1	2	3	4	5	6	7	8	9	10	11	12	13	14	15	
	1.2	1.2	1.2	1.2	1.2	1.2	1.2	1.2	1.3	2.1	2.8	10.7	6.2	4.4	2.1	
	16	17	18	19	20	21	22	23	24	25	26	27	28	29	30	31
	1.9	1.5	1.5	1.3	1.3	1.2	1.3	2.0	1.4	1.4	1.5	1.8	6.9	14.8	11.8	3.0
NOV	1	2	3	4	5	6	7	8	9	10	11	12	13	14	15	
	1.9	1.6	1.4	1.5	1.7	2.6	2.1	3.3	4.1	12.8	63.5	57.8	16.0	12.2	14.5	
	16	17	18	19	20	21	22	23	24	25	26	27	28	29	30	31
	35.0	22.9	12.1	6.6	6.1	4.5	3.5	4.5	4.6	3.4	4.0	3.1	2.9	2.9	16.4	
DEC	1	2	3	4	5	6	7	8	9	10	11	12	13	14	15	
	37.3	19.8	12.6	11.0	10.8	10.6	6.1	7.3	9.5	18.4	24.9	9.4	5.3	8.7	18.8	
	16	17	18	19	20	21	22	23	24	25	26	27	28	29	30	31
	20.2	13.1	8.9	28.3	104.9	207.2	162.4	63.4	17.8	9.0	14.3	24.1	55.5	28.6	30.7	67.9

Table 39. Synthetic daily inflow skew from spatial disaggregation for McCloud River from 50 simulations of 61 year ensembles using random annual inflow selection.

SKEW	1	2	3	4	5	6	7	8	9	10	11	12	13	14	15	
JAN	7.7	6.0	4.2	2.9	2.3	3.3	4.6	2.3	3.7	3.1	3.3	3.6	2.8	2.9	2.9	
	16	17	18	19	20	21	22	23	24	25	26	27	28	29	30	31
	5.2	3.5	3.0	2.7	2.3	2.8	4.1	5.6	5.6	4.7	3.1	3.9	2.4	3.5	2.9	1.6
FEB	1	2	3	4	5	6	7	8	9	10	11	12	13	14	15	
	2.1	1.9	2.9	2.6	2.1	2.2	3.3	3.0	2.5	3.0	1.9	1.7	2.3	2.3	2.7	
	16	17	18	19	20	21	22	23	24	25	26	27	28			
	3.3	3.5	3.4	2.9	2.4	3.1	4.7	2.9	4.0	5.1	4.0	2.9	2.0			
MAR	1	2	3	4	5	6	7	8	9	10	11	12	13	14	15	
	2.5	2.6	2.5	1.7	3.5	2.0	1.6	2.0	2.6	3.4	4.7	2.6	3.6	5.9	5.7	
	16	17	18	19	20	21	22	23	24	25	26	27	28	29	30	31
	2.5	2.8	2.8	2.5	1.7	3.7	2.9	2.9	4.1	2.1	1.8	1.1	2.5	3.9	6.0	3.7
APR	1	2	3	4	5	6	7	8	9	10	11	12	13	14	15	
	3.1	2.9	2.4	2.1	3.9	2.5	3.1	2.2	1.7	1.6	1.5	2.7	2.6	3.1	3.0	
	16	17	18	19	20	21	22	23	24	25	26	27	28	29	30	31
	2.4	2.0	1.6	1.5	1.4	1.3	1.3	1.1	0.9	0.8	0.8	1.0	1.0	1.0	1.2	
MAY	1	2	3	4	5	6	7	8	9	10	11	12	13	14	15	
	1.1	1.1	0.9	0.9	0.9	0.9	1.0	1.2	1.1	1.0	1.0	1.0	0.9	0.9	0.9	
	16	17	18	19	20	21	22	23	24	25	26	27	28	29	30	31
	0.9	1.0	1.8	2.5	1.0	0.9	0.9	0.9	0.9	0.9	0.9	0.9	1.2	1.0	1.0	0.9
JUN	1	2	3	4	5	6	7	8	9	10	11	12	13	14	15	
	0.8	1.1	1.1	1.1	1.0	1.0	1.2	2.0	1.7	1.3	1.2	1.3	1.2	1.2	1.2	
	16	17	18	19	20	21	22	23	24	25	26	27	28	29	30	31
	1.2	1.2	1.2	1.2	1.3	1.2	1.2	1.3	1.3	1.2	1.2	1.2	1.2	1.2	1.2	
JUL	1	2	3	4	5	6	7	8	9	10	11	12	13	14	15	
	1.19	1.20	1.20	1.21	1.20	1.20	1.21	1.20	1.12	1.20	1.20	1.20	1.20	1.21	1.21	
	16	17	18	19	20	21	22	23	24	25	26	27	28	29	30	31
	1.22	1.23	1.23	1.21	1.22	1.22	1.23	1.27	1.28	1.29	1.26	1.24	1.21	1.24	1.23	1.22
AUG	1	2	3	4	5	6	7	8	9	10	11	12	13	14	15	
	1.21	1.21	1.21	1.20	1.18	1.18	1.18	1.18	1.17	1.18	1.17	1.17	1.16	1.16	1.16	
	16	17	18	19	20	21	22	23	24	25	26	27	28	29	30	31
	1.16	1.17	1.17	1.17	1.16	1.16	1.16	1.16	1.16	1.16	1.16	1.16	1.21	1.17	1.16	1.16
SEPT	1	2	3	4	5	6	7	8	9	10	11	12	13	14	15	
	1.16	1.15	1.15	1.15	1.15	1.14	1.14	1.18	1.18	1.15	1.17	1.16	1.18	1.16	1.15	
	16	17	18	19	20	21	22	23	24	25	26	27	28	29	30	31
	1.15	1.13	1.22	1.16	1.13	1.14	1.15	1.17	1.15	1.15	1.15	1.87	1.24	1.13	1.14	
OCT	1	2	3	4	5	6	7	8	9	10	11	12	13	14	15	
	1.13	1.12	1.13	1.13	1.12	1.13	1.12	1.11	1.13	2.35	3.30	6.50	5.70	3.37	1.94	
	16	17	18	19	20	21	22	23	24	25	26	27	28	29	30	31
	1.80	1.29	1.24	1.19	1.12	1.08	0.90	1.42	0.98	1.00	1.42	2.29	6.67	7.67	7.49	4.30
NOV	1	2	3	4	5	6	7	8	9	10	11	12	13	14	15	
	2.60	1.85	1.54	1.36	1.25	1.60	1.20	2.71	2.15	4.83	5.80	5.77	4.95	3.23	3.35	
	16	17	18	19	20	21	22	23	24	25	26	27	28	29	30	31
	4.32	3.86	3.82	2.87	2.33	2.14	1.55	1.56	1.74	1.11	1.72	1.14	1.23	1.09	3.13	
DEC	1	2	3	4	5	6	7	8	9	10	11	12	13	14	15	
	4.11	2.32	2.10	3.68	4.73	2.77	1.46	2.36	2.19	3.64	4.25	2.55	1.93	2.00	4.67	
	16	17	18	19	20	21	22	23	24	25	26	27	28	29	30	31
	3.36	2.93	1.98	4.60	6.77	6.30	7.16	6.61	4.78	3.75	3.68	3.58	3.87	2.88	3.22	3.73

Appendix B: Additional Monthly Weather Statistics

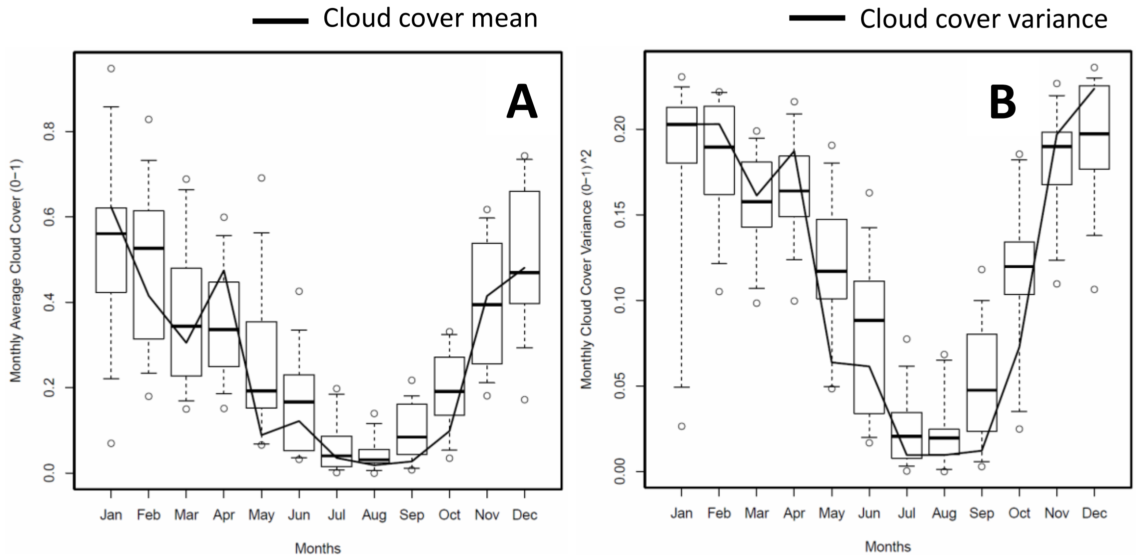

Figure 36. Statistical analysis of cloud cover generation using median synthetic streamflow year as input from 50 simulations of 61 year ensembles of the streamflow generator using random annual inflow selection. Solid lines represent simulated statistics. Boxplots represent interquartile range of historical statistics: (A) mean monthly cloud cover; (B) mean monthly cloud cover variance.

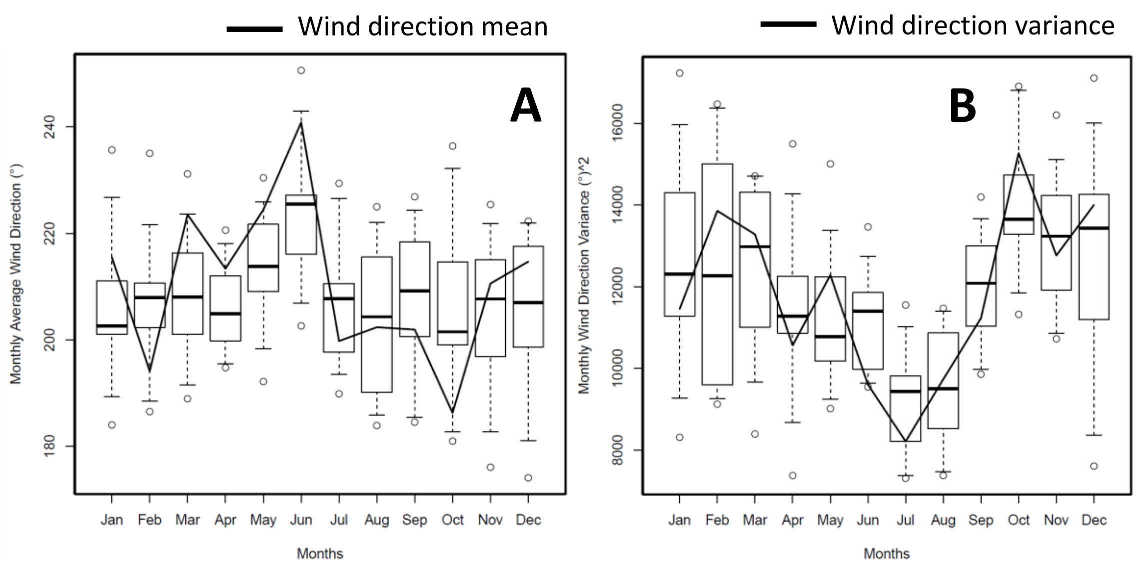

Figure 37. Statistical analysis of wind direction generation using median synthetic streamflow year as input from 50 simulations of 61 year ensembles of the streamflow generator using random annual inflow selection. Solid lines represent simulated statistics. Boxplots represent interquartile range of historical statistics: (A) mean monthly wind direction; (B) mean monthly wind direction variance.

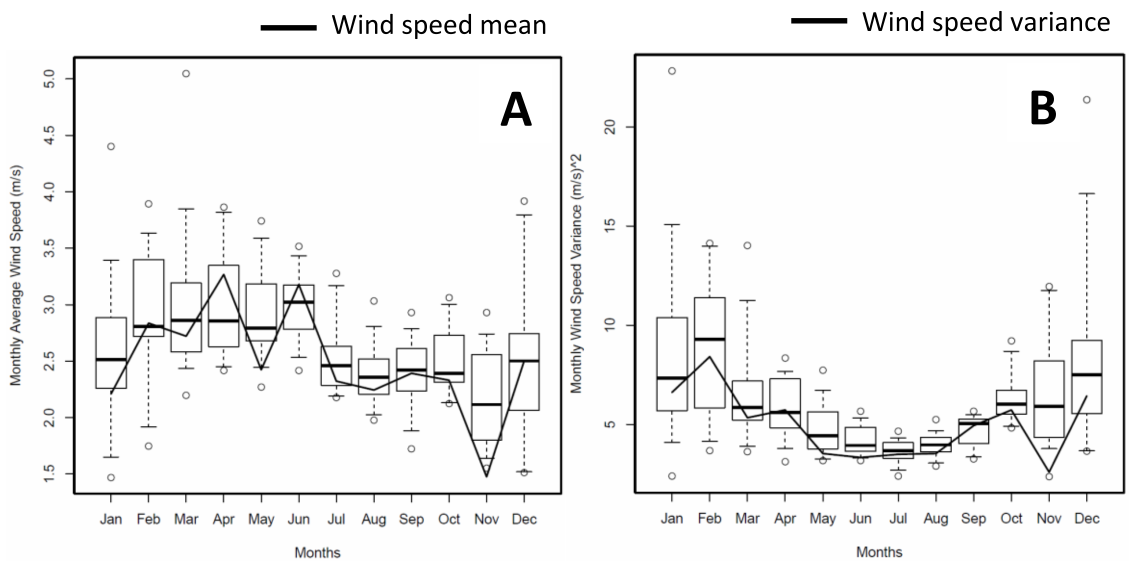

Figure 38. Statistical analysis of wind speed generation using median synthetic streamflow year as input from 50 simulations of 61 year ensembles of the streamflow generator using random annual inflow selection. Solid lines represent simulated statistics. Boxplots represent interquartile range of historical statistics: (A) mean monthly wind speed; (B) mean monthly wind speed variance.

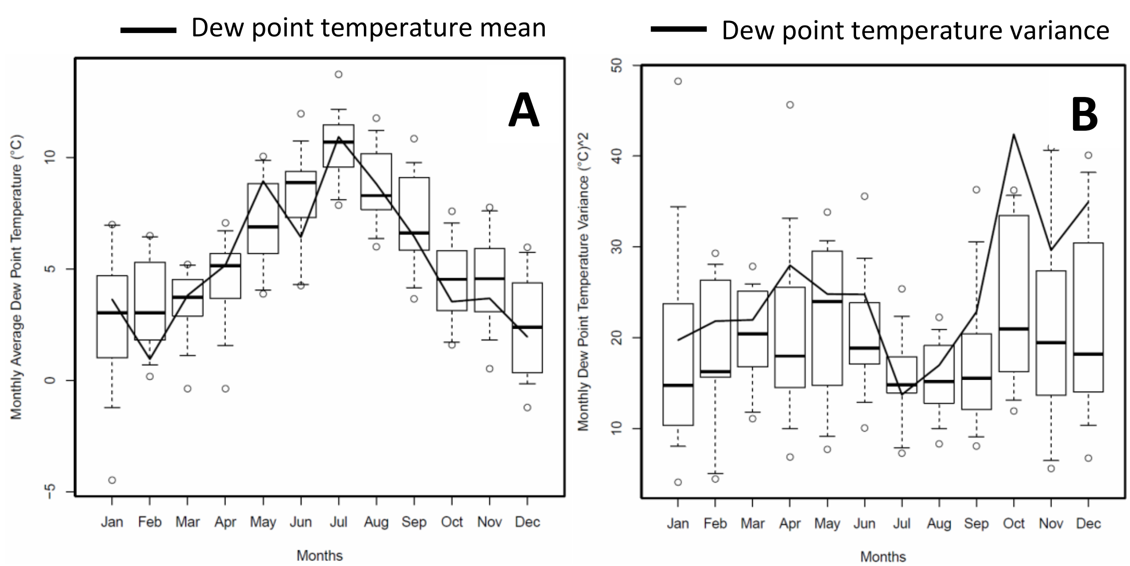

Figure 39. Statistical analysis of dew point temperature generation using median synthetic streamflow year as input from 50 simulations of 61 year ensembles of the streamflow generator using random annual inflow selection. Solid lines represent simulated statistics. Boxplots represent interquartile range of historical statistics: (A) mean monthly dew point temperature; (B) mean monthly dew point temperature variance.

Appendix C: Additional Temperature Output Figures

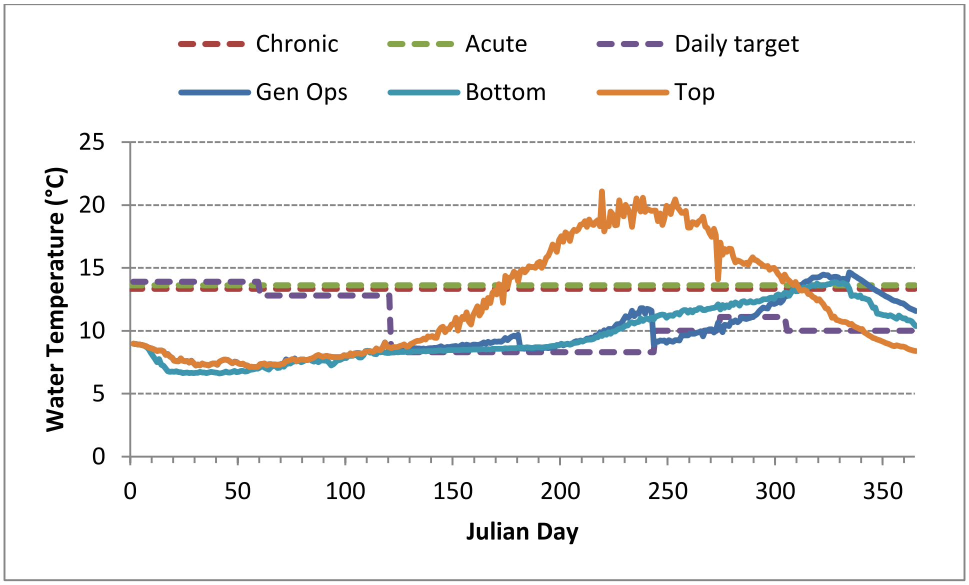

Figure 40. W2 simulated outflow temperatures for the wet year with a dry fall. Solid lines are outflow temperatures for the extreme dry year for each TCD schedule (bottom, uppermost and generalized operations). Dashed lines are the water temperature threshold standards (acute and chronic) and the outlet temperature targets.

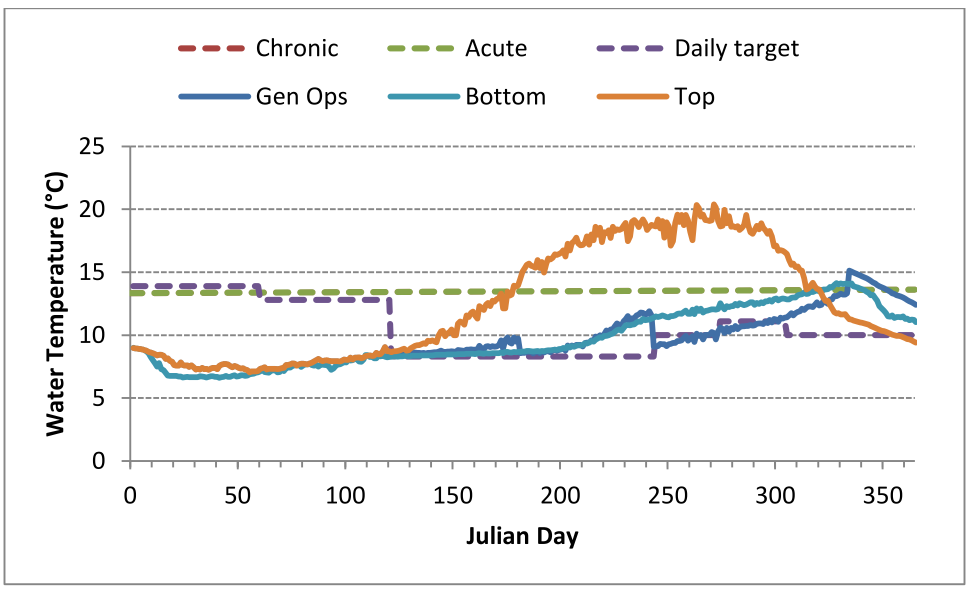

Figure 41. W2 simulated outflow temperatures for the wet year with a warm fall. Solid lines are outflow temperatures for the extreme dry year for each TCD schedule (bottom, uppermost and generalized operations). Dashed lines are the water temperature threshold standards (acute and chronic) and the outlet temperature targets.

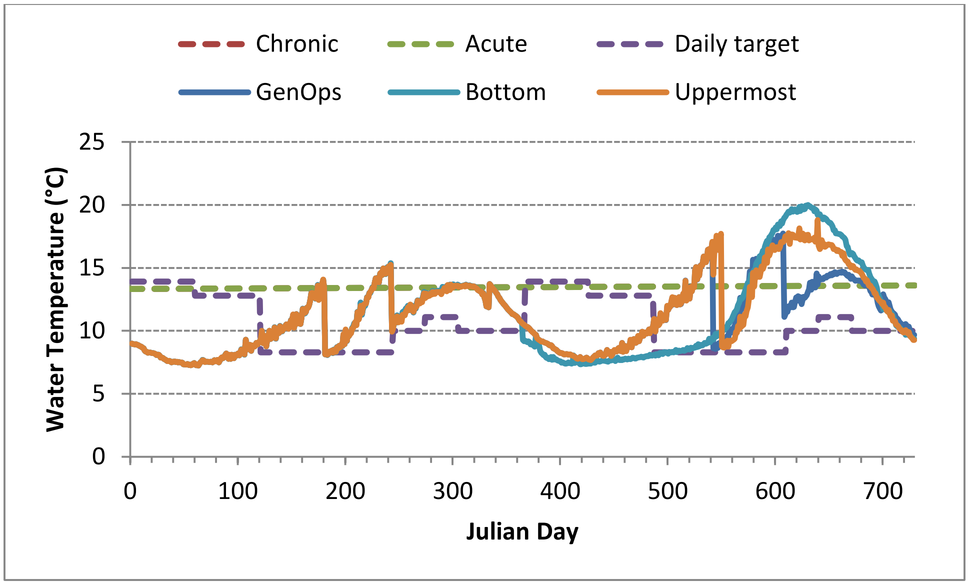

Figure 42. W2 simulated outflow temperatures for the two year drought. Solid lines are outflow temperatures for the extreme dry year for each TCD schedule (bottom, uppermost and generalized operations). Dashed lines are the water temperature threshold standards (acute and chronic) and the outlet temperature targets.

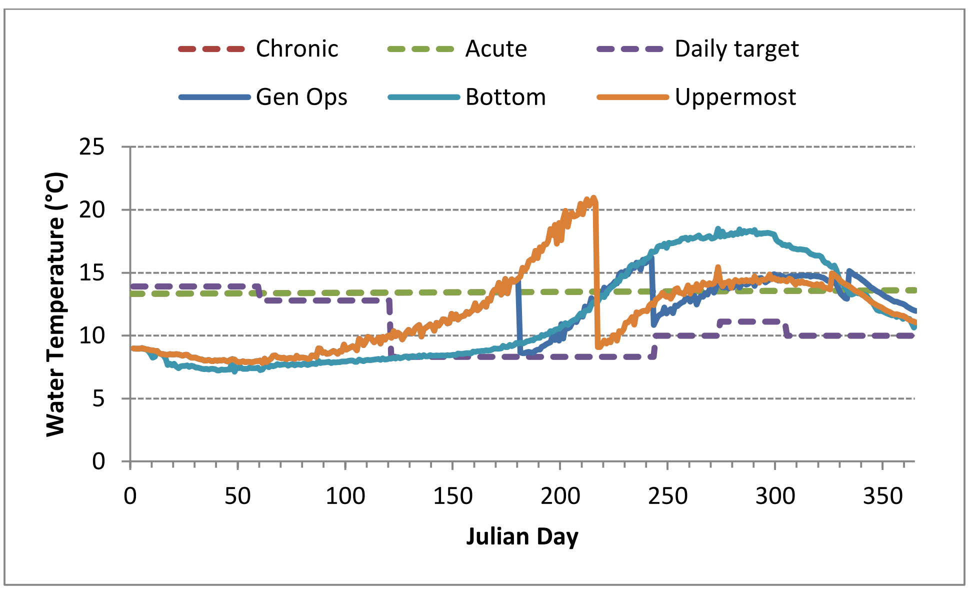

Figure 43. W2 simulated outflow temperatures for the extreme dry year with low emissions air temperature increases. Solid lines are simulated outflow temperatures for the extreme dry year for each TCD schedule (bottom, uppermost and generalized operations). Dashed lines are the water temperature threshold standards (acute and chronic) and the outlet temperature targets.

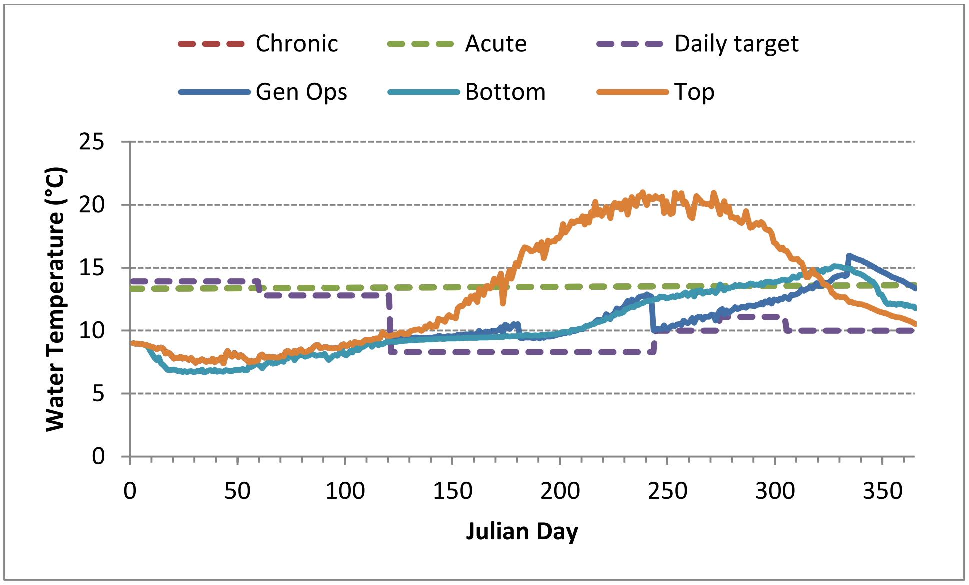

Figure 44. W2 simulated outflow temperatures for the extreme wet year with low emissions air temperature increases. Solid lines are simulated outflow temperatures for the extreme dry year for each TCD schedule (bottom, uppermost and generalized operations). Dashed lines are the water temperature threshold standards (acute and chronic) and the outlet temperature targets.

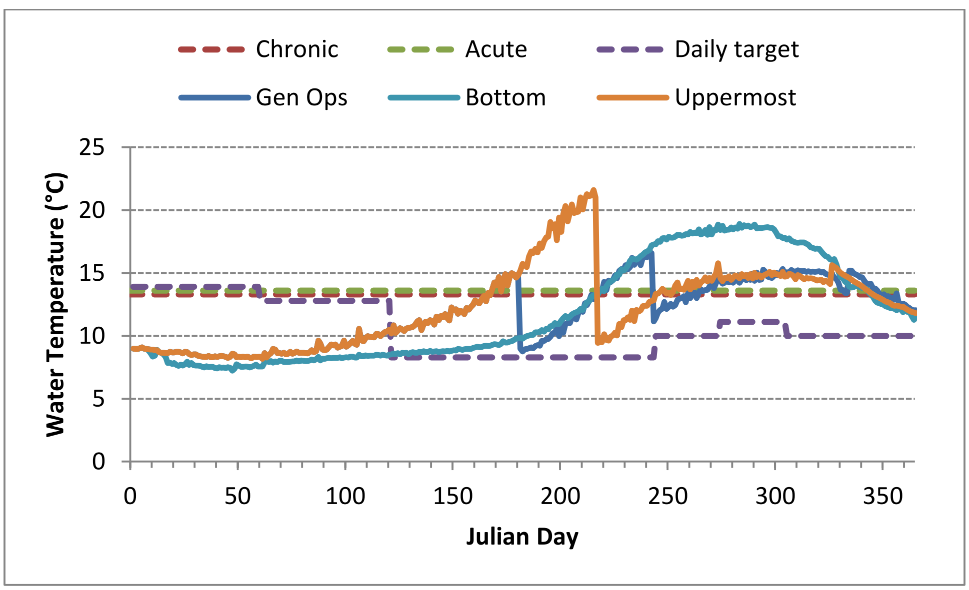

Figure 45. W2 simulated outflow temperatures for the extreme dry year with high emissions temperature increases. Solid lines are simulated outflow temperatures for the extreme dry year for each TCD schedule (bottom, uppermost and generalized operations). Dashed lines are the water temperature threshold standards (acute and chronic) and the outlet temperature targets.

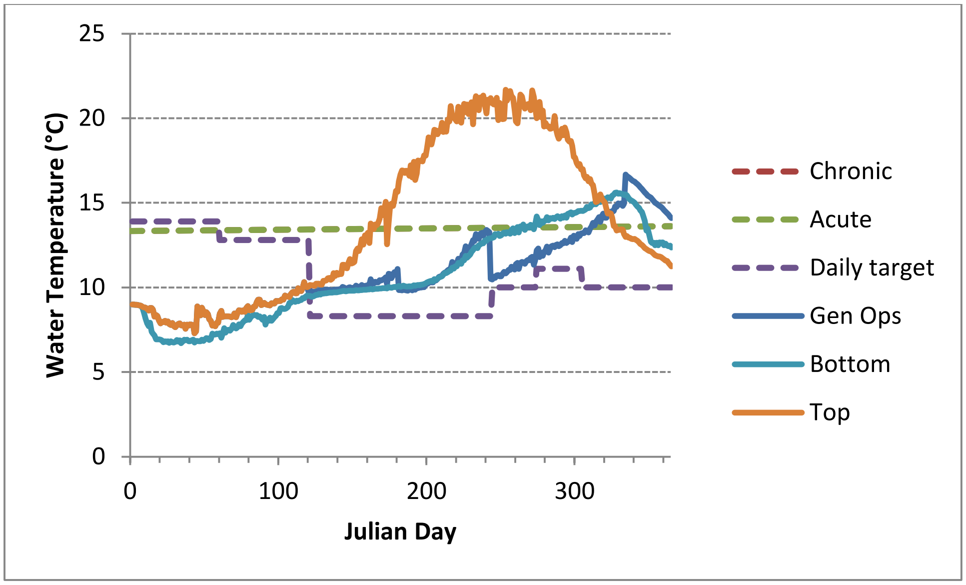

Figure 46. W2 simulated outflow temperatures for the extreme dry year. Solid lines are simulated outflow temperatures for the extreme dry year for each TCD schedule (bottom, uppermost and generalized operations). Dashed lines are the water temperature threshold standards (acute and chronic) and the outlet temperature targets.

Appendix D: Results for Climate Change Scenarios

Table 40. Low emissions climate change degree-day exceedance results (°C x days) rounded to the nearest integer organized by scenario, temperature threshold standard and TCD operations schedule. The best performing TCD schedule for each temperature standard for each scenario is bolded. "Bottom" is the all-out-the-bottom TCD schedule, "Uppermost" is the all-out-the-uppermost TCD schedule and "Gen Ops" is the generalized operations TCD schedule.

Scenario	Standard	TCD Schedule		
		Bottom	**Uppermost**	**Gen Ops**
Extreme Wet Year	Chronic	62	736	**54**
	Acute	43	693	**41**
	Temp Target	520	1514	**396**
Extreme Dry Year	Chronic	392	255	**123**
	Acute	360	220	**93**
	Temp Target	904	971	**762**

Table 41. High emissions climate change degree-day exceedance results (°C x days) rounded to the nearest integer organized by scenario, temperature threshold standard and TCD operations schedule. The best performing TCD schedule for each temperature standard for each scenario is bolded. "Bottom" is the all-out-the-bottom TCD schedule, "Uppermost" is the all-out-the-uppermost TCD schedule and "Gen Ops" is the generalized operations TCD schedule.

Scenario	Standard	TCD Schedule		
		Bottom	**Uppermost**	**Gen Ops**
Extreme Wet Year	Chronic	103	834	**91**
	Acute	80	787	**75**
	Temp Target	621	1635	**501**
Extreme Dry Year	Chronic	455	319	**166**
	Acute	420	279	**133**
	Temp Target	1004	1061	**847**

Table 42. In-reservoir cold water pool reserve for the low emissions temperature increase climate change (million cubic meters) below the cold pool temperature threshold (12.8°C) rounded to the nearest integer organized by scenario, date of calculation and TCD operations schedule model runs. The best performing TCD schedule for each calculation date for each scenario is bolded. "Bottom" is the all-out-the-bottom TCD schedule, "Uppermost" is the all-out-the-uppermost TCD schedule and "Gen Ops" is the generalized operations TCD schedule.

Scenario	Date	TCD Schedule		
		Bottom	**Uppermost**	**Gen Ops**
Extreme Wet Year	28-May	**5390**	**5390**	**5390**
	1-Nov	23	**2681**	104
	31-Dec	699	**5615**	791
Extreme Dry Year	28-May	2215	**2415**	**2415**
	1-Nov	8	**294**	40
	31-Dec	**2814**	**2814**	**2814**

Table 43. In-reservoir cold water pool reserve for the high emissions temperature increase climate change model (million cubic meters) below the cold pool temperature threshold (12.8°C) rounded to the nearest integer organized by scenario, date of calculation and TCD operations schedule runs. The best performing TCD schedule for each calculation date for each scenario is bolded. "Bottom" is the all-out-the-bottom TCD schedule, "Uppermost" is the all-out-the-uppermost TCD schedule and "Gen Ops" is the generalized operations TCD schedule.

Scenario	Standard	TCD Schedule		
		Bottom	**Uppermost**	**Gen Ops**
Extreme Wet Year	28-May	5215	**5390**	5215
	1-Nov	14	**2572**	66
	31-Dec	294	**5615**	403
Extreme Dry Year	28-May	**2215**	**2215**	**2215**
	1-Nov	8	**228**	23
	31-Dec	614	**2814**	**2814**

Appendix E: Additional Cold Pool Volume Figures

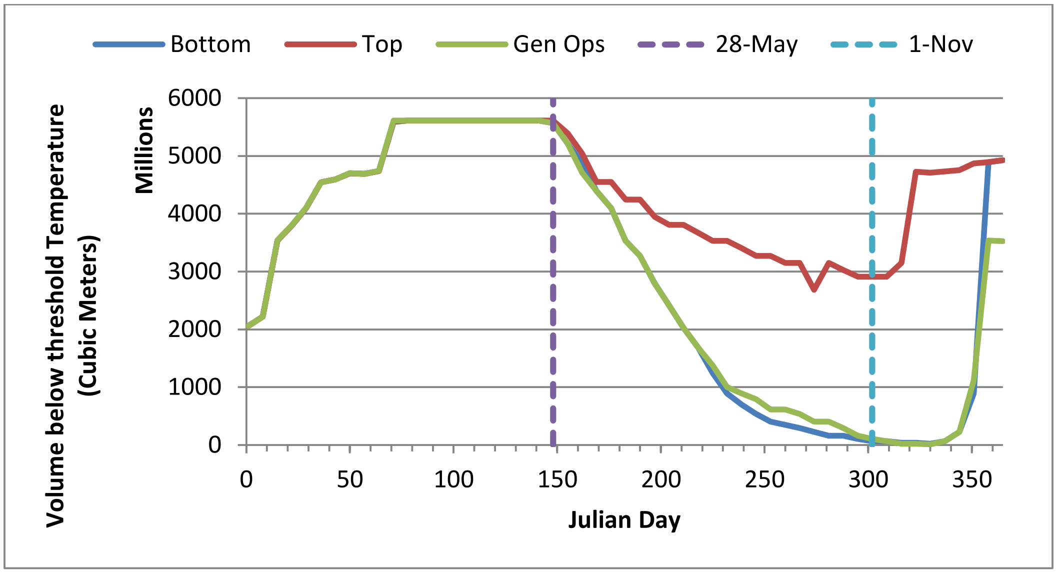

Figure 47. In-reservoir cold pool volume for the wet year with a dry fall, calculated weekly, at or below the cold pool temperature threshold of 12.8°C for each TCD Schedule (bottom, uppermost and generalized operations). "28-May" and "1-Nov" refer to their corresponding calendar dates.

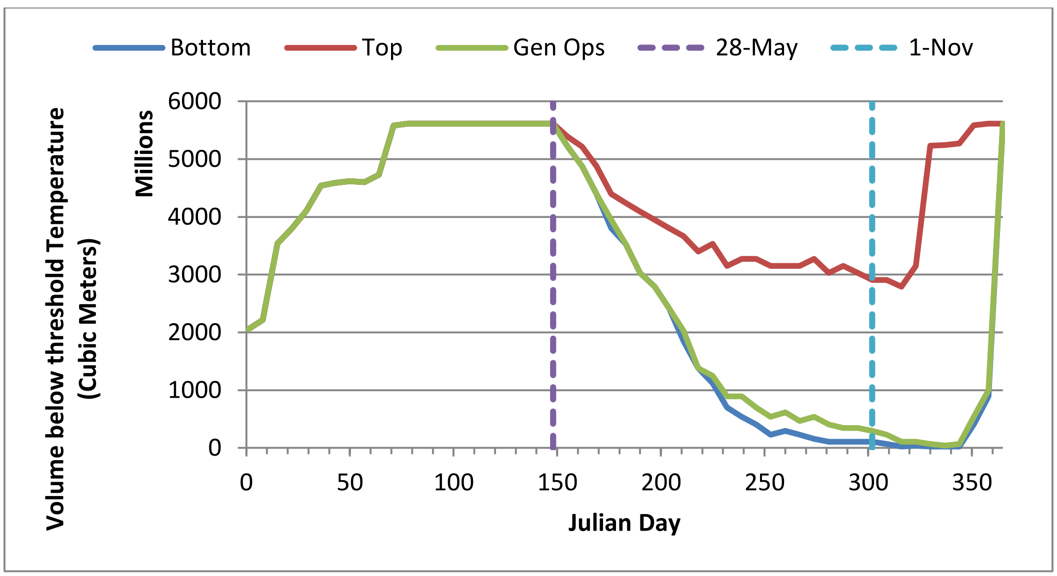

Figure 48 In-reservoir cold pool volume for the extreme wet year with a warm fall, calculated weekly, at or below the cold pool temperature threshold of 12.8°C for each TCD Schedule (bottom, uppermost and generalized operations). "28-May" and "1-Nov" refer to their corresponding calendar dates.

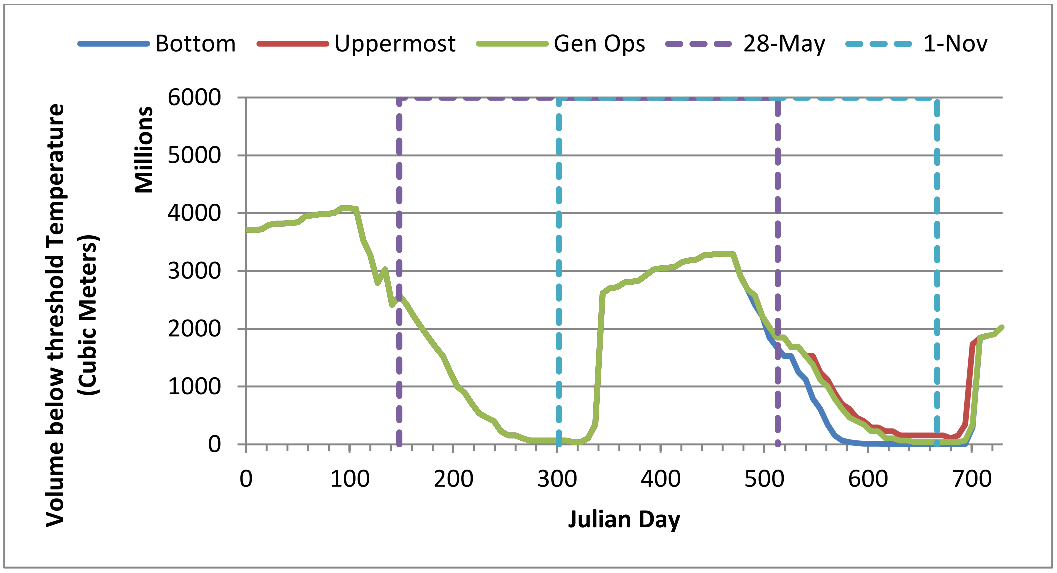

Figure 49. In-reservoir cold pool volume, calculated weekly for the two year drought, at or below the cold pool temperature threshold of 12.8°C for each TCD Schedule (bottom, uppermost and generalized operations). "28-May" and "1-Nov" refer to their corresponding calendar dates.

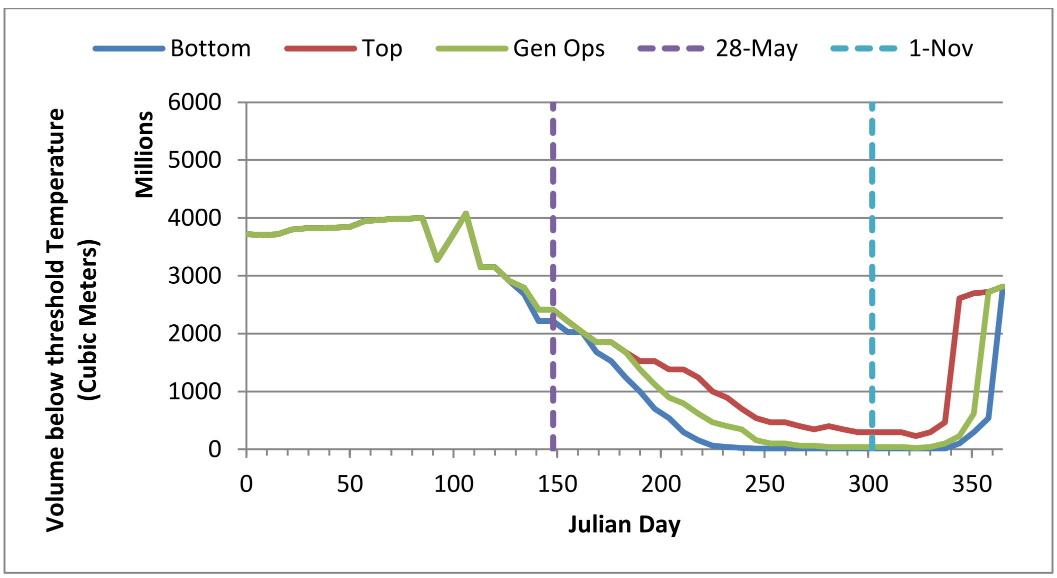

Figure 50. In-reservoir cold pool volume for the extreme dry year with low emissions air temperature increases, calculated weekly, at or below the cold pool temperature threshold of 12.8°C for each TCD Schedule (bottom, uppermost and generalized operations). "28-May" and "1-Nov" refer to their corresponding calendar dates.

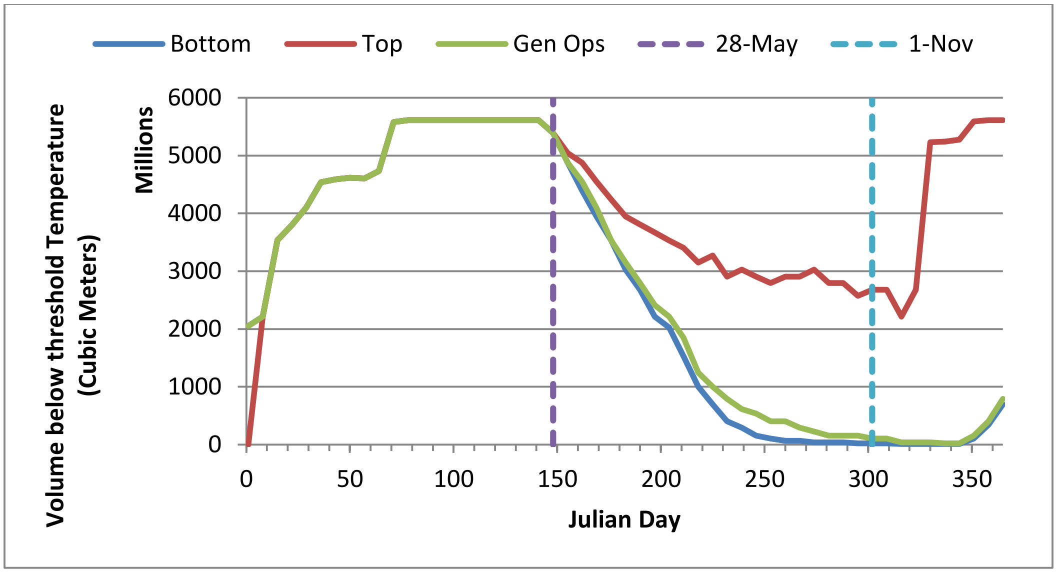

Figure 51. In-reservoir cold pool volume for the extreme wet year with low emissions temperature increases, calculated weekly, at or below the cold pool temperature threshold of 12.8°C for each TCD Schedule (bottom, uppermost and generalized operations). "28-May" and "1-Nov" refer to their corresponding calendar dates.

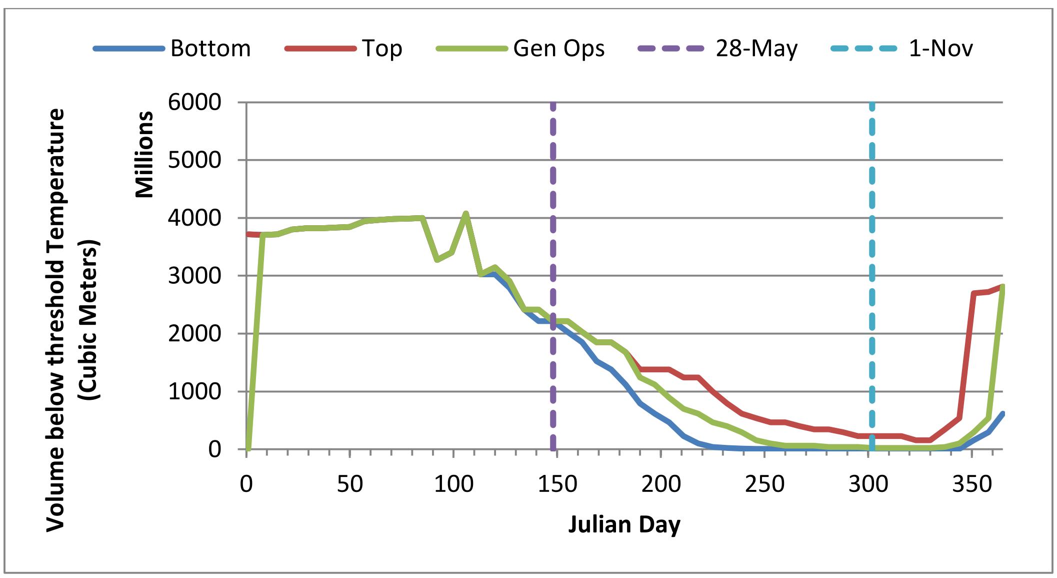

Figure 52. In-reservoir cold pool volume for the extreme dry year with high emissions air temperature increases, calculated weekly, at or below the cold pool temperature threshold of 12.8°C for each TCD Schedule (bottom, uppermost and generalized operations). "28-May" and "1-Nov" refer to their corresponding calendar dates.

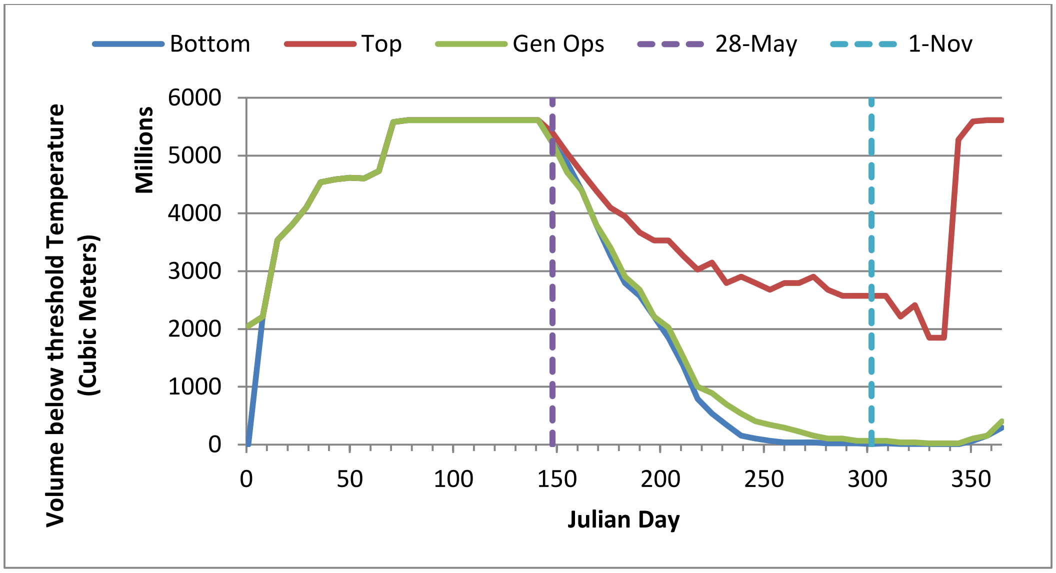

Figure 53. In-reservoir cold pool volume for the extreme wet year with high emissions air temperature increases, calculated weekly, at or below the cold pool temperature threshold of 12.8°C for each TCD Schedule (bottom, uppermost and generalized operations). "28-May" and "1-Nov" refer to their corresponding calendar dates.

Appendix F: Generalized Operations Sensitivity Analysis

A sensitivity analysis was conducted for the generalized operations schedule where the gate elevation dropdowns and increases for the generalized operations schedule was moved earlier one month and later one month (Figure 54). All schedules were adjusted for the months of December – March to run outflows through the top gate as prescribed in the methods of Hanna et al. (1999). All other methods for W2 simulation were the same as chapter 3.

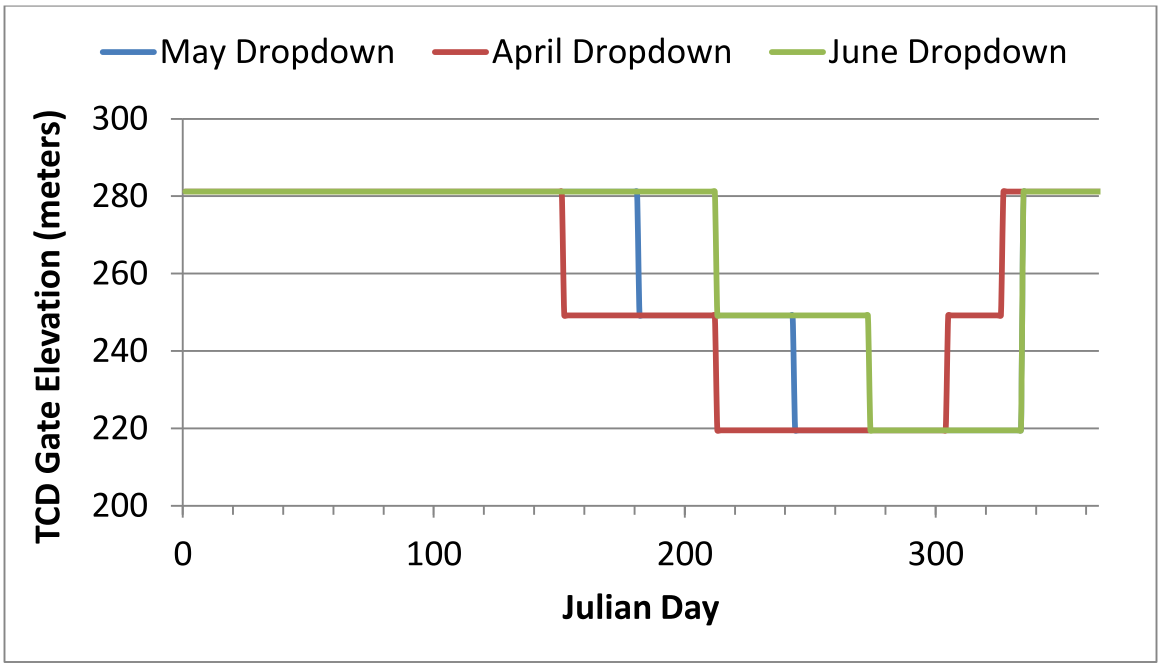

Figure 54. Changes to the dropdown schedule of the generalized operations. "May Dropdown" is the original generalized operations schedule. "April Dropdown" is the generalized operations dropdowns moved earlier one month. "June Dropdown" is the generalized operations dropdowns moved later one month.

The results for the sensitivity analysis for the extreme dry year show that the original dropdown schedule (May) reduced degree day exceedances overall. However, 1-Nov outflow temperatures for the June schedule were nearly at the temperature target while the May and June schedules were 5˚C and 10˚C higher, respectively.

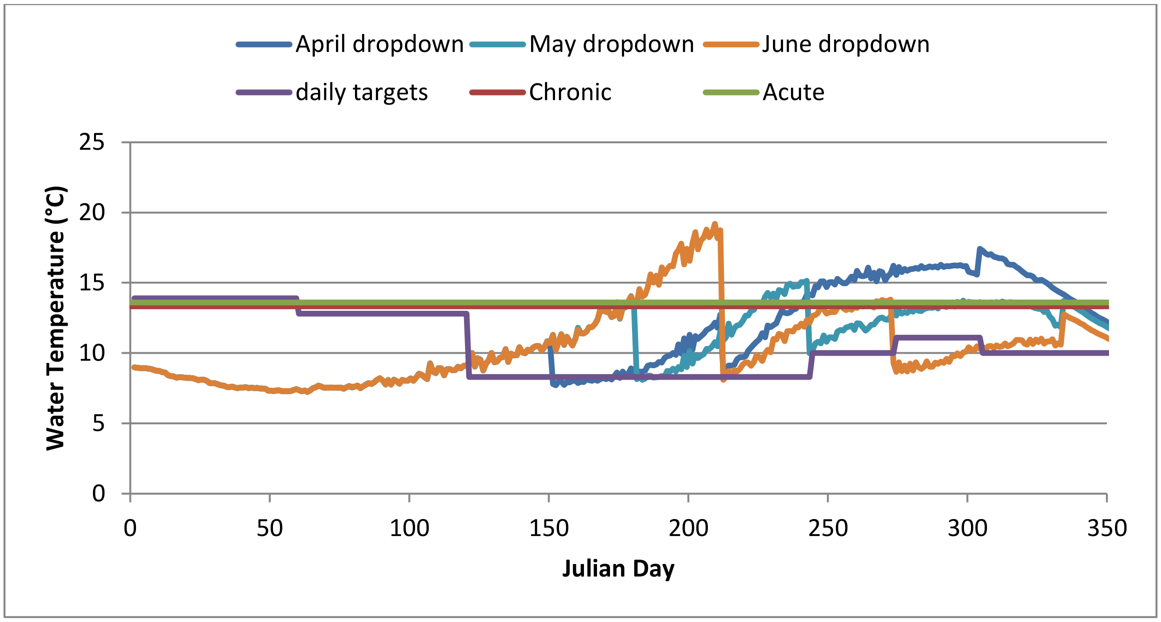

Figure 55. Sensitivity analysis outflow temperature results. "April Dropdown" is the generalized operations dropdowns moved back one month. "June Dropdown" is the generalized operations dropdowns moved forward one month.

Table 44. Sensitivity analysis degree-day exceedance results (°C x days) rounded to the nearest integer organized by scenario, temperature threshold standard and TCD operations schedule. The best performing TCD schedule for each temperature standard for each scenario is bolded. "April Dropdown" is the generalized operations dropdowns moved back one month. "June Dropdown" is the generalized operations dropdowns moved forward one month.

Scenario	**Standard**	**TCD Schedule**		
		April	May	June
Extreme Dry Year	Chronic	399	**52**	192
	Acute	349	**28**	172
	Temp Target	1264	**1030**	1084

Appendix G: Calsim2 January 1st Shasta Storage by Water Year Type

CALSIM storage was provided by Kristin White (USBR) on June 17, 2014 and are public information (http://baydeltaoffice.water.ca.gov/swpreliability/). The water year types are defined in the CalSim model files under DRR2013_FutureNoCC_082913\CONV\Run\Lookup\wytypes.table and used the "Sac Index" for determining wet (1)/critical (5). The Shasta storage results are also in the CalSim model files under DRR2013_FutureNoCC_082913\CONV\DSS\DRR2013_FutureNoCC_20130829_DV.dss and the Shasta storage is variable S4 (B part).

CalSim Shasta Storage Results organized by Wet Years on the Sacramento							CalSim Shasta Storage Results organized by Critical Years on the Sacramento				
NO CLIMATE CHANGE							NO CLIMATE CHANGE				
Date	Calendar Year	Month	Shasta Storage (TAF)	Sac River Index			Date	Calendar Year	Month	Shasta Storage (TAF)	Sac River Index
30Sep1927	1927	9	2659.4	1			30Sep1924	1924	9	845.5	5
30Sep1938	1938	9	3200.0	1			30Sep1929	1929	9	1820.6	5
30Sep1941	1941	9	3198.3	1			30Sep1931	1931	9	650.0	5
30Sep1942	1942	9	3186.6	1			30Sep1933	1933	9	789.8	5
30Sep1943	1943	9	2831.1	1			30Sep1934	1934	9	550.0	5
30Sep1952	1952	9	3360.7	1			30Sep1976	1976	9	2779.1	5
30Sep1953	1953	9	3187.7	1			30Sep1977	1977	9	588.2	5
30Sep1956	1956	9	3238.1	1			30Sep1988	1988	9	1769.8	5
30Sep1958	1958	9	3348.0	1			30Sep1990	1990	9	2129.3	5
30Sep1963	1963	9	2870.8	1			30Sep1991	1991	9	1623.6	5
30Sep1965	1965	9	3008.7	1			30Sep1992	1992	9	784.7	5
30Sep1967	1967	9	3293.1	1			30Sep1994	1994	9	1768.0	5
30Sep1969	1969	9	3200.0	1							
30Sep1970	1970	9	2315.0	1						Average:	1341.5
30Sep1971	1971	9	3291.1	1						Max:	2779.1
30Sep1974	1974	9	3364.2	1						Min:	550.0
30Sep1975	1975	9	3328.9	1							
30Sep1982	1982	9	3400.0	1							
30Sep1983	1983	9	3400.0	1							
30Sep1984	1984	9	2833.8	1							
30Sep1986	1986	9	2921.9	1							
30Sep1995	1995	9	3400.0	1							
30Sep1996	1996	9	3229.3	1							
30Sep1997	1997	9	2236.8	1							
30Sep1998	1998	9	3400.0	1							
30Sep1999	1999	9	3200.0	1							
		Average:	3111.7								
		Max:	3400.0								
		Min:	2236.8								

Appendix H: Historical TCD Operations Analysis

Arthur Dai calculated the average of the historical TCD gate levels was found by examining gate operations from 1997 to 2011 (data were missing for years 2004, 2006, 2007, and 2009). Movements between gate levels were distinguished in the following way: starting from a single elevation level, one full movement on a given day was a complete transition to an adjacent level within one day, with no gates left open on the previous level. A partial movement was a transition to an adjacent level that also kept gates open on the previous level on a given day. Many partial movements resulted in varying proportions of outflow between the gates, but all were counted as having the same change.

Historical TCD gate movements were quantified by assigning values of 7 to Side gates, 8 to Lower gates, 9 to Middle Gates, and 1 to Upper gates. Transitions between gates were accounted for by subtracting or adding 1 for a full movement and 0.5 for partial movements between gates. Using these values, a biweekly schedule of the average gate levels was calculated for a full calendar year. From that schedule of averages, Arthur Dai linearly interpolated the proportional distribution of outflows between the closest two gate levels (Table 45).

Table 45. Proportional Distribution of Average Historic Outflow through TCD gates, for years 1997 - 2011 (percent).*

	Side	Lower	Middle	Upper
1-Jan	0	45	55	0
15-Jan	0	32	68	0
1-Feb	0	14	86	0
15-Feb	0	0	91	9
1-Mar	0	0	59	41
15-Mar	0	0	36	64
1-Apr	0	0	36	64
15-Apr	0	0	45	55
1-May	0	0	55	45
15-May	0	0	82	18
1-Jun	0	0	91	9
15-Jun	0	14	86	0
1-Jul	0	41	59	0
15-Jul	0	59	41	0
1-Aug	0	95	5	0
15-Aug	18	82	0	0
1-Sep	36	64	0	0
15-Sep	55	45	0	0
1-Oct	59	41	0	0
15-Oct	59	41	0	0
1-Nov	59	41	0	0
15-Nov	59	41	0	0
1-Dec	50	50	0	0
15-Dec	0	68	32	0
*Note: Missing data for years 2004, 2006, 2007, 2009				

Appendix I: USBR Shasta Lake Flood Control Curve

Provided in a personal communication by Russ Yaworsky, USBR (June 9, 2014).

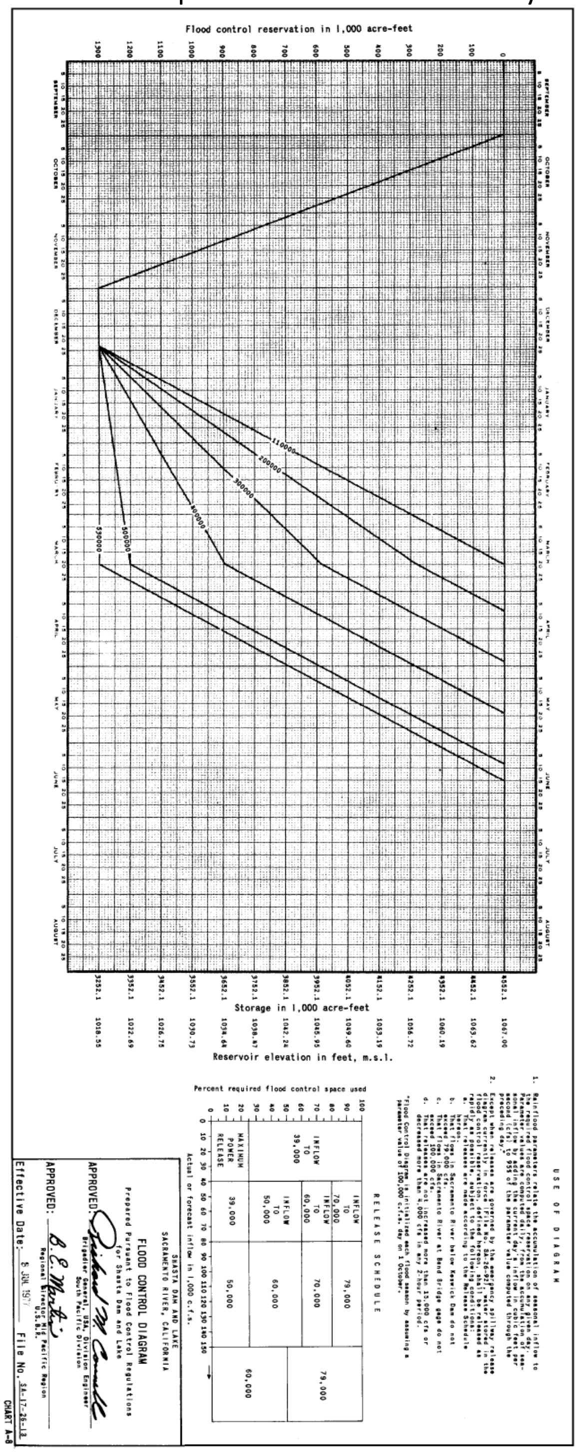

Appendix J: Correlation Analysis for Stream Temperature

Stream temperature, unfortunately, has a very limited record compared to other hydrologic and climate variables in the historical record. A correlation between stream temperature and another variable with a longer historical record would allow us to model stream temperature using a regression fit to the other variable. Therefore, the first step of this task was to determine if there was a correlation between stream temperature and other measured values in the historical record. Variables examined for correlation with stream temperature for all four tributaries included stream flow and air temperature.

All streamflow, snowpack and air temperature datasets were analyzed for correlation with the stream temperature datasets. In most cases, datasets were analyzed for many different conditions including whole dataset correlations, lag correlations, discrete temporal correlations (such as monthly) and log transform correlations. No significant correlation was found between February 1st snowpack on Mount Shasta and stream temperature for the Sacramento River. In addition, no significant correlation was found between air temperature at Redding airport and stream temperatures at the Sacramento, McCloud and Pit Rivers.

Table 46. Datasets analyzed for correlation with streamflow datasets for the Sacramento, McCloud and Pit Rivers. "NC" means no strong correlation was found while "C" means that there was a strong correlation found.

Variable Analyzed for correlation with stream temperature	Time period	Sacramento River	McCloud River	Pit River
Daily Average Air Temperature	Whole dataset	NC	NC	NC
Lag-1 Air Temperature	Whole dataset	NC	NC	NC
February 1^{st} snowpack	Whole dataset	NC	NC	NC
Log Transform Air Temperature	Whole dataset	NC	NC	NC
Daily Average Stream Temperature	Whole dataset	NC	NC	NC
Daily Average Air Temperature	Monthly	NC	NC	NC
Lag-1 Air Temperature	Monthly	NC	NC	NC
Log Transform Air Temperature	Monthly	NC	NC	NC
February 1^{st} snowpack	Monthly	NC	NC	NC
Daily Average Stream Streamflow	Monthly	C	C	C

The strongest correlations were found between stream temperature and streamflow for the months of May, June and July for the Sacramento, McCloud and Pit Rivers (Table 47). The correlations between stream temperature and streamflow for other months of the year for the Sacramento, McCloud and Pit Rivers, however, were determined to be rather weak compared to the months of May, June and July previously mentioned.

Table 47. May, June and July correlations between streamflow and stream temperature for the Sacramento, *McCloud and Pit Rivers. Numbers represent the calculated correlation coefficient value of the river for the specified month with the USGS streamflow data as the independent variable and the CDEC stream temperature data as the dependent variable*

	May	**June**	**July**
Sacramento River	-0.725	-0.555	-0.47
McCloud River	-0.411	-0.578	-0.646
Pit River	-0.262	-0.266	-0.156

After assessing the correlations between stream temperature and other variables it was decided that the most prudent approach to selecting stream temperatures for a given day's flow was to develop a k-NN algorithm similar to that described in the streamflow generator where the stream temperatures of days with streamflows similar in magnitude were selected.